University of Alberta

Soil Bearing Capacity for Crawler Cranes

by

Xiteng Liu

A thesis submitted to the Faculty of Graduate Studies and Research in

partial fulfillment of the

requirements for the degree of *Master of Science*

in

Geotechnical Engineering

Department of *Civil & Environmental Engineering*

Edmonton, Alberta

Spring 2005

ABSTRACT

Loadings imposed on the ground by cranes have been increased substantially. Large cranes such as the 1250mt capacity DEMAG CC8800 crawler crane can impose a pressure as much as 2.0Mpa on the ground. For these cranes, site preparation is required for heavy lifts. Site preparation usually includes placing mats under crane tracks to limit the ground pressure less than the allowable bearing pressure recommended by a geotechnical engineer. The current method of calculation of the allowable bearing capacity for cranes is based on the formulas used for spread footing and shallow foundation. However, there are differences in applying the traditional bearing capacity calculations for building foundations to a crane because the duration of loading for a crane is relatively short and the allowable settlements for cranes are higher. It is understood that total settlement is not a concern. Typically a crane can tolerate a maximum differential settlement of 1/200, which is much larger than 1/500 required for most buildings.

Computer simulation and field studies have been carried out to study the allowable bearing capacity for crawler cranes. A series of equations modified from the classical bearing capacity equations for foundations have been proposed for crawler cranes on different soils. A design procedure used to estimate the allowable bearing capacity for crawler cranes has also been suggested in the paper.

ACKNOWLEDGEMENT

I would like to express my gratitude to all those who gave me the possibility to complete this thesis. I want to thank the Natural Sciences and Engineering Research Council of Canada for providing the fund to do the necessary research work in the first instance.

I have furthermore to thank Sterling Crane for allowing me to carry out field studies on their lifts as well as their financial support.

I'm deeply indebted to my supervisor Prof. Dr. Dave Chan from the University of Alberta whose help, stimulating suggestions and encouragement helped me in all the time of research for and writing of this thesis.

I'm very grateful to the engineer manager of Sterling Crane, Mr. Brian Gerbrandt who spared no effort to help me understanding cranes and doing some measurement in the field.

I also want to thank Mr. Marvin Cherniawski from AMEC who gave me valuable suggestions on my research.

My classmates from University of Alberta supported me in my research work as well. I want to thank them for all their help, support, interest and valuable hints.

Especially, I would like to give my special thanks to my wife Dongmei whose patient love enabled me to complete this work.

TABLE OF CONTENTS

LIST OF TABLES

LIST OF FIGURES

LIST OF SYMBOLS

B - footing width, supporting track width of crane
B' - equivalent footing width, crane track pressure spread width through mat
B_t - width of crane track
c - cohesion of soil
C_u - undrained shear strength of soil
d - thickness of crane mat
D - footing depth
e - load eccentricity
E - modulus of elasticity
E_m - modulus of elasticity of crane mat
E_s - modulus of elasticity of soil
E_u - undrained modulus of elasticity of clay
$[f_b]$ - allowable bending strength of mat
$[f_v]$ - allowable longitudinal shear strength of mat
FS - factor of safety
G - shear modulus
I_m - influence factor of footing dimension on rotation
I_r - rigidity index
I_w - influence factor of footing dimension on settlement
L - footing length, supporting track length
L' - equivalent footing length
L_m - length of crane mat
L_t - length of crane track
N - SPT blow count
q - surcharge load
q_a - allowable bearing capacity of soil
q_{max} - max track pressure
q_{min} - min track pressure under the same track as q_{max}
q_n - net footing pressure
q_u - ultimate bearing capacity of soil
$\tilde{q}$ - equivalent track pressure
S - crane track span
α - crane rotation angle
β - relative rotation of foundation
γ - unit weight of soil
γ' - effective unit weight of soil
δ - settlement of soil
$[\delta]$ - allowable settlement of soil
δ_d - different settlement of soil
$[\delta_d]$ - allowable different settlement of soil
δ_u - immediate settlement
θ - tilt angle of crane base
λ - ratio of undrained modulus to undrained shear strength of clay

ν - Poisson's ratio
σ - normal stress
φ - friction angle of soil

LIST OF APPENDICES

1 INTRODUCTION

1.1 Background

Bearing capacity for soils traditionally has been determined based on the shear strength of the foundation material. Most studies on bearing capacity for buildings have been carried out from 1920s to 1970s. The classical equations proposed by Terzaghi, Meyerhof and Vesić are still being used nowadays. A factor of safety is commonly used to account for many uncertainties in the bearing capacity calculation such as the variability of soil resistance, limitations of the bearing capacity theory and deformation of the ground etc. Normally a factor of safety of 2.5 to 3.5 is used for shallow foundations.

From the 1950s, people started to recognize that excessive deformation of ground has great impact on the structural damage of the building. Another concern on the settlement of foundation has been studied from 1950s to 1980s. It is widely accepted that there are two criteria associated with foundation design: strength and settlement.

The history of crane can be dated back to 3000 B.C. when the first lifting device emerged in ancient Egypt. During the period of Renaissance, crane technology had been well developed with a large amount of new buildings and the development of specialized building methods. The first machine-driven crane was invented in 1839 and mobile cranes in early days are rail-mounted until the first excavator on crawler appeared in 1912 in the United States and then in Europe in the 1920s. From then, the development of crane has been boosted by the application of rubber tire, diesel engine, telescopic boom and hydraulic system. Varies types of cranes were also developed for different lifting purposes. The lift capacity of mobile crane increased dramatically in 1970s with the use of high strength fine-grained steel. DEMAG had broken through the 800mt limit in 1978 and the maximum lift capacity of a crawler crane exceeds 2600mt today.

1.2 The need of soil bearing capacity study for crawler cranes

It is believed that directly application of the soil bearing capacity calculation for foundations to cranes is conservative. Shapiro (1999) suggested using a presumable bearing capacity 33.3% to 50% higher for cranes than that for foundations in his book "Cranes and Derricks 3rd ed.". Another book "Crane Stability On Site - An Introduction Guide" (CIRIA1996) suggests using a factor of safety of 2.0 or even 1.5 in the determination of bearing capacity for mobile crane, but it deals mostly with outrigger cranes with small loading area and therefore settlement is not as critical as the crawler cranes. No previous study on soil bearing capacity has been done for crawler cranes due to the lack of demand. There were not many cranes with large lifting capacity ten years before. Even today there are no more than fifty mobile cranes having a capacity of over 1000mt in the world. Track pressures for crawler cranes with a capacity less than 500mt are not considerably high. Therefore, the bearing capacity of soil is usually not a big issue for majority of the cranes.

However, with the emerging of larger capacity crawler cranes, the demand of finding an appropriate value of soil bearing capacity for these cranes becomes greater. The track pressure of large cranes can be extremely high; for example, the maximum track pressure of a 1250mt DEMAG CC8800 crane can reach about 2000kPa. The use of traditional bearing capacity for buildings will lead to considerable cost and time in general site preparation. Therefore, the study on the soil bearing capacity for crawler cranes to reduce the cost and time in site preparation becomes more feasible.

1.3 The difference in soil bearing capacity for cranes and foundations

There are differences in applying the traditional bearing capacity calculations for foundations to a crane because of the following reasons:

- Proper factor of safety

The selection of a factor of safety is mainly based on experience, the level of uncertainty, the consequence of failure and the probability of design load ever actual occurs. The factor of safety for buildings is usually about 2.5 to 3.5. Since the load duration for a crane is relatively short, the uncertainty in crane load is less than buildings, and the consequence of failure is not as severe as buildings, the proper factor of safety used in soil bearing capacity for cranes should be less than that for buildings.

- Allowable differential settlement

The maximum allowable differential settlement should not exceed 1/500 for most buildings to avoid any structural damage or sever cracking of the wall. Whereas, the allowable out of levelness for crane during operation is about 1/200, which is less critical than that for buildings.

- Immediate settlement vs. total settlement

The settlement of building is generally comprised of immediate settlement, consolidation settlement and creep. While the crane settlement can be treated as the immediate settlement which is only about 0.2~0.6 of the total settlement for cohesive soil.

- Design pressure

In order to not overstress the soil under some point and to eliminate tilting of the footing, the eccentricity of load on a footing is usually limited to $e/L<1/6$ by adjusting the footing dimension for buildings. Therefore, the design pressure is equal to or slightly over the average pressure for footing. However, the load eccentricity for cranes can easily exceed the $e/L=1/6$ limit and results in triangular distributed pressure over partial length of the crane track. In this case, the maximum pressure is much higher than the average pressure over the whole length of crane track. This maximum pressure is commonly used as the design pressure in practice.

- Load duration

The load duration for a crane is relatively short compared to that for a foundation of buildings. The ground may not be able to fully respond to the change of pressure during crane operation. Although a typical lift usually does not exceed 2 or 3 hours, the crane may hold the load for quite a long period for other operation in some cases. Therefore, the effect of short loading duration is not considered as a major factor in the soil bearing capacity study for cranes.

- Dynamic load

Although the crane load is not a static load, the dynamic effect is usually neglected in the evaluation of track pressure. However, this effect can be significant if the soil is sensitive or has a potential of liquefaction.

- Actual versus design groundwater condition

The most adverse ground water level that might happen during the service life of the building is used for footing design. While the ground water level is relative constant during the crane operation and usually differs from the worst case. Therefore, it is more logical to use the actual water level in the determination of soil bearing capacity for cranes.

1.4 Objective

The objective of this study is to improve on the current method to evaluate the bearing capacity of soils for crawler cranes. It is mainly focused on the first four aspects in which cranes are different from foundations. Only cranes sitting on flat ground surface are being studied, no slope stability issues are concerned. This study also does not include any case with underground structure or pipeline close to crane working area that the crane track pressure may have impact on them. Both in-situ measurement and numerical analysis are carried out to form some equations of allowable bearing capacity of typical soils for crawler cranes. A series of simplifications and transformations are used to convert the problem of allowable bearing capacity for cranes to a typical foundation problem. Based on these, the equations for crane can be modified from the existing equations for

foundations. The influence of ground water level and crane mat on the bearing capacity is also considered in these equations. Finally, a design procedure including all equations that involved for evaluating the allowable bearing capacity for crawler cranes is proposed.

2 REVIEW OF SOIL BEARING CAPACITY FOR SHALLOW FOUNDATIONS

The soil must be capable of carrying the loads from any engineered structure or temporary facility placed on it without a shear failure and with the resulting settlements being able to be tolerated by the structure. That means the soil must meet both strength and serviceability requirement.

The ultimate bearing capacity q_u, defined as the maximum load a soil could sustain before shear failure will occur is based on the shear strength of the material. While the allowable bearing capacity q_a, is the maximum allowable load on of the ground under any circumstances, taking into consideration the bearing capacity, the settlement and other uncertainties. In most cases, especially for granular soils, the allowable bearing capacity is nearly almost controlled by settlement.

2.1 Determination of the ultimate bearing capacity q_u

2.1.1 Modes of failure

Bearing failure of a foundation usually results shear failure of the foundation soil. Shear failure are commonly separated into three modes: (a) general shear failure, (b) local shear failure, and (c) punching shear failure, depending on the relative compressibility of the soil and the particular geometrical and loading conditions. Figure 2-1 shows the feature of three failure modes.

General shear failure is usually associated with dense soil of relatively low compressibility; the slip surface is continuous from the edge of the footing to the soil surface, and full shear resistance of the soil is developed along the failure surface. The failure surface of local shear failure extends from the edge of the footing to approximately the boundary of the Rankine passive zone. The shearing resistance is fully developed over only part of the failure surface. Punching shear failure is commonly associated with loose and very compressible soils; the failure pattern is not easily detected. The vertical shear deformation is visible with no apparent bulging of the soil around the footing.

Vesić (1963 and 1973) carried out model footing tests in Chattahoochee sand and showed that the mode of failure in sand is a function of relative density and relative depth D/B (Figure 2-2). But there are no general numerical criteria that can be used for predicting the mode of shear failure; the only rational parameter to evaluate the relative compressibility of the soil mass is the rigidity index, I_r, which is defined as:

$$I_r = \frac{G}{c + \sigma \tan\phi} \qquad (2\text{-}1)$$

where G = shear modulus of soil

c = cohesion of soil

ϕ = friction angle of soil

σ = normal stress acting on the failure surface of soil

2.1.2 Classical earth pressure theory

The study of the ultimate bearing capacity of soil can be traced back to as early as 1850's, initiated by Rankine (1857) and Pauker (1850's) with the classic earth pressure theory.

This theory assumes that on exceeding a certain stress state, rupture surface are formed in the soil mass. Thus, the stresses, developing upon the formation of rupture surfaces may be considered as the ultimate bearing capacity of soil. Based on the above assumption, the ultimate bearing capacity can be determined using the static or kinematic methods. Most methods developed from this theory are abandoned nowadays.

2.1.3 Prandtl's theory of plastic equilibrium

Many of the fundamental principles regarding bearing capacity determination began with Prandtl's theory of plastic equilibrium found in the early 1920's. Prandtl studied the process of penetration of hard bodies, such as metal

punchers, into a softer, homogeneous, isotropic material from the viewpoint of plastic equilibrium. The theory was adopted to calculate the soil bearing capacity where a rigid footing penetrates into a relative soft soil. However, the soil is not a homogeneous isotropic material and the contact surface between the footing and the soil is not as smooth as that for metals.

The theory assumes that the soil is a rigid-plastic solid, which means that the soil exhibits no deformation prior to shear failure and flows plastically at constant stress after failure. Thus prediction of soil bearing capacity is only limited to relatively incompressible soils or to the general shear failure where the elastic deformation is relatively small. With the increase of load on the long footing (say, L/B>5), three zones are developed in the soil, resulting in bearing failure. Figure 2-3 illustrates the rupture surface and these three zones. Zone I is a wedge in active state, which will remain intact during failure. Zone II is in plastic state with an approximately logarithmic spiral to circular boundary. Zone III is in the passive Rankine state.

Assuming full shearing resistance is developed along the rupture surface and ignoring the weight of soil mass within the failure zone, the ultimate bearing capacity of a soil based on Prandtl's theory is given by:

$$q_u = \frac{c}{\tan\phi}\left[\tan^2\left(\frac{\pi}{4}+\frac{\phi}{2}\right)e^{\pi\tan\phi}-1\right] \qquad (2\text{-}2)$$

To prevent Prandtl's bearing capacity q_u from becoming equal to zero when c=0, Terzaghi suggested to account for the weight of the soil in the failure zone: a factor c' was added to c in Prandtl's equation:

$$q_u = \frac{(c+c')}{\tan\phi}\left[\tan^2\left(\frac{\pi}{4}+\frac{\phi}{2}\right)e^{\pi\tan\phi}-1\right] \qquad (2\text{-}3)$$

where $c' = \gamma t \tan\phi$

γ = unit weight of soil

$$t = \text{equivalent height of soil} = \frac{\text{area of failure zone}}{\text{length of failure plane}}$$

Taylor improved Equation 2-2 by adding a term $\frac{\gamma B}{2}\tan(\frac{\pi}{4}+\frac{\phi}{2})$ to account for the shear strength induced by the overburden pressure as:

$$q_U = \left[\frac{c}{\tan\phi} + \frac{\gamma B}{2}\tan(\frac{\pi}{4}+\frac{\phi}{2})\right]\left[\tan^2(\frac{\pi}{4}+\frac{\phi}{2})e^{\pi\tan\phi} - 1\right] \qquad (2\text{-}4)$$

2.1.4 Terzaghi's equation

Based on Prandtl's theory of plastic failure, Terzaghi presented a modified system in 1943 as illustrated in Figure2-4. In Terzaghi's system, he included the influence of foundation depth D and assumed the soil above the bottom of foundation has no shear strength and serves only as a surcharge load q = γD. Terzaghi believed that the rough base of the foundation would restrain the soil right beneath the foundation to spread laterally. Therefore he revised the angle between bottom of footing and rupture plane of wedge zone from Prandtl's $\psi = \frac{\pi}{4}+\frac{\phi}{2}$ to $\psi = \phi$ in his calculation.

Terzaghi proposed the equations for the ultimate bearing capacity for the general shear condition as a superposition of three contributions (c, γB, and q) to the bearing capacity:

$$q_{u=cN_c} + \frac{1}{2}\gamma B N_\gamma + qN_q \qquad (2\text{-}5)$$

where N_c, N_q and N_γ are bearing factors expressed as:

$$N_c = \cot\phi\left[\frac{a^2}{2\cos^2(\pi/4+\phi/2)}-1\right]$$

$$N_q = \frac{a^2}{2\cos^2(\pi/4+\phi/2)}$$

$$N_\gamma = \frac{1}{2}\tan\phi\left(\frac{K_{p\gamma}}{\cos^2\phi}-1\right)$$

$a = e^{(3\pi/4-\phi/2)\tan\phi}$ for rough base

$a = e^{\pi/2\tan\phi}$ for smooth base

The $K_{p\gamma}$ term used to calculate the N_γ in Terzaghi's equation was not thoroughly explained by the original author, however, it is not so important since it is only an intermediate value.

For the local shear and punching shear cases, Terzaghi suggested using reduced strength parameters as:

$$c' = \frac{2}{3}c$$
$$\tan\phi' = \frac{2}{3}\tan\phi \qquad (2\text{-}6)$$

Terzaghi also introduced factors for other shapes of footing:

For square footings:

$$q_{u=1.3cN_c} + 0.4\gamma BN_\gamma + qN_q \qquad (2\text{-}7)$$

For circular footings:

$$q_{u=1.3cN_c} + 0.3\gamma BN_\gamma + qN_q \qquad (2\text{-}8)$$

The Terzaghi's equations have been very widely used since they were the first proposal and were believed to be conservative. But Ko (1973) pointed out that bearing capacities calculated from Terzaghi's method are always greater than

those obtained by means of plasticity theory. Experiments also showed that the computation from Terzaghi's equation did not provide as good correlations as those given by Meyerhof's or Hansen's to the test results. Most scholars after Terzaghi preferred to accept Prandtl's failure pattern and express N_c and N_q with no influence of base roughness.

Although Terzaghi's equation are getting abandoned nowadays, its basic form is still used in others formulas. The N_γ is the mostly disputed term, Meyerhof suggested $N_\gamma = (N_q - 1)\tan(1.4\phi)$, Hansen used N_γ=1.5(N_q-1)tanϕ, and Vesić proposed N_γ=2(N_q+1)tanϕ.

2.1.5 Vesić's general equation

Based on theoretical and experimental findings from former researchers work, Vesić developed a general bearing capacity equation that is considered to be the alternative to Terzaghi's:

$$q_u = cN_c s_c d_c i_c b_c g_c + qN_q s_q d_q i_q b_q g_q + 0.5\gamma B N_\gamma s_\gamma d_\gamma i_\gamma b_\gamma g_\gamma \qquad (2\text{-}9)$$

It remains the same form as Terzaghi's equation but five influence factors are added to represent the general case.

Shape Factors

A broad range of footing shapes are considered by the shape factor:

$$\begin{aligned} s_c &= 1 + \left(\frac{B}{L}\right)\left(\frac{N_q}{N_c}\right) \\ s_q &= 1 + \left(\frac{B}{L}\right)\tan\phi \\ s_\gamma &= 1 - 0.4\left(\frac{B}{L}\right) \end{aligned} \qquad (2\text{-}10)$$

where B = width of footing

L = length of footing

For continuous footing, $B/L \rightarrow 0$, s factors become equal to 1.

Depth Factors

There is no limitation on the depth of the footing in Vesić's equations. It might even be used for deep foundation. The depth factor is defined as:

$$d_c = 1 + 0.4k$$
$$d_q = 1 + 2k\tan\phi(1-\sin\phi)^2 \qquad (2\text{-}11)$$
$$d_\gamma = 1$$

where k = D/B for shallow foundations(D≤B)

k = $\tan^{-1}(D/B)$ for deep foundations (D>B)

Load Inclination Factors

The load inclination factors are for loads that do not act perpendicular to the base of footing:

$$i_c = 1 - \frac{m \cdot V}{A \cdot c \cdot N_c}$$
$$i_q = \left[1 - \frac{V}{P + \frac{A \cdot c}{\tan\phi}}\right]^m \geq 0 \qquad (2\text{-}12)$$
$$i_\gamma = \left[1 - \frac{V}{P + \frac{A \cdot c}{\tan\phi}}\right]^{m+1} \geq 0$$

For loads inclined in the B direction:

$$m = \frac{2 + B/L}{1 + B/L}$$

For loads inclined in the L direction:

$$m = \frac{2 + L/B}{1 + L/B}$$

where V = applied shear load

P = applied normal load

A = base area of footing

Base Inclination Factors

The vast majority of footings are built with horizontal bases. However, the base might be inclined if the applied load is at a large angle from vertical. The base inclination factors are:

$$b_c = 1 - \frac{\alpha}{147^\circ}$$
$$b_q = b_\gamma = \left(1 - \frac{\alpha \tan\phi}{57^\circ}\right)^2 \qquad (2\text{-}13)$$

where α = the angle between the footing base and horizon, α≥0.

Ground Inclination Factors

The ground inclination factor is to account for the reduction of bearing capacity of a footing located near the top of a slope. They are:

$$g_c = 1 - \frac{\beta}{147^\circ}$$
$$g_q = g_\gamma = (1 - \tan\beta)^2 \qquad (2\text{-}14)$$

where β = the angle between the slope surface and the horizon, β ≥0.

2.1.6 Other factors to be considered

- **Ground water**

The effects of ground water on the ultimate bearing capacity are the decrease of shear strength at the failure surface and decrease of the effective unit weight above the footing base. The decrease of unit weight above the footing base is straightforward, while the effect of a decrease of shear strength at the failure surface is usually expressed as the decrease of unit weight γ in the N_γ term in Equation 2-5. The unit weight γ is computed as the average effective unit weight from the base of footing to a depth of B+D.

There is no influence of ground water when performing total stress analysis since the effects are implicit in the method.

- **Eccentricity of Load**

Meyerhof introduced the concept of effective footing dimension B' and L' to account for the effect of eccentric or moment loads. They are defined as:

$$B' = B - 2e_B$$
$$L' = L - 2e_L \qquad (2\text{-}15)$$
$$q_{eqv} = \frac{P + W_f}{B'L'}$$

where e_B = load eccentricity in footing width direction

e_L = load eccentricity in footing length direction

q_{eqv} = equivalent design bearing pressure

Instead of explicitly reducing the bearing capacity due to the load eccentricity, this method increases the calculated equivalent bearing pressure. It is a practical method in footing design rather than evaluating the load eccentricity effect on bearing capacity.

- **Layered soil**

Many soil profiles are not uniform but layered due to the depositional process. Therefore, the bearing capacity equations are not valid because the failure surfaces of layered soil are not the same as that assumed in the bearing capacity

theory and the strength parameters of soil are not uniform but vary with depth. However, there are three primary ways to use the bearing capacity equations to calculate the bearing capacity of layered soils with consideration of soil parameter variation:

The first option is to evaluate the bearing capacity using the lowest values of c, φ, and γ in the zone between the bottom of the footing and a depth B below the bottom, this is the zone where bearing failures occur. This method is obviously conservative. However, in most cases settlement controls the allowable bearing capacity of soil.

The second option is to use weighted average values of c, tanφ, and γ based on the relative thickness of each stratum in the zone between the bottom of the footing and a depth of B below the bottom. This method can provide acceptable results so long as the differences in the strength parameters are not too great.

The third and the most complex option is to consider a series of trial failure surfaces and evaluate the bearing capacity using the methods similar to those employed in slope stability analysis. This method is more precise but requires more effort to implement.

- **Adjacent footings**

The effects of adjacent footings may vary considerably with the friction angle φ. For low φ values they can be negligible; however, for high φ values they appear to be significant particularly if a footing is surrounded by others on both sides. These effects are considerably reduced as $L/B \rightarrow 1$.

Vesić recommended not considering the interference effects in bearing capacity computations.

- **Rate of loading**

Researchers found that the mode of failure on both dense sand and compacted clay changes from general shear to punching shear as the rate of loading

increased from static loading condition ($2.5x10^{-3}$ mm/sec) to impact loading condition ($2.5x10^{2}$ mm/sec). Footings on dense sand show a slightly drop of bearing capacity with the increase of loading rate while footings on compacted clay showed a considerable increase of bearing capacity as the rate of loading increases. It appears that the conventional static analysis of bearing capacity can be used for footing subjected to moderately rapid loadings if the strength parameters introduced in the analysis are modified for strain rate effects.

2.1.7 Bearing capacity for cohesive soils

The ultimate bearing capacity of c-φ soils is apparently a function of soil's c, φ, and γ, foundation width B, foundation depth D, and other factors as discussed in Vesić's equations. However, strength of saturated cohesive soil will increase with time due to consolidation. Therefore, the bearing capacity of cohesive soils is usually determined by its undrained strength c_u with friction angle $\phi=0$ since the undrained condition is usually the most critical condition. In this case, the failure surface becomes a circle and the bearing capacity can be expressed as:

$$q_u = cN_c + qN_q \qquad (2\text{-}16)$$

It is obvious that there is no influence of footing size on the ultimate bearing capacity for cohesive soils in total stress analysis.

2.2 Determination of allowable bearing capacity q_a

There are two concerns in determining the allowable bearing capacity in geotechnical foundation design: There should be some conservation against failure and there should be no structural damage caused by foundation settlement. Thus, the allowable bearing capacity is evaluated from both the failure criterion and the settlement criterion, and the minimum value should be used.

2.2.1 Factor of safety

Nearly all bearing capacity analyses are currently implemented using allowable stress design (ASD) method although the load resistance factor design (LRFD) methods are prevailing in structural analysis these days. In the ASD method, the allowable bearing capacity is obtained by dividing the ultimate bearing capacity by a factor of safety (FS) as:

$$q_a = \frac{q_u}{FS} \tag{2-17}$$

The factor of safety is to accommodate the uncertainties in soil profile, soil strength parameters, bearing capacity theory and simplification in analysis. The selection of the value of factor of safety is based on:

- Past experience
- The quality of information can be obtained from site investigation
- Soil type
- The cost of the foundation
- The serviceability of the structure
- The importance of the structure and consequence of a failure
- The probability of design load ever actual occurring

Geotechnical engineers usually use a factor of safety between 2.5 and 3.5 for bearing capacity analyses of shallow foundations. However, values as low as 2.0 or as high as 4.0 have be used.

2.2.2 Settlement of foundation

Since it is impossible to build a foundation without settlement, there is always a major concern of limiting the settlement to a certain value to avoid any induced damage to the structure in foundation design. A foundation designed with an

adequate factor of safety against a bearing capacity failure does not guarantee that it will not settle excessively. In most cases, settlement analysis is needed to obtain the proper allowable bearing capacity.

The structural load applied to the footing is the major cause of settlement. However, other sources of settlement also may be important. These include:

- Settlements caused by falling groundwater table
- Settlements caused by underground mining or tunneling
- Settlements caused by secondary consolidation
- Settlements caused by lateral movement from nearby excavation

Allowable settlement and structure damage

It is believed that the settlements of the foundations are the major cause of distress in buildings. But if the entire structure moves vertically by some amount or rotates as a plane rigid body, this will not generally cause structural or architectural distress. Most structural damages are related to the differential settlement δ_d. Skempton and McDonald (1955) introduced the concept of tilt ω and angular distortion (relative rotation) β to quantify the effect of differential settlement on structural damage. Figure 2-5 shows the definitions of these terms in foundation movement.

Two best known studies in early days on allowable settlements of structures are those of Skempton and McDonald (1956) and Polshin and Tokar (1957). Both studies gave similar recommendations: relative rotation β>1/150 (or 1/200 by Polshin and Tokar) will cause structural damage; β>1/300 will cause cracks in walls and partitions; β<1/500 is recommended and if it was particularly desired to avoid any settlement damage this figure might well be reduced to 1/1000.

Burland and Wroth (1974) introduced the concept of critical tensile strain that the onset of visible crack in a given material was associated with this limiting critical

tensile strain. His theory generally agreed with previous works by Skempton and McDonald and Polshin and Tokar and provided a theoretical basis to them.

The allowable value of relative rotation also depends on soil type and structure type. Steel frame may undergo much more differential settlement than brick wall before any damage occurs due to its flexibility.

In practice, it is convenient to use differential settlement δ_d rather than relative rotation β in settlement control since the former is more directly.

The origins of differential settlement may include the variation in the soil profile, the variation in the structural loads, construction tolerances and soil structure interaction etc.

Bjerrum (1963) compared the total and differential settlements of spread footings on clays and sands as shown in Figure 2-6 and Figure 2-7. His study led to the method of using the available δ_d/δ ratio on local soil conditions and the calculated total settlement to estimate the differential settlement. In the absence of local data, the generic δ_d/δ ratio are listed in Table 2-1 may be used to predict differential settlement.

Table 2-1 Design value of δ_d/δ for spread footings (from Coduto 2001)

Predominant Soil Type Below Footings		Design value of δ_d/δ	
		Flexible Structures	Rigid Structures
Sandy	Natural soils	0.9	0.7
	Compacted fill over stiff natural soils	0.5	0.4
Clayey	Natural soils	0.8	0.5
	Compacted fill over stiff natural soils	0.4	0.3

Based on Bjerrum's correlation between the differential settlement and total settlement, it is wise to set a criterion on total settlement to limit the value of differential settlement. However, total settlement itself can be very large without any structural or architectural damage. Therefore, the settlement requirements on foundation design are stated as follows:

$$\delta \le [\delta]$$
$$\delta_d \le [\delta_d] \qquad (2\text{-}18)$$

where δ, δ_d = total settlement and differential settlement

$[\delta]$, $[\delta_d]$ = total allowable settlement and differential settlement

The general guideline on allowable settlements is given in Table 2-2.

Table 2-2 Guideline of allowable settlement in foundation design

Soil Type	Foundation Type	Allowable Total Settlement [δ] (mm)	Allowable Differential Settlement [δ_d] (mm)
Sandy	Spread footing	25	<=75%[δ]
	Raft	50	
Clayey	Spread footing	65	40
	Raft	65 - 100	40

Time dependent settlement

The settlement of footing is a time-dependent behavior and can be divided into immediate settlement (δ_u), consolidation settlement (δ_{con}), and secondary consolidation settlement (δ_{sec}) by the time framework as:

$$\delta = \delta_u + \delta_{con} + \delta_{sec} \qquad (2\text{-}19)$$

Immediate settlement is the settlement due to the increase of load to the foundation during construction; it is mainly elastic deformation of soil and usually has a time span from 0 day to perhaps10 days. Consolidation settlement is the process of expelling pore water out of the soil skeleton under the applied load. Based on Terzaghi's consolidation theory, this process in clayey soil may be very slow due to its low hydraulic conductivity k. Secondary consolidation settlement is the "creep" of soil with no change of effective stress in the soil. Figure 2-8 illustrates the development of these three parts of settlement with time.

The immediate settlement predominates in cohesionless soils and nearly all settlement will be developed during the construction period. The other two parts

of settlement can be ignored in most cases for cohesionless soils. The consolidation settlement can be predominant in cohesive soil, especially in normally consolidated (NC) clay. In highly organic deposits the secondary consolidation settlement is likely to predominate.

Since the load duration for crawler cranes is very short, the ground mainly undergoes elastic deformation. Only immediate settlement should be considered in the study of soil bearing capacity for crawler cranes.

Estimation of immediate settlement

The immediate settlement may be calculated using various procedures and those seem to be of most use in practice can be in general classified into three categories: Theoretical approach, empirical approach and the finite element method.

The theoretical approach is based on the elastic solution of load on a half space infinite body. The equations proposed usually have similar form as the elastic solution:

$$\delta_u = q_n B \frac{1-\nu^2}{E} I_w \qquad (2\text{-}20)$$

where δ_u = immediate settlement

q_n = net bearing pressure

B = the width of footing

E, v = elastic properties of soil

I_w = influence factor account for footing shape, depth, and rigidity

The rotation of rigid footing caused by an eccentric load P acting at a distance e from the center of footing is:

$$\tan\theta = \frac{Pe}{L^2 B}\frac{\left(1-\nu^2\right)}{E} I_m \qquad (2\text{-}21)$$

where e = load eccentricity in footing length direction

I_m = influence factor for footing shape

The formula proposed by Janbu et al (1956) is a representative one from elastic solution. This approach is commonly used for clays.

The empirical approach is based on the correlation between SPT blow count N or CPT cone resistance q_c and the Young's modulus of the soil. It is mainly used for sand and gravel due to the great difficulties in obtaining undisturbed samples. The formula usually has the form of:

$$\delta_u = \frac{q_n f(B)}{N} K \qquad (2\text{-}22)$$

where f(B) = factor account for the influence of footing width

N = SPT blow count

K= influence factor

For layered soil, the finite element method usually provides a satisfactory result with known soil properties. Schmertmann (1970, 1978) also developed a method to calculate the settlement of layered soil. He introduced the concept of equivalent modulus E_s and the strain influence factor I_ε. The equivalent modulus implicitly reflects the lateral strain of the soil and therefore greater than the Young's modulus of soil. The strain influence factor represents the vertical strain distribution below the footing. Knowing these two factors of each layer, the settlement of the footing can be calculated by summing the displacement of each layer as:

$$\delta_u = q_n \cdot \Sigma \frac{I_\varepsilon \Delta H}{E_s} \qquad (2\text{-}23)$$

where ΔH = thickness of each layer

Proportion of immediate settlement to total settlement

The proportion of immediate settlement to total settlement was extensively studied since there is a theoretical correlation $\frac{\delta_u}{\delta} = \frac{1-\nu_u}{1-\nu'}$ for uniform circular load on elastic half space. The theoretical undrained Poisson's ratio of saturated soil is ν_u=0.5. The drained Poisson's ratio v' is about 0.3 for normally consolidated clay and is about 0.15 for over-consolidated clay. Therefore the ratio of the immediate settlement to the total settlement is about 0.7 for NC clay. Table 2-3 shows the average value found from hundreds of real cases for different soils.

Table 2-3 Typical ratio of immediate settlement to total settlement

Material	Sand	Over consolidated clay	Normally consolidated clay
δ_u / δ	0.9 ~1.0	~0.6	~0.2

Accuracy of settlement estimation

Unlike bearing capacity, the prediction of settlement is not quite accurate and may range from 50% to 500% of the measured settlement. The errors in the settlement analysis may come from the uncertainties in soil profile, the errors in field and laboratory tests, the inaccuracy of methodology, the construction tolerance etc., however, major difficulty comes from determining the modulus of elasticity E of soil accurately and the net bearing pressure q_n applied by the footing.

The major causes of errors in determining the modulus of elasticity E includes:

- Non-linearity of the soil

Soil is not an ideal linear elastic material. The modulus of elasticity is not a unique value but dependent on the pressure level.

- Sample disturbance

Sample disturbance can not be avoided since at least the stress state of sample is different from its in-situ stress state after sampling. Laboratory tests are not often used to evaluate the modulus of elasticity. The modulus of elasticity of soil is usually correlated in-situ test results such as SPT blow counts or CPT cone resistance.

- Poor estimation from field test

The empirical correlations between modulus of elasticity and SPT or CPT are very weak. The modulus of elasticity from in-situ tests may vary as much as about one order of magnitude.

It is often assumed that the bearing pressure applied by central load of the footing is uniformly distributed under the footing. However, the actual stress distribution is highly dependent on the rigidity of the footing and the soil type. The soil structure interaction also plays an important role in the settlement of the footing, especially for rigid structures. When differential settlement takes place, it causes the redistribution of load within the structure so as to the load on the footings. This load redistribution tends to reduce the difference settlement and leads to less total settlement than predicted from those simplified methods.

2.2.3 Allowable bearing capacity from in-situ tests

Allowable bearing capacity from SPT result

The SPT N value has been used extensively for design of shallow foundations in granular soils. This is generally done by means of direct empirical correlations. Settlement rather than bearing capacity criteria usually control design of shallow foundations on sands with a least width greater than about 1.2m. Terzaghi and Peck (1948) provided a chart (Figure 2-9) for allowable bearing capacity as a

function of SPT N value and footing width B based on 25mm settlement for homogeneous sand with groundwater table below the failure zone. If the groundwater is within the failure zone, the allowable bearing capacity should be reduced 1/3 or 1/2 depending on the depth ratio D/B. Although the chart was widely used for a time after its introduction, subsequent field data have shown the chart to be too conservative.

Meyerhof proposed equations for determining the allowable bearing capacity from the same criteria, and these equations yields similar curves to those of Terzaghi and Peck.

$$\begin{aligned} q_a &= 12000Nk_d && B \le 1.2m \\ q_a &= 8000\left(\frac{B+0.3}{B}\right)^2 Nk_d && B > 1.2m \end{aligned} \qquad (2\text{-}24)$$

where N = SPT blow count

$k_d = 1+0.33(D/B) \le 1.33$

The above equations are suggested in the Canadian Foundation Engineering Manual to evaluate the allowable bearing capacity for sand.

Based on additional data Bowles makes the observation that Meyerhof's equations are also conservative. Hence, Bowles proposed a modification to Meyerhof's equations as:

$$\begin{aligned} q_a &= 18000Nk_d && B \le 1.2m \\ q_a &= 12000\left(\frac{B+0.3}{B}\right)^2 Nk_d && B > 1.2m \end{aligned} \qquad (2\text{-}25)$$

Equation 2-25 gives a value of 50% higher than Equation 2-24.

Allowable bearing capacity from CPT results

The allowable bearing capacity of shallow foundations can also be estimated directly from the CPT cone resistance using empirical correlations as illustrated in Equation 2-26.

$$\begin{aligned} q_a &= K_\phi \cdot q_{c(av)} && \textit{for granular soil} \\ q_a &= K_{su} \cdot q_{c(av)} + \gamma D && \textit{for cohesive soil} \end{aligned} \qquad (2\text{-}26)$$

where $q_{c(av)}$ = average CPT cone penetration resistance within the influence zone of footing z_f = B.

K_Φ = factor for granular soil

K_{su} = factor for cohesive soil

Meyerhof (1956) suggested K_Φ = 0.30 for granular soil. Eslaamizaad and Robertson (1996) suggested K_Φ = 0.16 ~ 0.30 depending on the footing shape and depth. In general, K_Φ is assumed to be 0.16 since settlement usually controls. The factor K_{su} ranges from 0.30 to 0.60 depending on the footing shape, depth and over consolidation ratio and sensitivity of the soil. K_{su} = 0.30 is usually used in the estimation of the allowable bearing capacity.

Correlations between allowable bearing capacity and other field test (Field vane, Plate load and Pressure Meter, etc.) results are also available. However, SPT and CPT are the most widely used field test methods in North America. For fine grain soils such as silt and clay, the SPT results may vary with the change of moisture content. It is not recommended to use SPT results to evaluate the allowable bearing capacity for these soils.

For layered soils with large contrast in stiffness, the stress distribution and influence zone may vary from the homogeneous one. A finite element or finite difference analysis is recommended to evaluate the allowable bearing capacity.

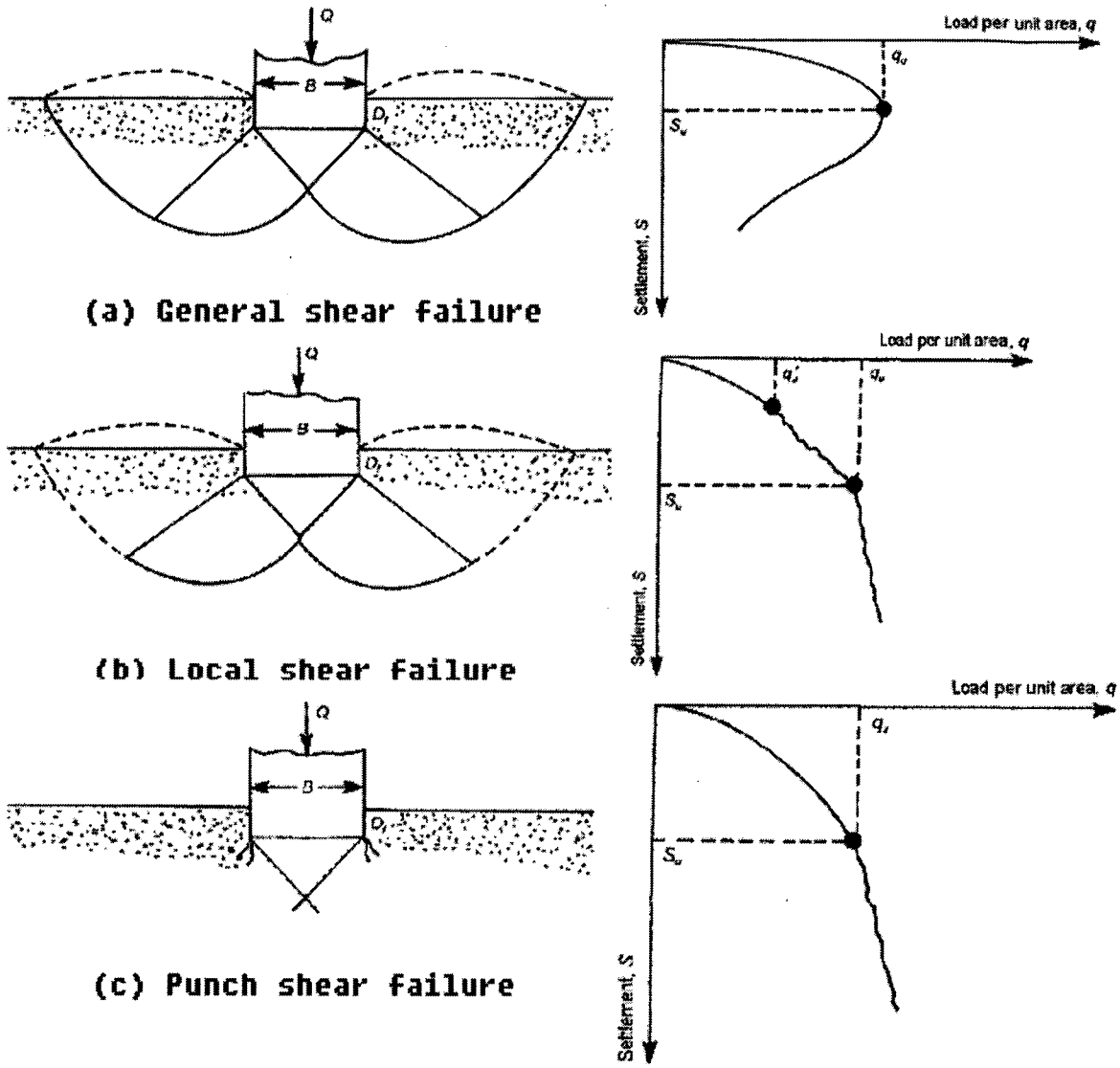

Figure 2-1 Modes of bearing capacity failure (from Vesić, 1963)

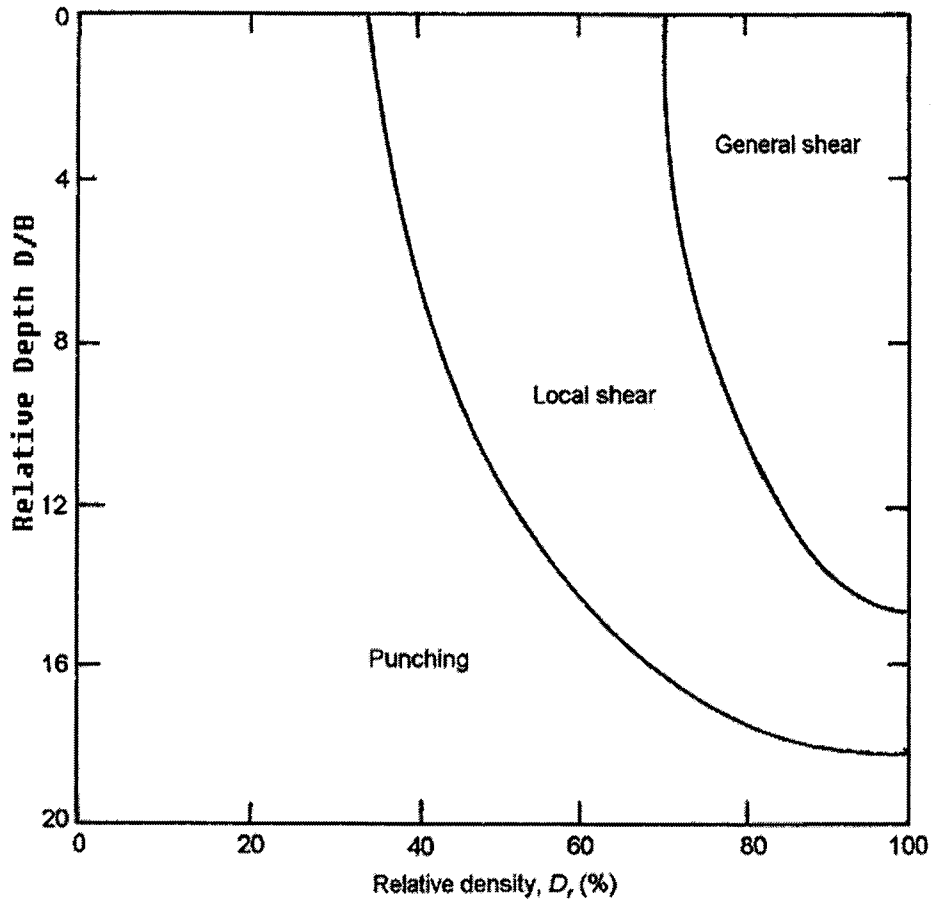

Figure 2-2 Classification of bearing capacity failure (from Vesić 1963, 1973)

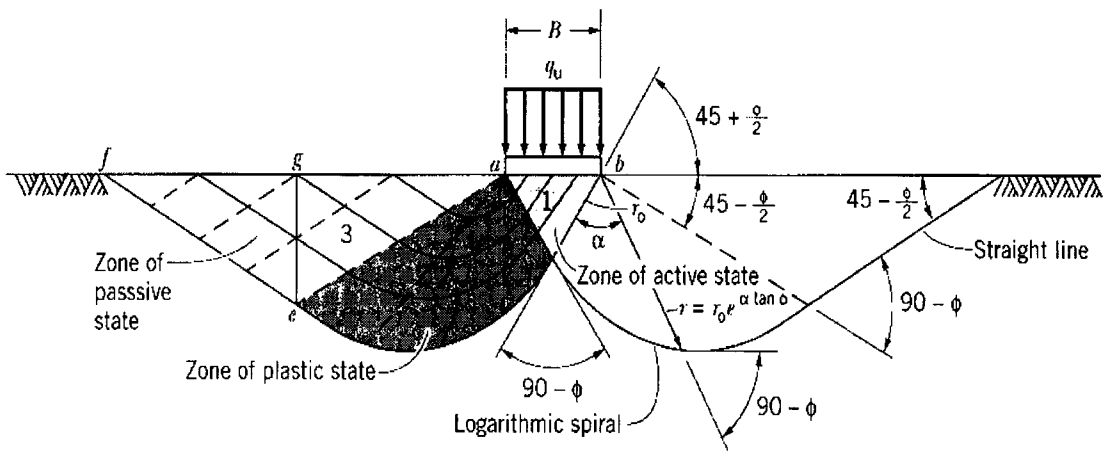

Figure 2-3 Prandtl's plastic equilibrium model

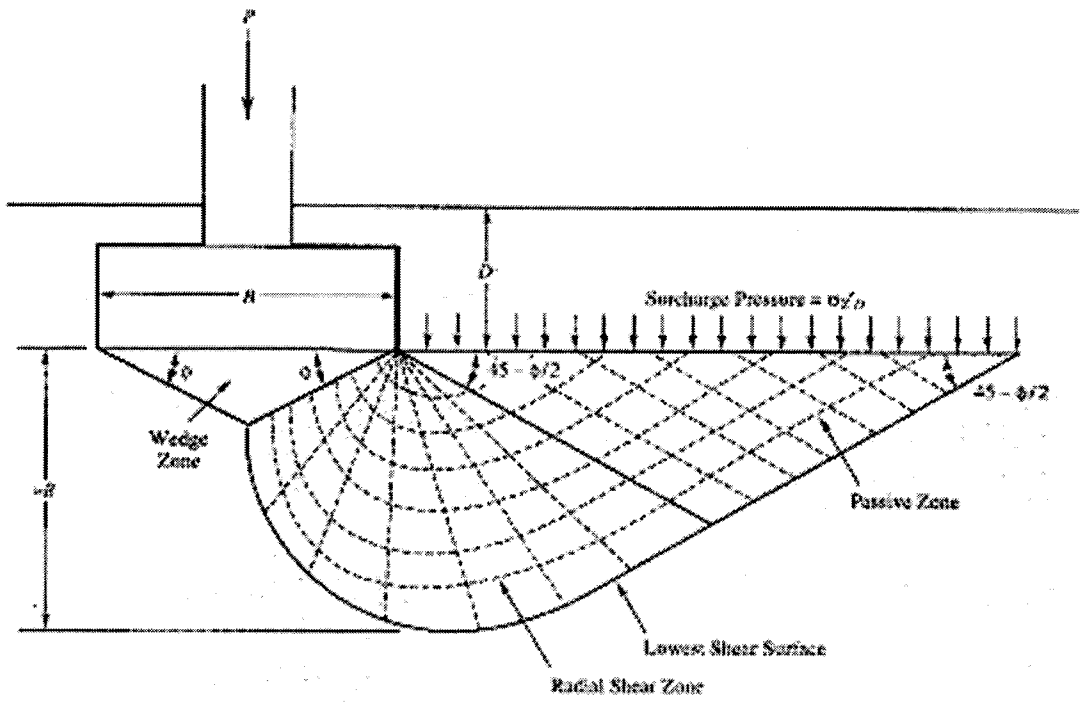

Figure 2-4 Geometry of Terzaghi's bearing capacity model

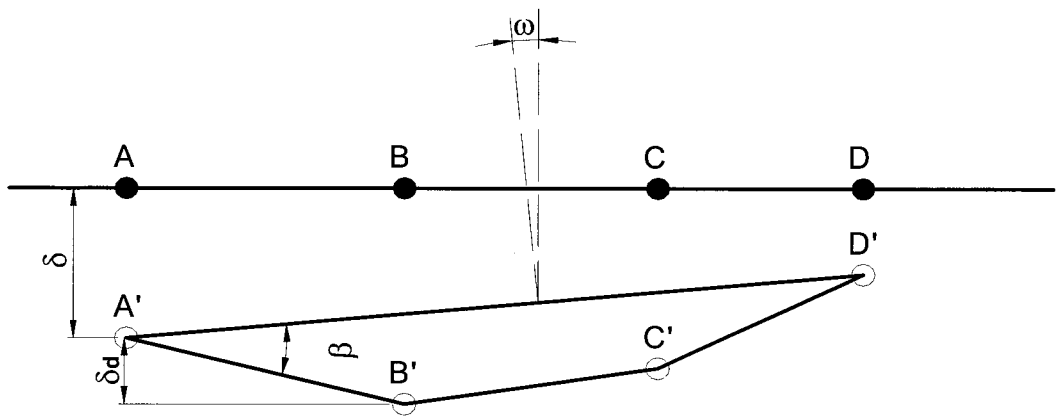

δ = settlement δ_d = differential settlement ω = tilt β = relative rotation

Figure 2-5 Definition of terms on foundation movement

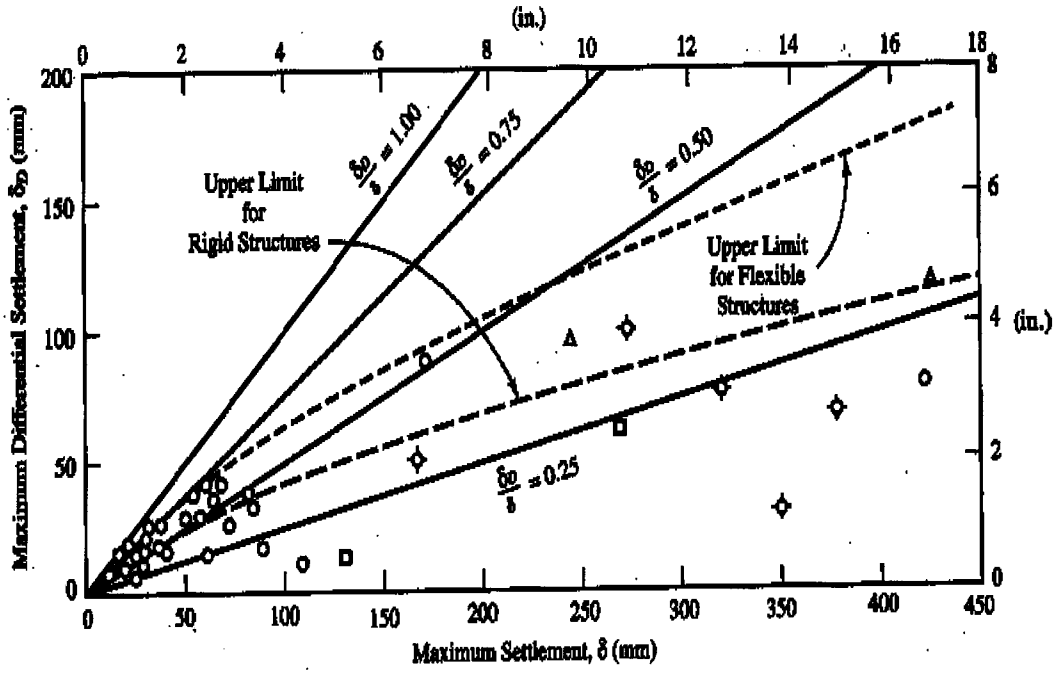

Figure 2-6 Total and differential settlement of spread footings on clays (from Bjerrum, 1963)

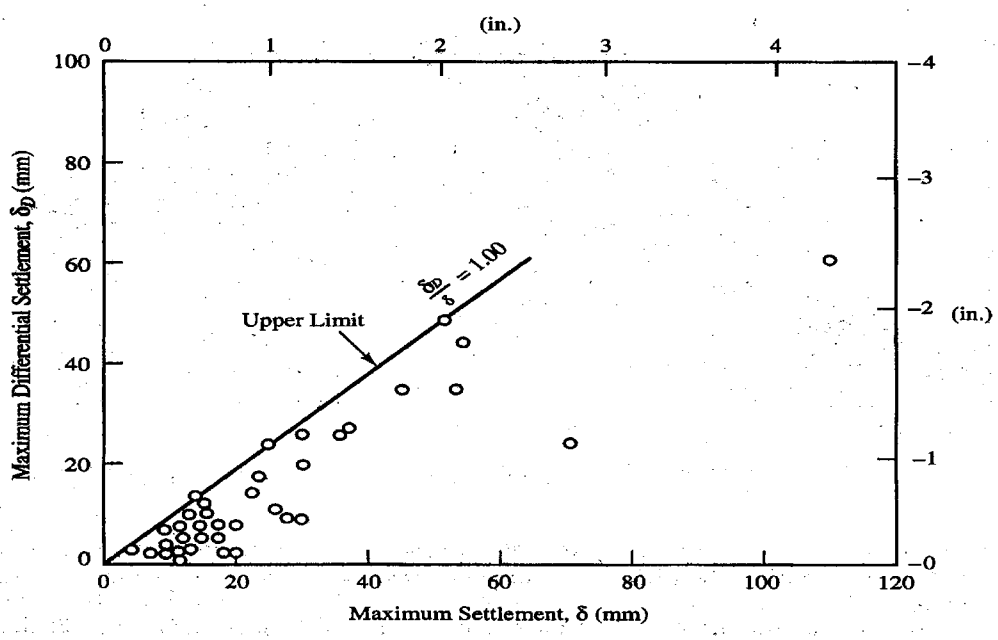

Figure 2-7 Total and differential settlement of spread footings on sands (from Bjerrum, 1963)

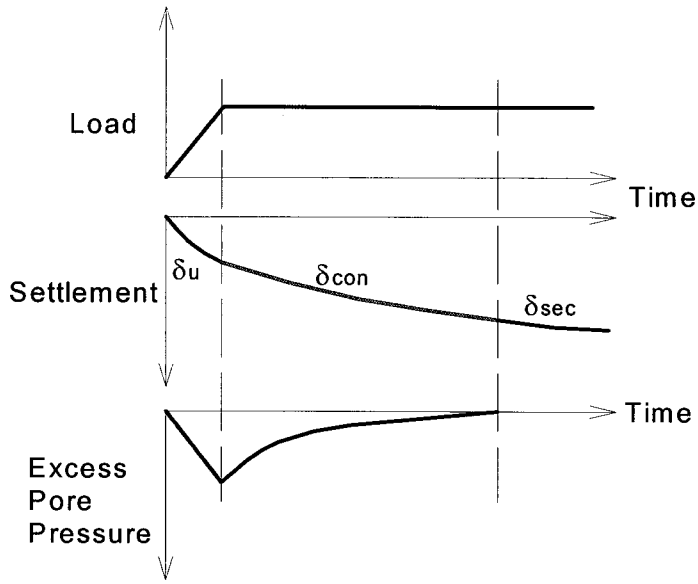

Figure 2-8 Development of settlement with time

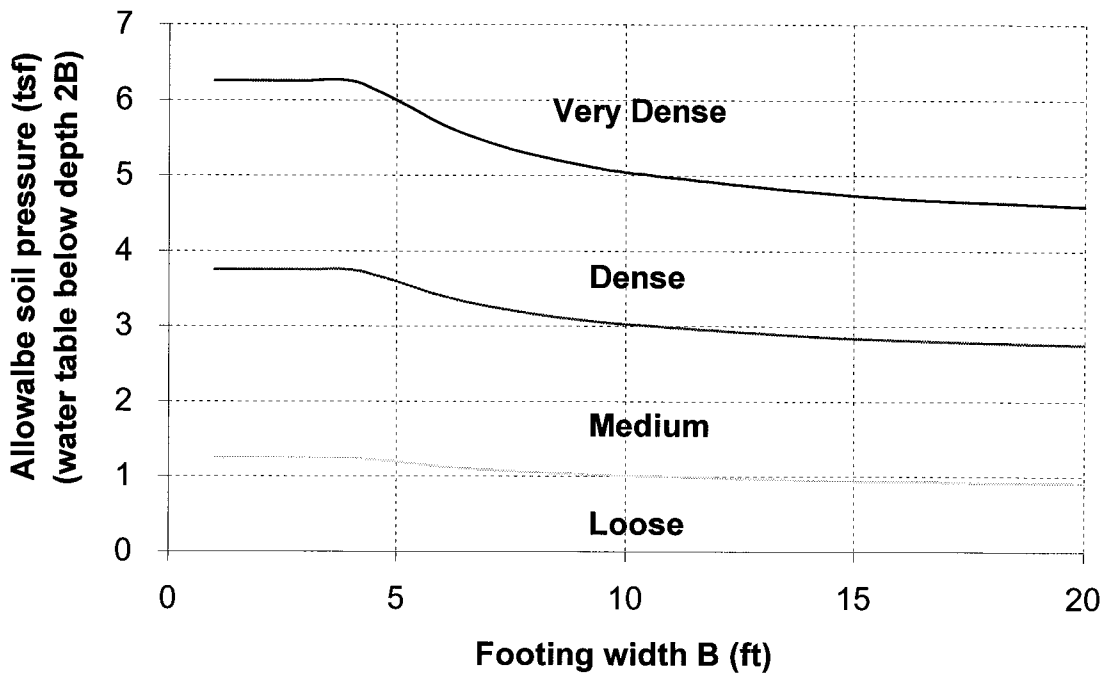

Figure 2-9 Allowable bearing capacity for sand (from Terzaghi and Peck, 1948)

3 REVIEW OF CRANE STABILITY AND TRACK PRESSURE

Mobile cranes make a large proportion in the crane industry due to their mobility. They are widely used for both the industrial plants and the construction of commercial buildings in North America. There are various types of mobile cranes to carry out different tasks. Truck crane, all terrain crane, rough terrain crane and crawler crane are the most widely used mobile cranes. The boom for a mobile crane can be either telescopic or lattice and the crane is usually supported by outriggers, tires or crawlers. Crawler crane with lattice boom usually has a large capacity. This capacity can be ranges from hundreds tonnes to thousand tonnes nowadays.

3.1 Terminology and definitions

A crane that can move freely about the jobsite under its own power without being restricted to a predetermined travel path requiring extensive preparation is called a mobile crane. The crane is called a crawler crane if the rotating superstructure of a mobile crane is mounted on a crawler carrier. The crawler carrier is usually comprised of car body, crawler frame and slewing unit. The drive unit is often mounted on the crawler frame.

To deal with the track pressure of a crawler crane, it is necessary to understand the supporting area of the crane track. Figure 3-1 shows the top view of a crane track and some typical dimension used in track pressure determination.

In Figure 3-1, the track length L_t is the distance between the ends of the crawler. The track width B_t is the overall length of a single track shoe. The track span S is the distance between the centerlines of two crawlers. Since the sprocket is usually raised and therefore does not participate in the transmission of ground pressure, the supporting track length L is usually shorter than the track length L_t and is taken as the distance between the first roller and last roller. Since the track shoe is usually rounded at both ends, the actual supporting track width B is also shorter than the track width B_t. Since only the supporting track length and width

are concerned in dealing the track pressure, for the sake of simplicity, the track length and track width called hereinafter means the supporting track length L and supporting track width B unless it is otherwise stated.

3.2 Stability based load rating of crane

The load rating is the maximum allowable load for a specific radius with the crane with a particular configuration while operating under defined conditions. The load rating of a crane can be limited by:

- Load-hoist rope strength
- Available line pull at the winch
- Structural strength of the boom
- Structural strength of the frame
- Structural strength of mountings
- Stability against overturning

However, with the usage of fine-grained high strength steel, the most important factor controlling load ratings now-days is stability against overturning. Most ratings of mobile cranes are governed by stability. Bulter (1978) studied 176 cases of accidents associated with mobile crane and concluded that more than 71% percent of accidents are overturning. Figure 3-2 and 3-3 illustrate the lift capacity limited by the above-mentioned factors. From these figures it can be seen that with greater load radius (outreach) stability will control since the trend line of stability is much steeper than the others. In most countries, it is accepted that the stability-based load rating is set as a percentage of the tipping load. For crawler crane, this percentage is set to be 75% in the United States and Canada, while it is set to be 66.7% in Europe (Shapiro et al, 1999).

Another approach is to use moments instead of loads as the basis for stability ratings. For cranes with long booms at long radii, the tipping load may be

considerably less than 1% of the machine weight. Under such conditions, the crane is very sensitive to wind load and dynamic effects. However, cranes behave very well with rated load at short radii.

ISO4305:1991(E) (International Organization of Standardization) came up with the combination of these two approaches by the equation:

$$P = \frac{T - 0.1A}{1.25} \tag{3-1}$$

where P = rated load

T = tipping load

A = boom tip weight, boom weight refer to the boom tip

Similar to structural design, the stability of crane is determined from varies load combinations. The major combinations include:

- 1.33 x P
- 1.25 x P + 0.1 x A
- 1.1 x P x ψ + W
- 1.1 x P + A x φ + W

where W = wind load

ψ = hoisting load coefficient on the load

φ = Intrinsic coefficient on boom

The first two combinations are identical to the two approaches in the stability-based load rating. Although the rated crane load is about 25% less than its tipping load, the manufacture's rated load must not be exceeded in any case.

3.3 Track pressure

Most track pressure analyses for crawler cranes are based on the assumption that the crawler frame and car body are absolutely rigid. Knowing the total vertical force and moments acting on the crane, the track pressure can be determined using the principle of equilibrium. Although the rigid assumption works well in general, the calculated track pressure never equal to the actual track pressure. Furthermore, because of the rigidity assumption, both tracks will have a common value for eccentricity. Another problem associated with the rigidity assumption is that it ignores the interaction between crane tracks and the ground.

The essential feature of the track pressure is its eccentricity, which is the major cause of the differential settlement of the ground. The maximum track pressure is frequently generated when the total center of gravity of the crane weight and load are swung out at right angles to the direction of travel by approximately 50-60°.

3.4 Track pressure distribution through mat

The maximum track pressure for larger cranes can be as high as 2Mpa, which is beyond the ground bearing capacity for most soils. In case where the track pressure is high and the ground is not able to sustain such a pressure itself, timber mats are usually used to spread the pressure to a larger area. Figure 3-4 illustrates the track pressure distribution and spreading through mat.

Traditionally, the soil pressure under the mats is assumed to be equally distributed and the lateral spread width B' is governed by the strength of the mat, usually by the longitudinal shear strength of the mat. Assuming the mat is a reverse cantilever beam supported by the crane track in the middle and loaded by a distributed pressure by the ground, the maximum spreading width can be evaluated knowing the shear strength of mat.

But this method is only focused on the strength of mat: if the mat is not overstressed the spreading width is then deemed as the length of the mat.

However, the actual track pressure might not be able to spread over such a large area. The extent of the spreading area is controlled by a lot of factors including the thickness of the mat, the relative stiffness of the mat and soil, the intensity of load etc. The study of this spreading width is very important because it directly affects the magnitude of the design pressure in the ground stability evaluation.

3.5 Crane levelness and maximum tilt angle

The rated load of crane is based on the assumption that the machine is standing on a firm, uniform level supporting surface (up to 1% gradient). This means that the ratings given are appropriate to use only if the tracks are properly supported so that throughout operations the crane will remain level to within ±1%. Some manufactures such as DEMAG specifies the levelness of site preparation should be within ±0.5%. Nevertheless, it is practical to set the ground deformation criterion as ±0.5% or 0.3° throughout the crane operation.

The tilting of the crane track (or the differential settlement of the ground) is different from the tilting of crane body. The crane body and boom are flexible and may deflect considerably under bending moment. Therefore, the tilt angle of the superstructure is much higher than the ground surface. For example, the allowable tilt angle during the operation of a DEMAG CC8800 is ±2°, and the limiting value is ±4°. There is no international standard for the maximum tilt angle a crane can tolerate. It is only specified in Dutch Standard, where the maximum tilt angle at stationary condition is 4.5°. Although allowed by the standards, it should be ensure that none of the support is lifted off the ground with the normal loads in the supported state.

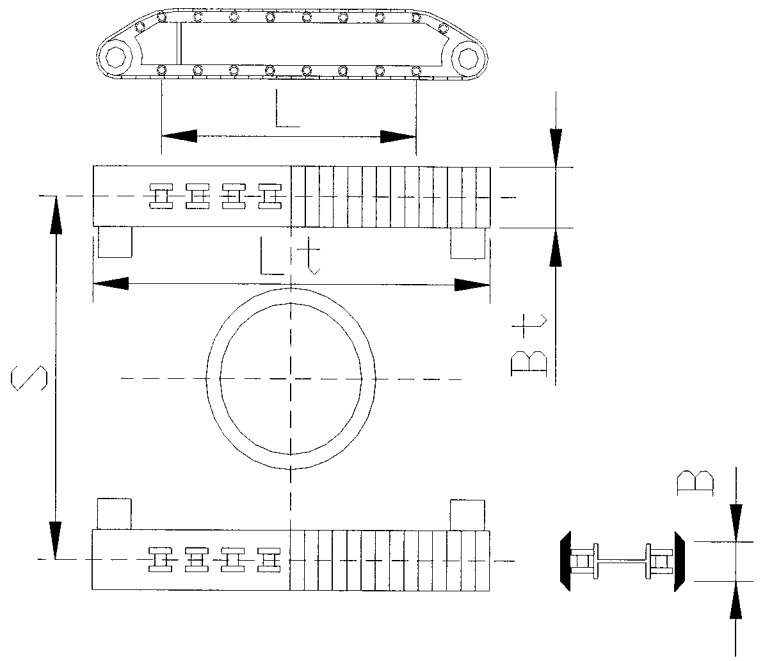

Figure 3-1 Dimensions of supporting area of crane tracks (Modified from Becker 2001)

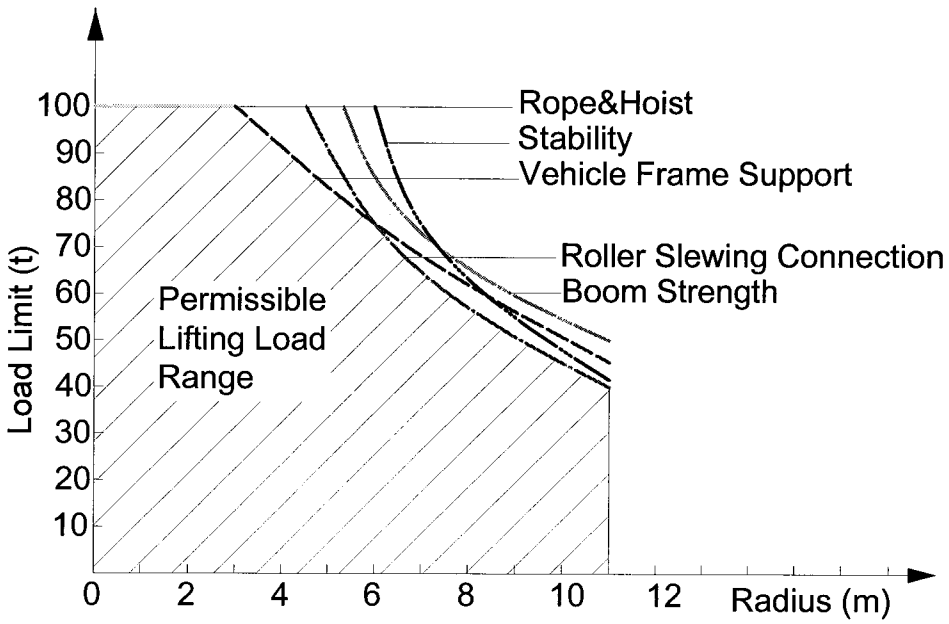

Figure 3-2 Load limits of crane with short boom (Modified from Becker 2001)

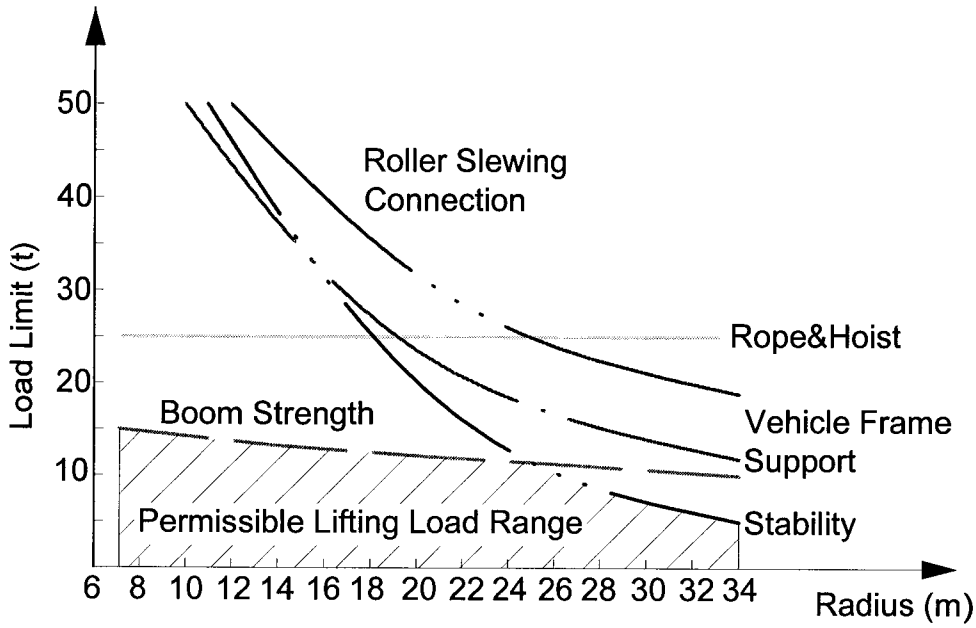

Figure 3-3 Load limits of crane with long boom (Modified from Becker 2001)

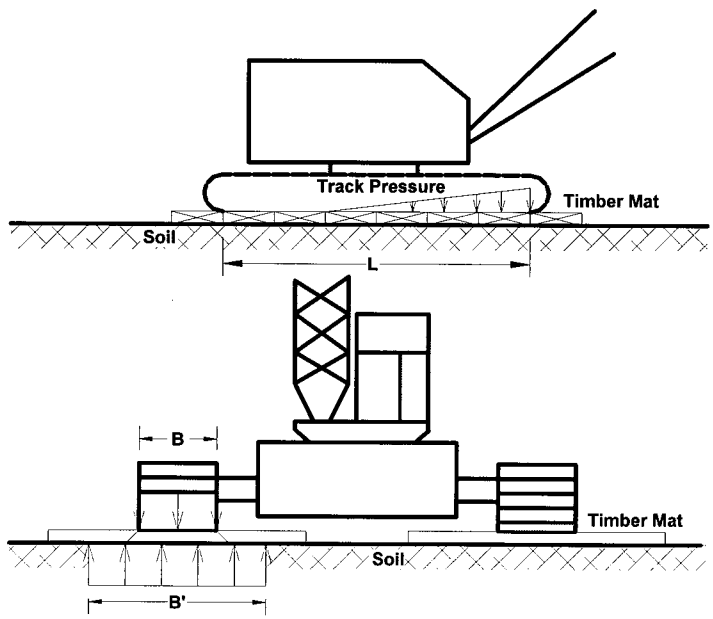

Figure 3-4 Crane track pressure distribution through timber mats (Modified from Shapiro 1999)

4 SIMPLIFICATIONS FOR THE STUDY OF BEARING CAPACITY

Since there are some fundamental features lying between the soil bearing capacity for foundations and for cranes, it is possible to convert the problem of bearing capacity for cranes to the traditional bearing capacity problem for foundations. Three major steps should be taken to achieve this. First, convert the levelness criterion for crane to the maximum allowable settlement. In this way, the bearing capacity for cranes is governed by the maximum settlement during its operation. Second, convert the crane track pressure to an equivalent uniformly distributed pressure. This equivalent pressure should induce the same amount or more settlement than the actual track pressure to ensure that this simplification is on the safe side. Finally, use a proper equivalent footing width. The crane track and mat can be treated as a spread footing. The footing length is usually taken as the track length. However, the equivalent footing width is not that obvious. The determination of the equivalent footing width should be based on both the displacement and the stress aspect of the actual scenario of crane with mats.

Besides those three major simplifications, a series of assumptions are also made to quantify the problem. And the verification of models used in the study of bearing capacity for typical soils and for actual cases is also carried out here.

4.1 Assumptions

4.1.1 Soil is isotropic and homogeneous within each layer

Although soil is neither isotropic nor homogeneous in a natural deposit, it can be assumed to be isotropic and homogeneous within each soil layer without introducing significant errors in the analysis. And it is the most commonly used assumptions on geotechnical analysis.

4.1.2 Linear elastic behavior of soil under crane load

The stress-strain behavior of soil is highly dependent on its mineralogy, stress history, strain level and boundary conditions. If the soil is loaded at low stress level under undrained condition, the deformation of soil is mainly elastic and the

stress-strain relationship can be simplified as a straight line. For a linear elastic material only two elastic parameters the Young's modulus E and the Poisson's ratio v are needed to carry out the analysis.

Since the crane track load is a short-term behavior, fine grained soil is under undrained condition and nearly pure elastic deformation is often developed. Total stress analysis is appropriate in this case to evaluate the undrained bearing capacity and the immediate settlement. Groundwater has an effect on the buoyant unit weight and the undrained Poisson's ratio of the soil.

4.1.3 In-situ stress is only caused by gravity

High horizontal stress tends to increase the bearing capacity. However, in-situ stress can be affected by various factors and the measurement is not easily carried out. The in-situ stress is assumed to be caused only by gravity unless clear evidence shows that the soil is highly over consolidated which usually leads to high horizontal stress.

4.1.4 Crane tracks and mats acting as two spread footings

For sites where timber mat is needed to spread the crane track pressure, the layout of the mat is usually in such a way that each track sits at the center of one row of mats as shown in Figure 3-4. Although the two tracks can sit on only one row of mats for some small cranes, for large cranes with wide track span (say >8m) this configuration is nearly impossible due to the limit length of the timber.

The crane tracks and mats can be treated as two spread footings regardless whether the crane sits on the mats or directly on the ground.

In the case crane sitting directly on the ground, the dimension of the spread footing is the crane track width and crane track length. Since the length of the crane track is usually in the range of 7.2m to 10.5m and the corresponding track width is from 1.2m to 2.0m, the length to width ratio of spread footing L/B falls

into the range of 4 to 6. In this case, the two tracks should behave more like two strip footings (L/B>10).

It is not obvious on how to determine the dimension of the equivalent spread footing when crane mats are used. The width of the footing is limited by the timber length and the strength of the timber. Since the length of mat is usually 6 m and the thickness of is only about 30cm, this means that the footing is quite flexible and the whole timber mat length may not be fully utilized in calculating an equivalent footing size. It is a major topic on how to find an equivalent footing width representing the real case which will be discussed later in this chapter. The length of the footing usually differs from the track length as well since the mats are discontinuous in the direction of the track length. Therefore, the footing length should be taken as the distance between the end of the mats under the first and last rollers. It is generally greater than the track length but the maximum difference will not exceed the width of one piece of mat (usually 1.2m and 1.5m). Since this difference is relative small compared to the track length and can not be easily controlled, it can be ignored in practice and deem the track length as the footing length. A typical length to width ratio L/B for crane with mats is usually within the range of 1.2 to 2.0 and it seldom exceed 2.5 in practice. Therefore, the two tracks with mats behave more like two square footings (L/B=1.0).

4.1.5 The track pressure is equally distributed along the footing width

The actual pressure distribution is dependent on the soil type, the loading level and the rigidity of the footing etc. it is nearly impossible to determine the real pressure distribution for a footing. In practice, the concentrate load is usually assumed to be equally distributed over the entire footing area. This assumption may be applied to crane track pressure in the width direction where the load eccentricity can be ignored for each track.

4.1.6 No interference between two footings

If two footings are close enough, their zones of influence will interact and the failure surface may change from that of the isolate footing and will increase the bearing capacity in general. But this effect is highly dependent on the soil type, footing type and distance between the two footings. The effect is significant for two strip footings on dense sand with a center to center distance of less than three times of footing width, for other cases, especially for two square footings on soils with low friction angle this effect is negligible as pointed out by Vesić. For crane sitting directly on the ground, the distance between the tracks is much greater than the width of the track. Therefore, there is no interference between two tracks. For cranes with mats the track span is only about 1.5 to 1.8 times of footing width, since the two footings are generally square, the effect on bearing capacity can be ignored as well. This simplification is conservative in the determination of ultimate bearing capacity.

On the other hand, the adjacent footing will cause additional stress in the soil therefore induce more settlement than the isolate footing itself theoretically.

Figure 4-1 shows the additional settlement at the center of one footing caused by the adjacent footing varying with the distance of the two footings, the shape of footings and Poisson's ratio of soil. It assumes the two footings have the same dimension with same uniform pressure applied on the footings. The soil is assumed to be homogeneous and the depth to be considered is two times of the footing width. The settlement caused by the adjacent footing is expressed as the percentage of the settlement caused by the footing itself.

It can be found from Figure 4-1 that the influence of adjacent footing on settlement will drop dramatically with the increase of the distance between the footings. A typical range for span to width ratio S/B and length to width ratio L/B for crawler cranes with mats are about 1.5 - 1.8 and 1.2 - 2.0 respectively. If a Poisson's ratio of 0.3 is used for soils, the additional settlement caused by

adjacent footing is only about 2% to 10% comparing to the settlement caused by the footing itself.

4.1.7 Ignore the crane ground interaction

The track pressure calculated from the theory of rigid body equilibrium is based on the assumptions that the crane body is purely rigid, whereas, the actual track pressure distribution depends not only the load and moment applied on the crane but also on the relative rigidity of crane, mats and soils. The term soil structure interaction may apply to this situation as well. The rigidity of the crane track tends to redistribute the pressure along the track and yield a linear settlement; the rigidity of crane body tends to reduce the differential settlement between the tracks and reduce the pressure difference between the tracks. In general, the soil structure interaction tends to reduce the differential settlement and equalize the pressure distribution. But this effect is very complex and only evaluated in very important structural design. For most spread footing design, this effect is not considered either.

4.2 Computer modeling

4.2.1 Software selection

Computer modeling and field observation are the two techniques used in the study of soil bearing capacity for crawler cranes. Most of the works are carried out by computer simulation and the field observation provides a reference for calibrating the parameters used in the models. An adequate program should be able to model the composition of layered soil and timber mat, especially to model the interface between soil and mat. A program called FLAC2D developed by ITASCA CONSULTING GROUP INC. is used in the computer modeling for the reason of availability and applicability. It is a two-dimensional explicit finite difference program that simulates the behavior of soil, rock or other material originally developed for geotechnical engineering and mining. The advantages of this program include:

- More that ten types of soil and rock models are available in the program. Furthermore, it provides the facility to add user-defined constitutive model to it.
- It has interface elements to simulate distinct planes along which slip or separation can occur.
- It dose not require the grid points of one element to match exactly with adjacent elements. This provides the flexibility in the process of gird generation.
- It contains a built-in programming language FISH for users to write their own functions and solve specific problems.

4.2.2 Sections to be modeled

We usually only model the section along footing width direction for building footings since the load eccentricity for the foundation is small and only the maximum settlement is concerned. The limitation of two-dimensional program is that it can not simulate the actual 3-D behavior of the footing. The plane strain configuration used in the program assumes the footing is infinite long in the direction perpendicular to the section it modeled. It works well for strip footings and for those behave like strip footings. Therefore, the simulation on section perpendicular to the tracks will be more appropriate. And the simulation on sections along track length is not so reliable.

But in order to simulate the ground reaction during crane operation, the section along crane track length is more critical because the differential settlement mainly occurs in this direction. So three sections are modeled in the case studies: two along each track and on perpendicular to the tracks. Figure 4-2 shows the sections to be modeled. For general studies, only section perpendicular to crane tracks is used.

4.2.3 Model size verification

Theoretically, the ground settlement will increase with the increase of depth in calculation. In practice, the depth used in settlement calculation is usually chosen to be where the vertical stress induced by net contact pressure is less than 1/10 of the net contact pressure. From Boussinesq's elastic solution on semi-infinite half space, the zone of influence of square footing and strip footing on homogeneous soil is shown in Figure 4-3. The influence depth is about two times of footing width (2B) for square footing and about four times of footing width (4B) for strip footing in homogeneous soil.

The lateral influence zone of a strip footing is about three times of the footing width (3B) from the center of the footing for elastic analysis. At this distance, the induced horizontal stress by the footing is generally less than 1/10 of the applied pressure. In consideration of the bearing failure zone from Prandtl's plastic equilibrium theory, this distance is about the horizontal influence distance caused by a strip footing with a width of B in a homogeneous soil with a friction angle of 20°.

The problem associated with using 2-D program to model a 3-D footing is that it causes a larger zone of influence than the actual footing, especially in modeling the case of crane with mats which is more like a square footing (L/B=1.2~2.0) than a strip footing. Theoretically, the settlement at the center of a strip footing (L/B>10) is about two times of the settlement at the center of a square footing with the same width from elastic solution. To account for this effect, an adequate model depth should be applied in the simulation.

Two cases need to be considered in choosing the proper model depth for section perpendicular to the crane tracks: crane with mat and crane sitting directly on the ground. The model depth can be chosen to be 4B for crane sitting on the ground without mat since the two tracks behave more like a strip footing. For the case that the crane is sitting on the mats, a depth of 2B may be appropriate. To

evaluating the errors caused by using 2-D program with limit depth (2B) to simulate the settlement of a rectangular or square footing, a theoretical comparison based on the elastic equation (Equation 4-1) for a footing on finite soil depth is used.

$$\delta = qB\frac{1-\nu^2}{E}(F_1 + \frac{1-2\nu}{1-\nu}F_2)$$

$$F_1 = \frac{1}{\pi}\left[m\ln\frac{\left(1+\sqrt{m^2+1}\right)\sqrt{m^2+n^2}}{m\left(1+\sqrt{m^2+n^2+1}\right)} + \ln\frac{\left(m+\sqrt{m^2+1}\right)\sqrt{1+n^2}}{m+\sqrt{m^2+n^2+1}}\right] \qquad (4\text{-}1)$$

$$F_2 = \frac{n}{2\pi}\tan^{-1}\left(\frac{m}{n\sqrt{m^2+n^2+1}}\right)$$

where $m = \frac{L}{B}$, $n = \frac{H}{B}$

δ = settlement at corner of a footing

E, v = elastic properties of soil

q = vertical distributed load

L, B = footing length and width

H = depth used in calculation

Figure 4-4 shows the errors in settlement calculation using a model depth of 2B to simulate section perpendicular to the crane tracks from their theoretical solution. This error ranges from -16% to +8% with L/B from 1.0 to 2.0. It also shows that the use of 2B model depth will result in more settlement at high Poisson's ratio while less settlement at low Poisson's ratio. And the increase of L/B generally leads to the decrease in error. For most soils, the Poisson's ratio ranges from 0.15 to 0.5, the maximum difference of settlement between square footing and strip footing is within ±10%.

There should be more error in settlement using 2-D program to model section along two tracks. Figure 4-5 illustrates the errors in settlement calculation using a model depth of 2B to simulate sections along crane tracks from their theoretical solution. It should be pointed out here that the footing in the simulation has a width of L, the track length of the crane rather than the actual footing width B. This error ranges from +16% to -23% with the L/B from 1.0 to 2.0. It also shows that the use of 2B model depth tends to overestimate the settlement with low Poisson's ratio while underestimate it with high Poisson's ratio. And the increase of L/B generally leads to the increase in error. At Poisson's ratio from 0.3~0.4, this error falls within ±5% and can be negligible.

However, since soil is not homogeneous, this effect can not be easily evaluated. In general, modeling section along both tracks is not as accurate as modeling section perpendicular to the tracks.

In general, using 2-D model to simulate the settlement of a crane with mat should be appropriate by using a model depth of 2B. For cranes sitting on the ground without mat, the model depth is chosen to be 4B.

The model width has less influence on the settlement study unless it is too small, a distance of 3B from the center of the footing to both side walls is used for both cases where crane sitting on mats or not.

4.3 Convert the levelness criterion to allowable settlement

Similar to foundations of buildings, there are two criteria controlled the determination of soil bearing capacity for cranes during its operation: the ground should be strong enough to sustain the load applied and the tilting of the crane base should be within the 0.5% limit as stated in Chapter 3. It is reasonable to use a similar approach in calculating the allowable soil bearing capacity for cranes as that for foundations since there are so many similarities exists. In traditional bearing capacity calculation, the allowable total settlement is usually used to control the differential settlement. Based on the same logic, it is possible

to convert the levelness criterion of crane to a maximum settlement criterion as well.

It is well understood that the tilting of the crane is not only in one direction but it is a two-dimensional problem. The degree of tilting may vary while the superstructure of a crane slewing around without changing the load and radius. It is not practical to calculate the soil bearing capacity by evaluating the tilting of crane at various boom orientation angles. As a result, only the maximum tilting angle is used in bearing capacity analysis.

The maximum tilting angle usually occurs at three critical boom orientations as shown in Figure 4-2:

- The boom is perpendicular to the crane tracks, where tilting only in the direction perpendicular to the crane tracks occurs.
- The boom is parallel to the crane tracks, where tilting only in the direction parallel to the crane tracks occurs.
- The boom over one corner of the tracks where maximum track pressure usually occurs. In this case, tilting in both directions occurs.

The key factor to convert the tilting criterion to maximum allowable settlement criterion is to find a representative tilting angle not less than the actual maximum tilting angle. This representative tilting angle can be expressed as a function of maximum settlement so that a correlation between maximum allowable settlement and maximum allowable out of levelness is built.

The representative titling angle is found by observing and estimating and then testified by theoretical analysis. Consider a typical crane operation shown in Figure 4-6. Assume the total gravity of crane and load is G, the center of gravity is at a radius R from the crane rotation center and at an angle of α off the centerline perpendicular to crane tracks. The crane track has a dimension of B x L with a span of S between two tracks. For most cranes, the maximum pressure

occurs at an angle of α=50°~60°, and the track span S is often equal or a little bit greater than the track length L. Since the tilting angle is usually very small, it can be expressed as the differential settlement over the distance between two points.

Using the principle of equilibrium, the load at each track is:

$$\frac{P_1}{P_2} = \frac{G(S/2 \pm R\cos\alpha)}{S} \tag{4-2}$$

By introducing the factor t=2R/S, which represents the degree of eccentricity of the load, the above equations can be rewrite as:

$$\frac{P_1}{P_2} = \frac{1 \pm t\cos\alpha}{2} G \tag{4-3}$$

The pressure difference between two tracks is:

$$\Delta p = \frac{P_1 - P_2}{LB} = \frac{Gt\cos\alpha}{LB} \tag{4-4}$$

Assuming the crane track is rigid and the pressure is equally distributed in the track width direction, the differential settlement caused by the pressure difference from Equation 2-20 is:

$$\delta_d = \frac{\left(1-\nu^2\right)\Delta pB}{E} I_W = \frac{\left(1-\nu^2\right)Gt\cos\alpha}{E \cdot L} I_W \tag{4-5}$$

where I_w = influence factor for settlement of rigid footing

Therefore, the tilting angle when the boom is perpendicular to crane tracks (α=0°) is:

$$\theta_n \approx \tan\theta_n = \frac{\delta_d}{S} = \frac{\left(1-\nu^2\right)Gt\cos\alpha}{E \cdot L \cdot S} I_W \approx \frac{\left(1-\nu^2\right)Gt}{E \cdot L^2} I_W \tag{4-6}$$

Similarly, from Equation 2-21 the tilting angle when the boom is parallel to crane tracks (α=90°) is:

$$\theta_l = \tan\theta_l = \frac{P_1 e}{L^2 B}\frac{\left(1-\nu^2\right)}{E} I_m \approx \frac{\left(1-\nu^2\right)Gt}{4E \cdot L \cdot B} I_m \qquad (4\text{-}7)$$

where I_m = influence factor for rotation of rigid footing

e = load eccentricity in track length direction

The tilting angle when the boom is over one corner of the tracks (α=50°~60°) is:

$$\theta_\alpha = \tan\theta_\alpha \approx \frac{\sqrt{2}}{2}\frac{\left(1-\nu^2\right)G}{EL^2}\left[\left(t\cos\alpha\right)I_W + \frac{L \cdot t(1+t\cos\alpha)\sin\alpha}{4B} I_m\right] \qquad (4\text{-}8)$$

where α=50°~60°

Now define the representative tilting angle as the maximum settlement over the length of crane track L, which is:

$$\theta_{rep} = \tan\theta_{rep} = \frac{\delta_{\max}}{L} = \frac{\left(1-\nu^2\right)G(1+t\cos\alpha)}{2E \cdot L^2}\left(I_W + \frac{Lt\sin\alpha}{4B} I_m\right) \qquad (4\text{-}9)$$

where α=50°~60°

To testify whether this representative tilting angle is greater than or equal to those three angles at different boom locations, it is convenient to use ratios of those three angles to the representative angle to eliminate some common variables. These ratios are then simplified as:

$$r_n = \frac{\theta_n}{\theta_{rep}} = \frac{8t \cdot l_w}{(1+t\cos\alpha)(4l_w + m \cdot t \sin\alpha l_m)}$$
$$r_l = \frac{\theta_l}{\theta_{rep}} = \frac{2m \cdot t \cdot l_m}{(1+t\cos\alpha)(4l_w + m \cdot t \sin\alpha l_m)} \qquad (4\text{-}10)$$
$$r_\alpha = \frac{\theta_\alpha}{\theta_{rep}} = \frac{\sqrt{2}\left[4t\cos\alpha l_w + (1+t\cos\alpha)m \cdot t \sin\alpha l_m\right]}{(1+t\cos\alpha)(4l_w + m \cdot t \sin\alpha l_m)}$$

where α=50°~60°

If these three ratios are less than 1, the representative tilting angle is proven to be valid and the maximum settlement from Equation 4-9 can be used as the allowable settlement of the crane track during its operation.

Figure 4-7 shows the variation of these three ratios r_n, r_l and r_α with the length to width ratio L/B of the footing and the degree of load eccentricity t=2R/S.

Since the rated load of crane is based on one criterion that requires at least a factor of 1.33 against overturning, the load eccentricity t is rarely greater than 0.75 during normal crane operation, especially for heavy lift cranes which usually has a superlift counterweight that moves the center of gravity further away from its tipping axis.

The L/B ratio for crane with mats is usually between 1.2 and 2.0 and rarely over 2.5. Within this range, these three ratios are all less than 1 and the using of representative tilting angle is valid.

Since the allowable out of levelness (tilting) for cranes is 0.5%, the corresponding allowable settlement for crane with mats from Equation 4-9 is:

$$\delta_{\max} = \theta_{rep} \cdot L \le 0.5\% \cdot L = \frac{L}{200} = [\delta] \qquad (4\text{-}11)$$

where [δ] = allowable maximum settlement of crane during operation

For cranes sitting directly on the ground, the L/B ratio is generally between 4 and 6, another factor of 1.2 should be applied to the representative tilting angle to ensure it is no less than those three tilting angles. As a result, the allowable settlement for crane without mats is modified from Equation 4-11 as:

$$\delta_{\max} = \frac{\theta_{rep}}{1.2} \cdot L \leq \frac{0.5\%}{1.2} \cdot L = \frac{L}{240} = [\delta] \tag{4-12}$$

4.4 The concept of equivalent pressure

Unlike building foundations, the track pressure of a crane changes greatly during its operation. Even though the load and radius might be constant, the track pressure will change while the boom slewing around.

Another important feature of the crane track pressure is that the pressure is barely uniformly distributed along the track length due to the eccentricity of crane load. The most common track pressure shape under each track is either triangular or trapezoidal and the maximum pressure is usually used as the design pressure in the evaluation of soil bearing capacity. This maximum pressure usually occurs when the crane boom is over the corner of the crane tracks.

The use of maximum track pressure to represent the triangular or trapezoidal distributed pressure seems to be conservative. To find a design pressure that can better represent this pressure distribution lead to the concept of equivalent pressure. The equivalent pressure is a uniformly distributed pressure along the whole track length that will cause same amount of settlement at the point where the maximum pressure taking place. Since the crane tracks can be treated as a rigid footing, the settlement profile along the crane track is close to a straight line, the settlement under the maximum pressure can be considered as the maximum settlement. Therefore, the definition of equivalent pressure ensures it resulting in settlement not less than the actual maximum settlement.

4.4.1 Theoretical analysis

The equivalent pressure is first derived from theoretical analysis based on elastic assumption and then verified by computer simulation. Consider a rectangular footing with a dimension B x L sitting on an elastic semi-infinite half space as shown in Figure 4-8.

A linearly varying pressure q_1 to q_2 is applied in the track length direction and the pressure is uniform in track width direction. Using the theory of superposition, the actual load condition can be comprised of a uniform pressure $(q_1+q_2)/2$ and an antisymmetric pressure $(q_1-q_2)/2$.

From Equation 2-20, the settlement at point M and N in Figure 4-8 caused by the uniform load is:

$$\delta_I = \frac{(q_1+q_2)}{2}\frac{\left(1-\nu^2\right)B}{E}I_w \tag{4-13}$$

The rotation of footing caused by antisymmetric pressure from Equation 2-21 is:

$$\tan\theta = \frac{M}{L^2B}\frac{\left(1-\nu^2\right)}{E}I_m = \frac{(q_1-q_2)}{12}\frac{\left(1-\nu^2\right)}{E}I_m \tag{4-14}$$

Therefore, the total settlement at point M and N are:

$$\begin{matrix}\delta_M \\ \delta_N\end{matrix} = \delta_I \pm \frac{L}{2}\tan\theta = \frac{\left(1-\nu^2\right)}{E}\left[\frac{(q_1+q_2)B}{2}I_w \pm \frac{(q_1-q_2)L}{24}I_m\right] \tag{4-15}$$

Now, assume an equivalent uniformly distributed pressure $\tilde{q}$ will cause same amount of settlement at point M, the settlement can be expressed in the form of $\tilde{q}$ as:

$$\delta_M = \tilde{q}\frac{\left(1-\nu^2\right)B}{E}I_w \tag{4-16}$$

Substitute Equation 4-16 into Equation 4-15, the equivalent pressure $\tilde{q}$ is:

$$\tilde{q} = \frac{(q_1+q_2)}{2} + k\frac{(q_1-q_2)}{2}$$
$$k = \frac{I_m \cdot L}{12 I_w \cdot B} \tag{4-17}$$

Table 4-1 listed the variation of factor k with the footing length to width ratio L/B. The influence factor I_m and I_w used are from Bowles (1982).

Table 4-1 Correlation of factor k with footing L/B ratio

L/B	I_w	I_m	k
1	0.82	3.70	0.38
1.5	1.06	4.12	0.49
2	1.20	4.38	0.61
5	1.70	4.82	1.18

A plot of k as a function of L/B is also made to find an empirical correlation in Figure 4-9. It demonstrates a fairly good linear correlation between k and the ratio L/B with a regression coefficient R^2 = 0.9956. The ratio L/B for crane with mats is from 1.2 to 2.0. Within this range, the maximum factor k is about 0.7. In another word, the maximum equivalent pressure for crane with mats is:

$$\tilde{q} = \frac{q_1+q_2}{2} + 0.7\frac{q_1-q_2}{2} = 0.85q_1 + 0.15q_2 \tag{4-18}$$

For cranes sitting directly on the ground, the L/B ratio is generally greater than 4, the equivalent pressure is not valid and the maximum pressure should be used in the design.

4.4.2 Strength check for eccentricity

Since the crane track load is eccentric in nature, the allowable bearing capacity should also be checked using the equivalent bearing pressure introduced by Meyerhof (Equation 2-15):

$$q_{eqv} = \frac{P}{B'L'} = \frac{(q_1 + q_2)BL}{2(L - 2e_L)B} = \frac{3(1+s)^2}{4(1+2s)} q_1 \qquad (4\text{-}19)$$

where q_{eqv} = equivalent pressure from Meyerhof

$s = q_2/q_1$ $(0 \le s \le 1)$

It is easy to prove that the equivalent pressure proposed in Equation 4-18 for crane with mats is always larger than that from Meyerhof's for building foundations. That means that the proposed equivalent track pressure provides a higher factor of safety against bearing capacity failure due to load eccentricity.

4.4.3 Verification from computer simulation

Computer models were built to test the validation of the equivalent pressure. The footing used in the model is assumed to have a width of B=6m and length L. The size of the model is chosen to be Width x Depth = 6L x 2B which has demonstrated previously to be appropriate. The rigid crane track is simulated by a 1.5m high rigid block sitting on the soil. The Young's modulus of the block is reduced to 1/15 of steel's modulus to account for the ratio of its actual width to footing width. The soil is assumed to be elastic with modulus of elasticity of 50MPa since yielding and failure is not taken into account. The maximum pressure q_1 applied on the track is assumed to be 200kPa for general study. However, only the stress ratio q_2/q_1, L/B ratio, and the Poisson's ratio v have influence on the final result. The typical configuration of the model and the settlement contour is shown in Figure 4-10. The figure shows a typical finite difference mesh using FLAC program, non-uniform pressure is applied on the

footing directly. The soil in the foundation is discretized using 60 grids horizontally and 20 grid points vertically.

The model was run with the variation of the stress ratio, the shape factor and the Poisson's ratio. The ratio of settlement due to actual pressure q_1, q_2 to settlement due to equivalent pressure $\tilde{q}$ is used to evaluate the validation of the equivalent pressure.

Figure 4-11 illustrates the ratio of actual settlement to the settlement caused by equivalent pressure varies with stress ratio q_2/q_1, L/B ratio and Poisson's ratio v. In general, this ratio is less than 100%, which means the use of equivalent pressure is safe. However, the actual pressure tends to yield larger settlement (4%) than the equivalent pressure with high Poisson's ratio ($v \rightarrow 0.5$), low stress ratio ($q_2/q_1 \rightarrow 0$) and large L/B ratio (L/B = 2.5) from the simulation. This can be due to:

- The defect of 2-D simulation

  2-D plain strain analysis assumes the model is infinite in the direction perpendicular to the plane. Problem can be simplified to be plane strain if the ratio of the footing length to its width is greater than 10. In the above simulation, the width of model is L and the length of model is B, the ratio of footing length to its width is B/L which is generally less than 1, with the increase of L/B, the actual model differs more from plain strain condition, the result becomes less reliable.

- The shallow model depth for large L/B ratio

  The model depth of 2B is proven to be suitable to yield similar amount of settlement to the actual square footing. With the increase of L/B ratio, the actual influence depth of the footing becomes greater and the fixed model depth tends to underestimate the settlement due to uniformly distributed

pressure. While the settlement due to triangular pressure depends greatly on the shear deformation rather than the model depth.

- The change of relative rigidity between crane track and soil

With the increase of Poisson's ratio, the bulk modulus of soil increases and the relative rigidity between crane track and soil decreases, the crane track acts more like a flexible footing than rigid footing in the computer simulation. However, the actual footing is 3-D and the soil can be expelled around the footing in both directions. Therefore the actual relative rigidity between crane track and soil is greater than that appears in the model.

Due to the above-mentioned reasons, it can be concluded that the equivalent pressure is verified to be valid from computer simulation.

4.5 Track pressure distribution in the lateral direction

The traditional way to determine the track pressure distribution along mat length is based on the shear strength of timber mat.

Consider the crane track with width B sitting on timber mat and thickness d as shown in Figure 4-12. The track pressure q is equally applied over the track width. By assuming the pressure under mat is uniformly distributed over a wider range, the cantilever length a can be determined by the strength of mat:

$$qB = q_1(2a + 2d + B)$$
$$\frac{3q_1 \cdot a}{2d} \le [f_V] \qquad (4\text{-}20)$$
$$\frac{3q_1 \cdot a^2}{d^2} \le [f_b]$$

where q_1 = distributed pressure under timber mat

$[f_v]$ = allowable shear strength parallel to grain of timber mat

$[f_b]$ = allowable modulus of rupture of timber mat

Since the modulus of rupture of timber is usually one order of magnitude higher than shear strength, the length a is usually governed by the shear strength of the mat.

$$a \le \left[\frac{2B + 4d}{3qB/[f_V] - 4d} \right] \cdot d \tag{4-21}$$

The lateral spread width is:

$$B' = B + 2a + 2d = \left[\frac{3qB + 6qd}{3qB - 4d[f_V]} \right] \cdot B \le L_m \tag{4-22}$$

where B' = spread width of track pressure

L_m = length of timber mat

However, the lateral track pressure spreading is not only limited by the strength of mat, but a function of the following factors:

- The soil type
- The elastic properties of soil (E, v)
- The strength of soil (c, φ)
- The elastic properties of mat (E, v)
- The strength of mat (f_v, f_b)
- The thickness of mat (d)
- The length of mat (L_m)
- The track width (B)
- The stress level (q)

The spread pressure calculated from Equation 4-22 might be very different from the actual pressure distribution. And since the allowable shear strength of the mat [f_v] is only about 1/10 of its ultimate shear strength (in another word, an overall factor of safety of about 10 is used), the calculated pressure is usually higher than the actual value.

To adequately estimate the spreading area is of great importance since it will provide two major parameters in footing design: the bearing pressure and the appropriate footing width. Computer simulation was used to find the correlation between the factors listed above and the lateral spreading width of track pressure.

Two sets of computer models were analyzed with the variation of soil type, elastic parameter of soil (E and v), type of mat, track width B, thickness of mat d and stress level q. Variables used in the simulation is listed in Table 4-2.

Table 4-2 Parameters used in modeling lateral spread width

	Clay and glacial till	Sand and Gravel
Young's modulus E (MPa)	10, 20, 50, 100, 200, 500	10, 20, 50, 100, 150, 200
Poisson's ratio v	0.3 (0.1, 0.45)	0.25
Mat thickness d (m)	0.2, 0.3, 0.4, 0.5, 0.6	0.2, 0.3, 0.4, 0.5, 0.6
Track width B (m)	1.0, 1.5, 2.0	1
The mat length L_m (m)	6 (9)	6
Mat type	Fir, Mora	Fir, Mora

The first set of model is constructed as the real world with crane track sitting on timber mats lying on homogeneous ground. Interference between two tracks is ignored and only half of the track is modeled for reason of symmetry. Figure 4-13 shows the typical configuration of the model. The model was then loaded to 10, 20, ... and 50mm deformation at the center of track. Stress and displacement at the ground surface as well as the track pressure were recorded for each stages of loading. Only stages with 30mm to 50mm settlement are concerned since it was shown previously that the allowable maximum settlement for most cranes is within this range.

Another set of model was then built without mat as illustrated in Figure 4-14. The ground is loaded by a uniformly distributed load, the width and intensity of load is adjusted by trial and error to induce similar stress and displacement and at the ground surface as the first model. In this way, the width of the load can be treated as the adequate spread width of the track pressure since it will cause similar amount and shape of stress and settlement.

Figure 4-15 shows the stress and settlement profile for a typical case where a 1m wide crane track is sitting on 6m long, 0.3m thick fir mats. The soil used in the model is hard clay with a property of E=50Mpa and v=0.3. The solid lines in the figure represent the results from the first set of models to cause a settlement of 30mm, 40mm and 50mm respectively. The dotted lines represent the results from the second set models by assuming the pressures from the first set models are equally distributed over a certain width. If both the stress and settlement profiles from the second set models are close to those from the first set models, the width is found to be appropriate to represent the lateral spread width. For this particular case, the spread width is B' = 4.0m.

From the results of simulation, it can be found that soil type, mat length, and Poisson's ratio have less impact on the lateral spread width. The major factors are the track width, Young's Modulus of mat and soil and the thickness of mat d. Figure 4-16 to Figure 4-19 show the plot of the lateral spread width versus the track width, the thickness of mat and the ratio of Young's modulus of mat and soil. From that, a regression expression is derived as:

$$B' = B + 2d \cdot \left(\frac{E_m}{E_s} \right)^{0.29} \leq L_m \qquad (4\text{-}23)$$

where B' = lateral spread width of track pressure

B = track width

d= thickness of timber mat

E_m = Young's modulus of mat

$E_m \approx 11$Gpa for Douglas fir

$E_m \approx 20$Gpa for Mora

E_s = Young's modulus of soil

L_m = length of timber mat

The calculated lateral spread widths using Equation 4-23 were also presented in Figure 4-16 to 4-19 for the convenience of comparison with those from computer simulations.

Results from computer models also show that the soil strength has little influence on the spreading width unless the soil fails. This can usually be avoided by using a factor of safety no less than 2.0 in practice.

The Young's moduli of typical soils are listed in Table 4-3. Laboratory or field test may be required to obtain more representative values of Young's modulus for a particular site.

Table 4-3 Typical range of Young's modulus and Poisson's ratio of soils (adapted from Bowles 1982)

Type of Soil		E (Mpa)	Poisson's ratio v
Clay	Very soft	2 – 15	0.1 - 0.3
	Soft	5 – 25	
	Medium	15 – 50	
	Hard	50 – 100	
	Sandy	25 - 250	0.2 - 0.3
Glacial Till	Loose	10 - 153	--
	Dense	144 - 720	
	Very Dense	478 - 1440	
Sand	Silty	7 – 21	0.15 for coarse-grained 0.25 for fine-grained
	Loose	10 – 24	
	Dense	48 – 81	0.2 - 0.4
Sand and Gravel	Loose	48 - 144	--
	Dense	96 - 192	

It should be pointed out that although there is no track pressure component in Equation 4-23, the lateral spread width is a function of the stress level, and the equation is based on the range of track pressure to cause 30-50mm settlement.

Equation 4-23 should incorporate the equations from strength of the mat to ensure that the mat is not overstressed. Then the complete expression for lateral spread width of crane track pressure based on 30-50mm settlement is:

$$B' = B + 2d \cdot \left(\frac{E_m}{E_s}\right)^{0.29} \leq \left[\frac{3qB + 6qd}{3qB - 4d[f_v]}\right] \cdot B \leq L_m \qquad (4\text{-}24)$$

Since the mat is usually formed by binding 4 or 5 pieces of 30cmx30cm timbers together, the track pressure on the mat should be the average pressure over one piece of mat. Comparisons have been done for some real cases between this average pressure and equivalent pressure, the average pressure is close to the equivalent pressure and the maximum difference is about 11%. Therefore, using equivalent pressure in Equation 4-24 seems to be adequate since it will eliminate some underestimation of the lateral spread width due to the low allowable shear strength used for mat and will not cause large error.

It should be pointed out that the allowable shear strength of mat $[f_v]$ is only about 1/10 of the strength measured. Therefore, the calculated spread width can be less than its actual spread width in some cases when the strength of the mat controls. A detailed study on the shear strength and other properties of mat is attached in Appendix A.

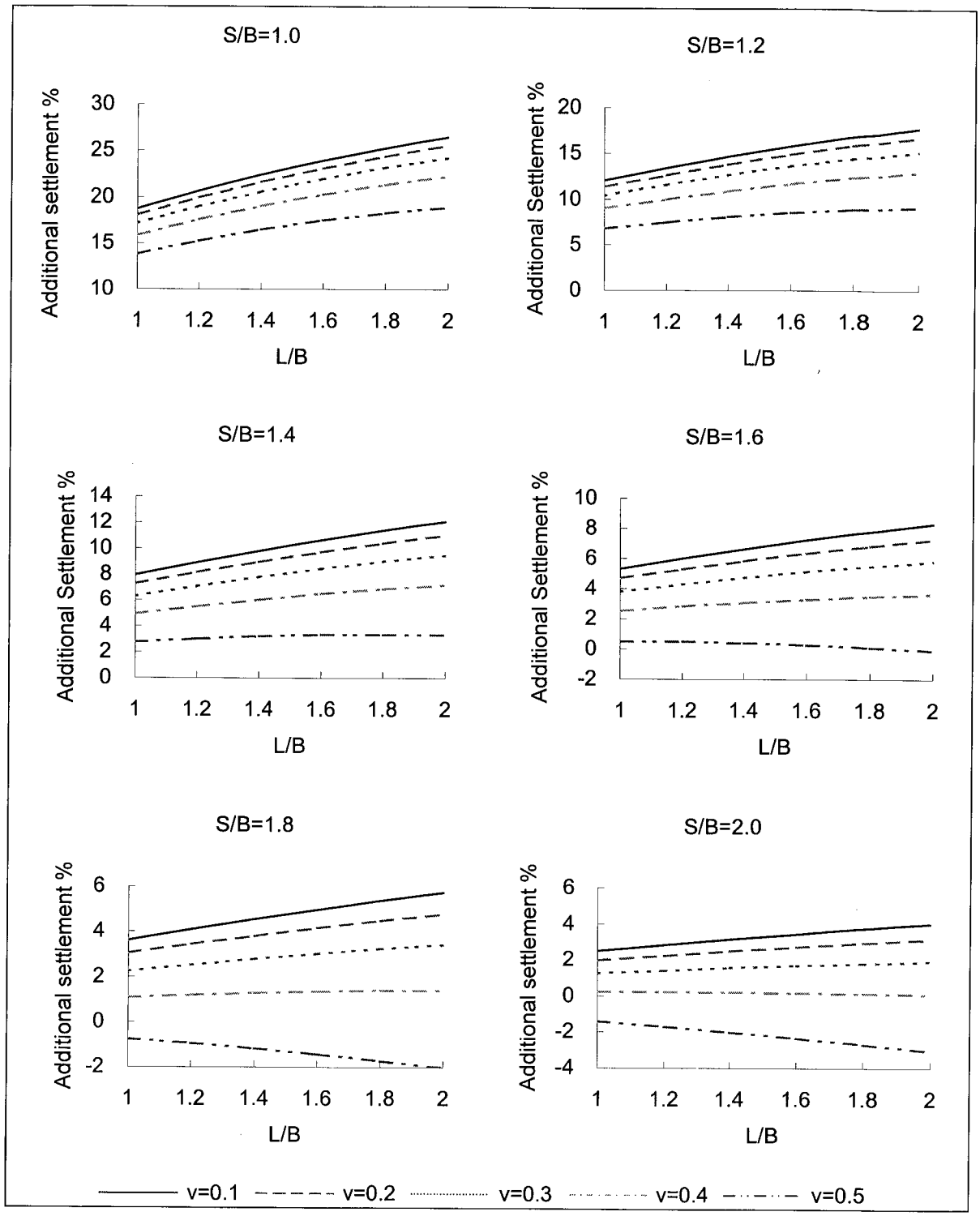

Figure 4-1 Additional settlement caused by adjacent footing

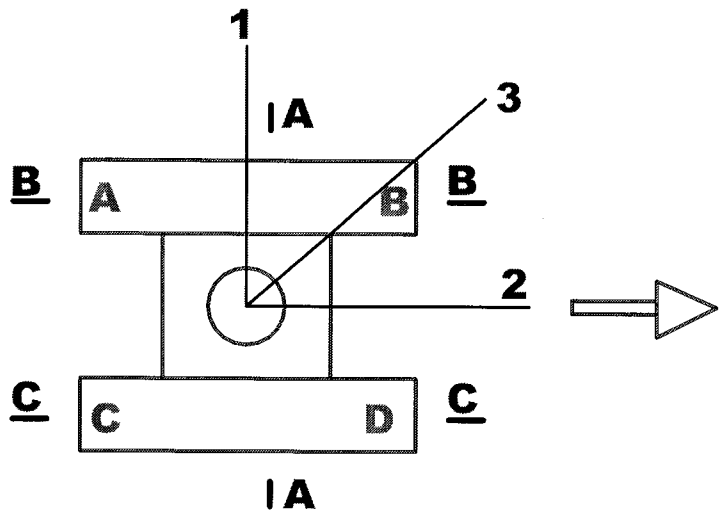

Figure 4-2 Sections to be modeled and critical boom orientations

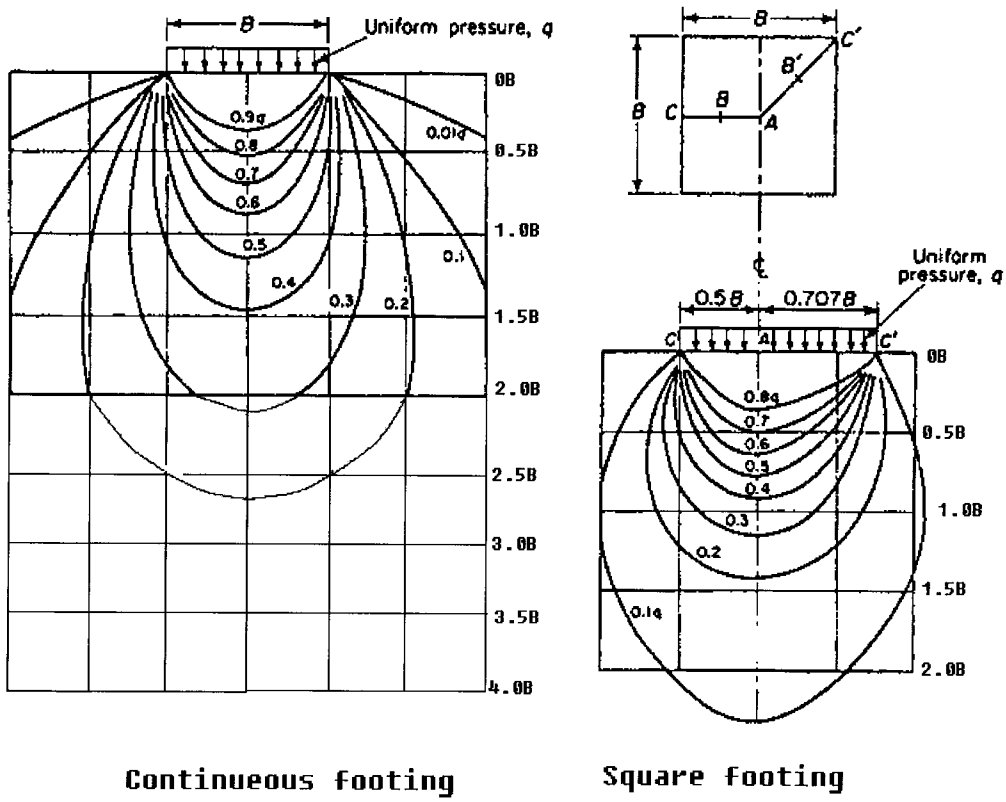

Figure 4-3 Vertical stress in soil under square footing and strip footing

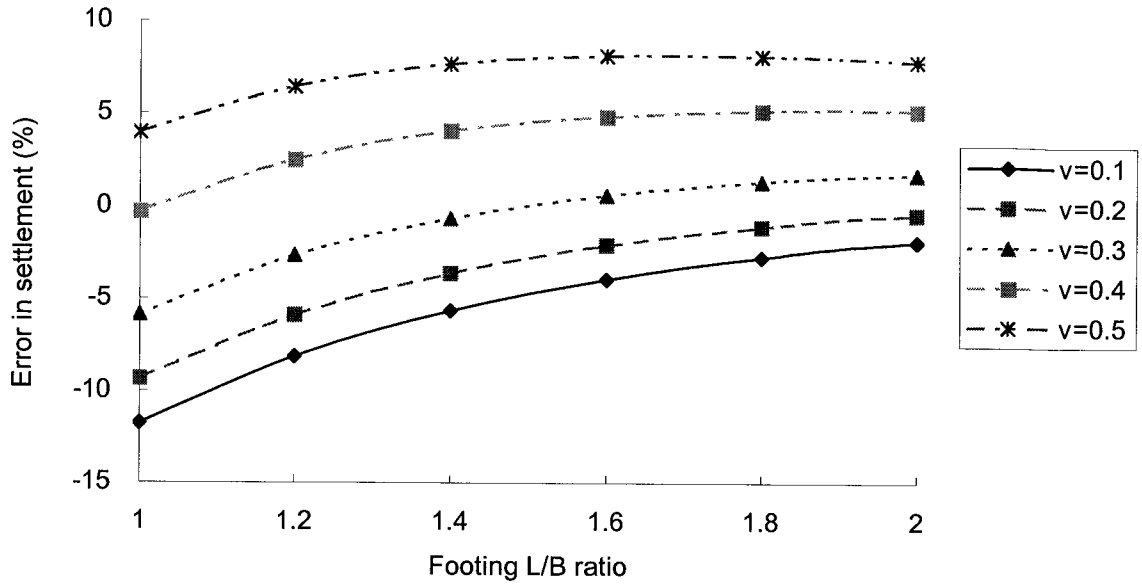

Figure 4-4 Errors in settlement using model depth of 2B to simulate the section perpendicular to crane tracks

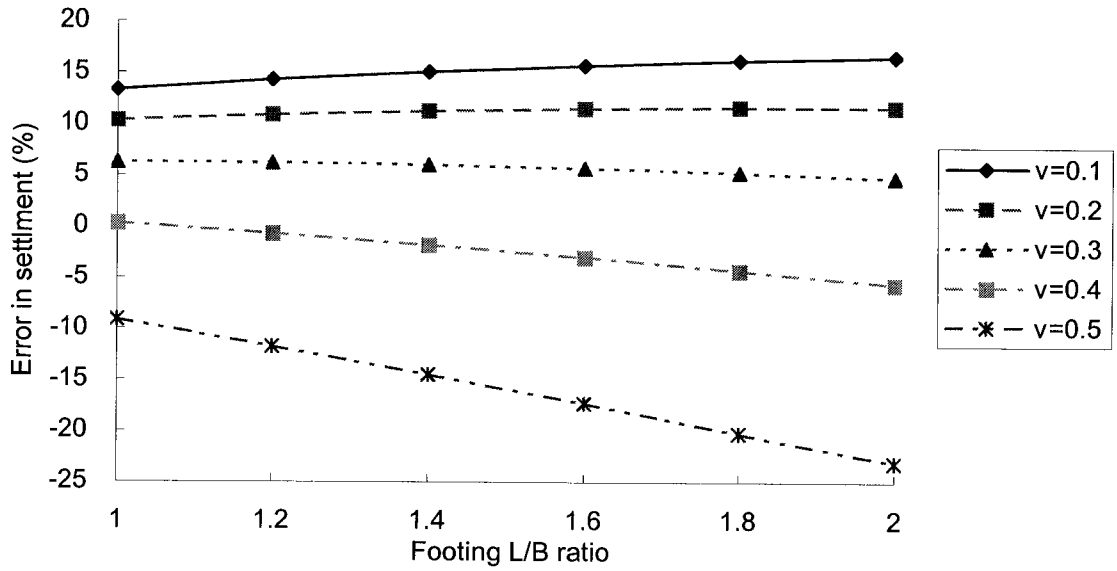

Figure 4-5 Errors in Settlement using model depth of 2B to simulate sections along crane tracks

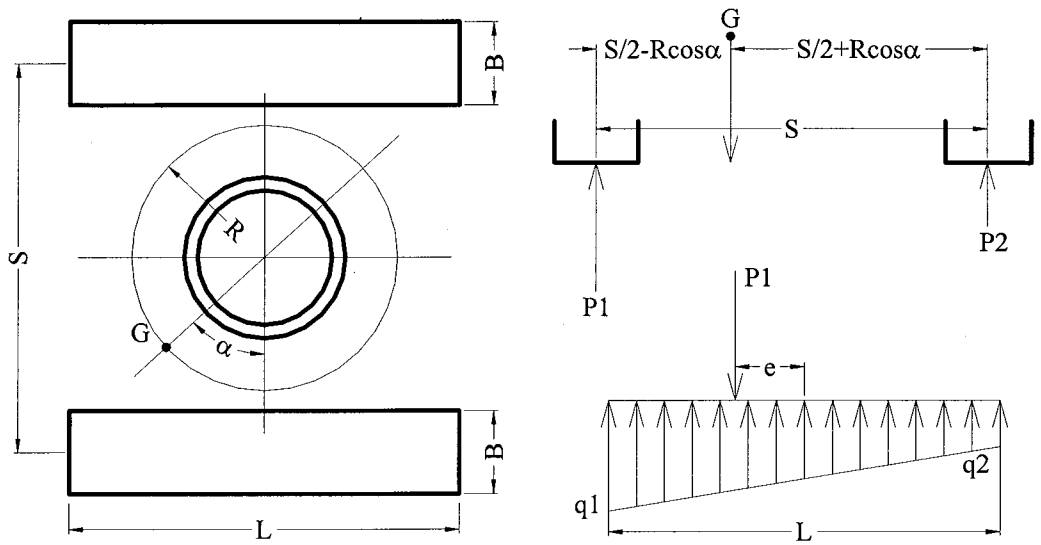

Figure 4-6 Diagram for crane tilting calculation

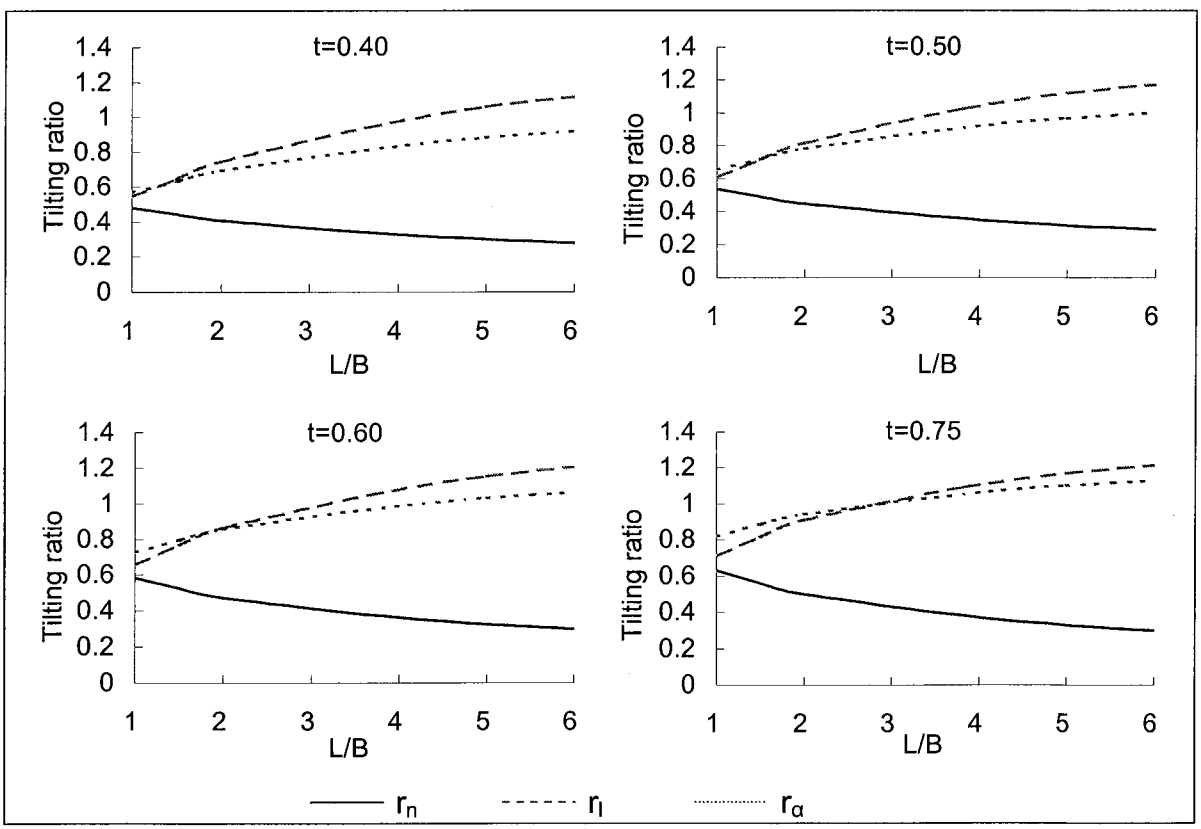

Figure 4-7 Variation of tilting ratios

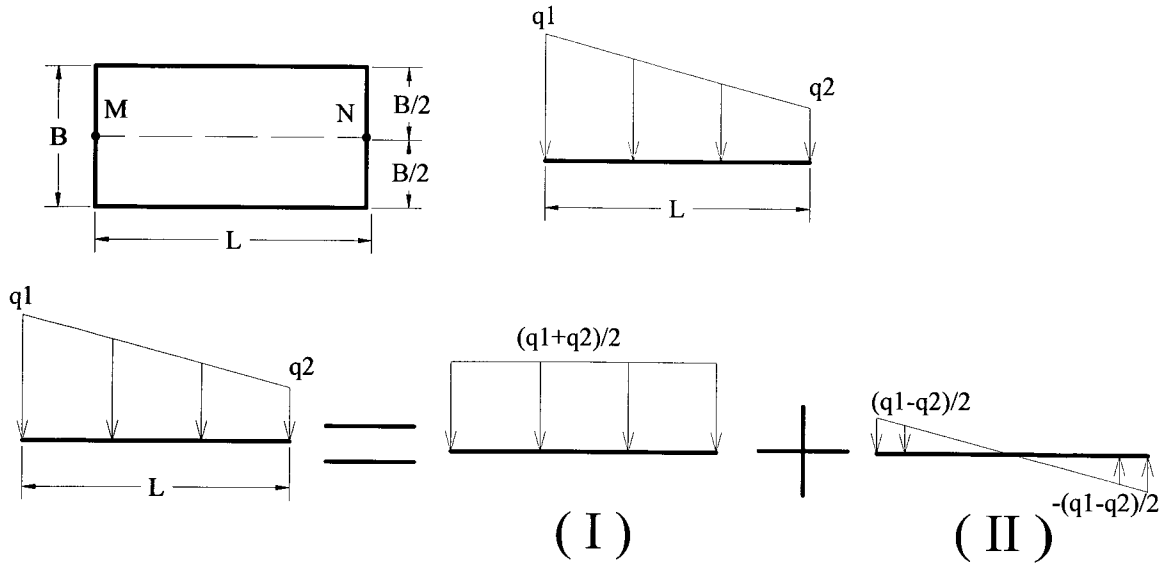

Figure 4-8 Diagram for calculating settlement of rigid footing

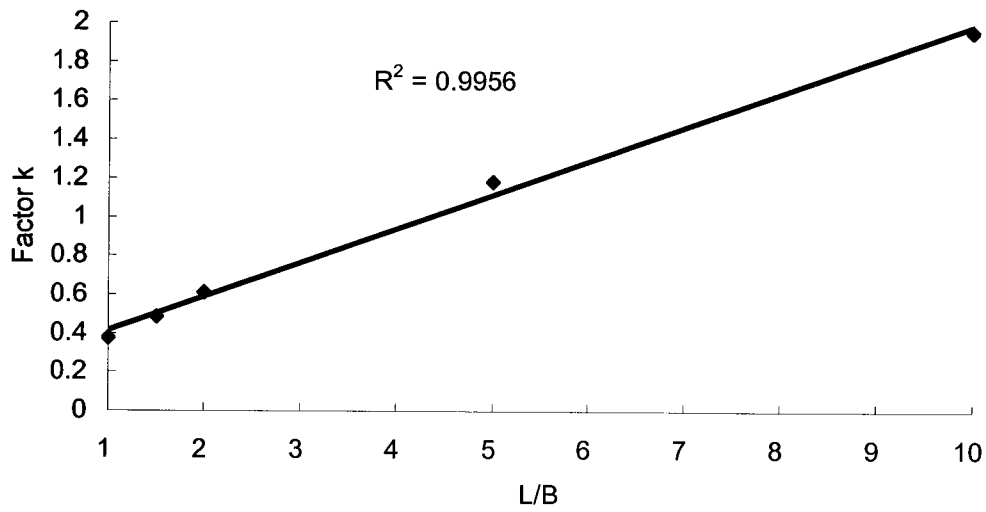

Figure 4-9 Correlation of factor k with L/B ratio

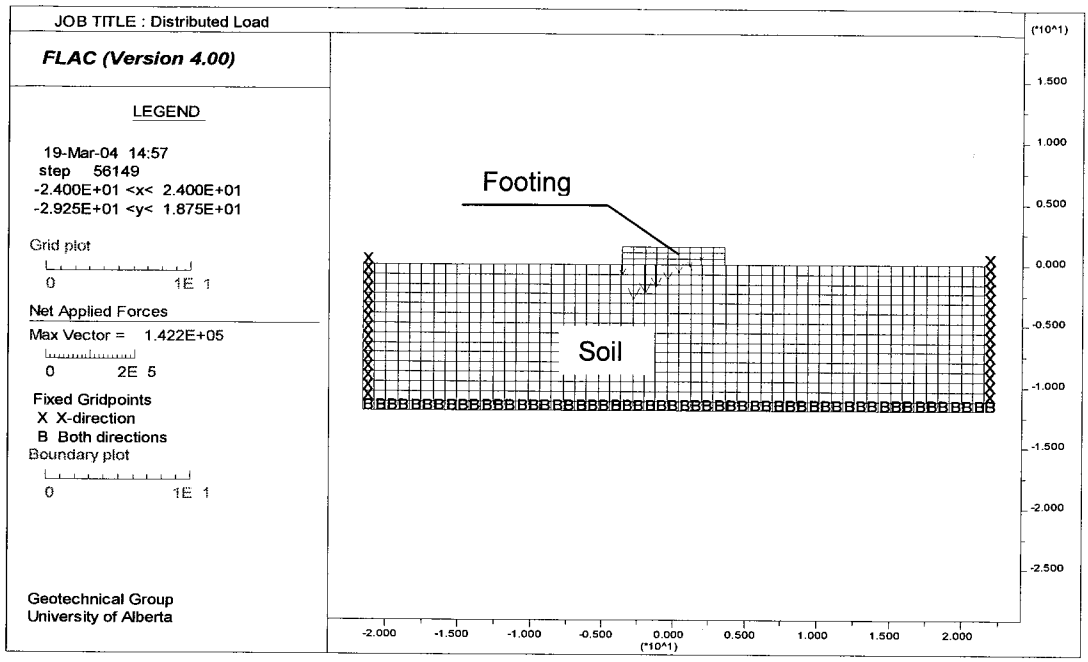

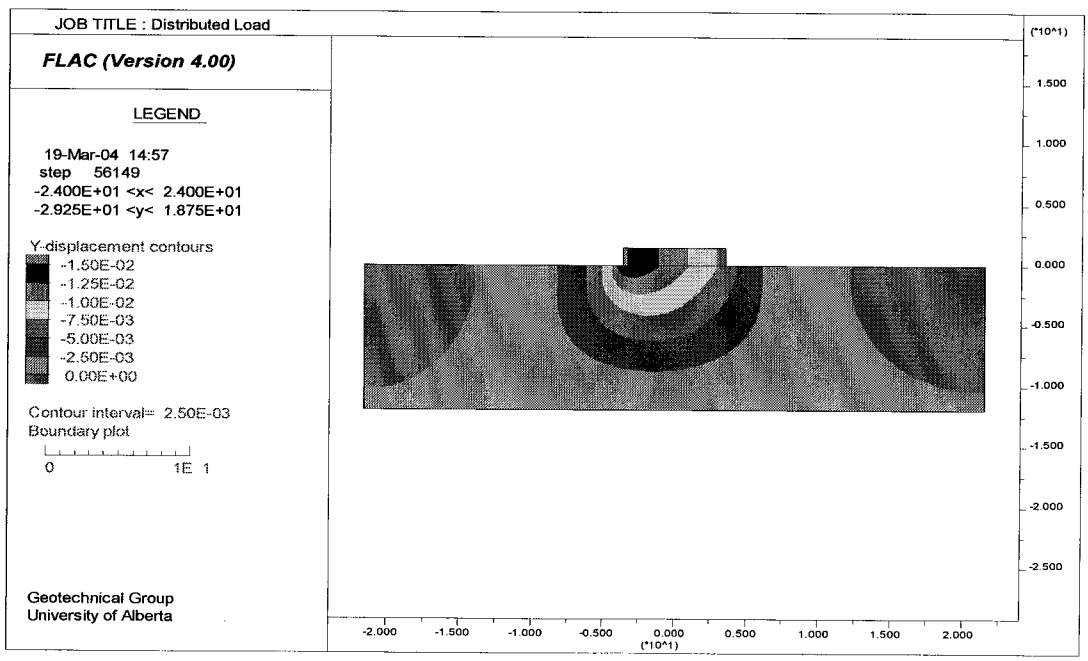

Figure 4-10 Typical model configuration and settlement profile for equivalent track pressure verification

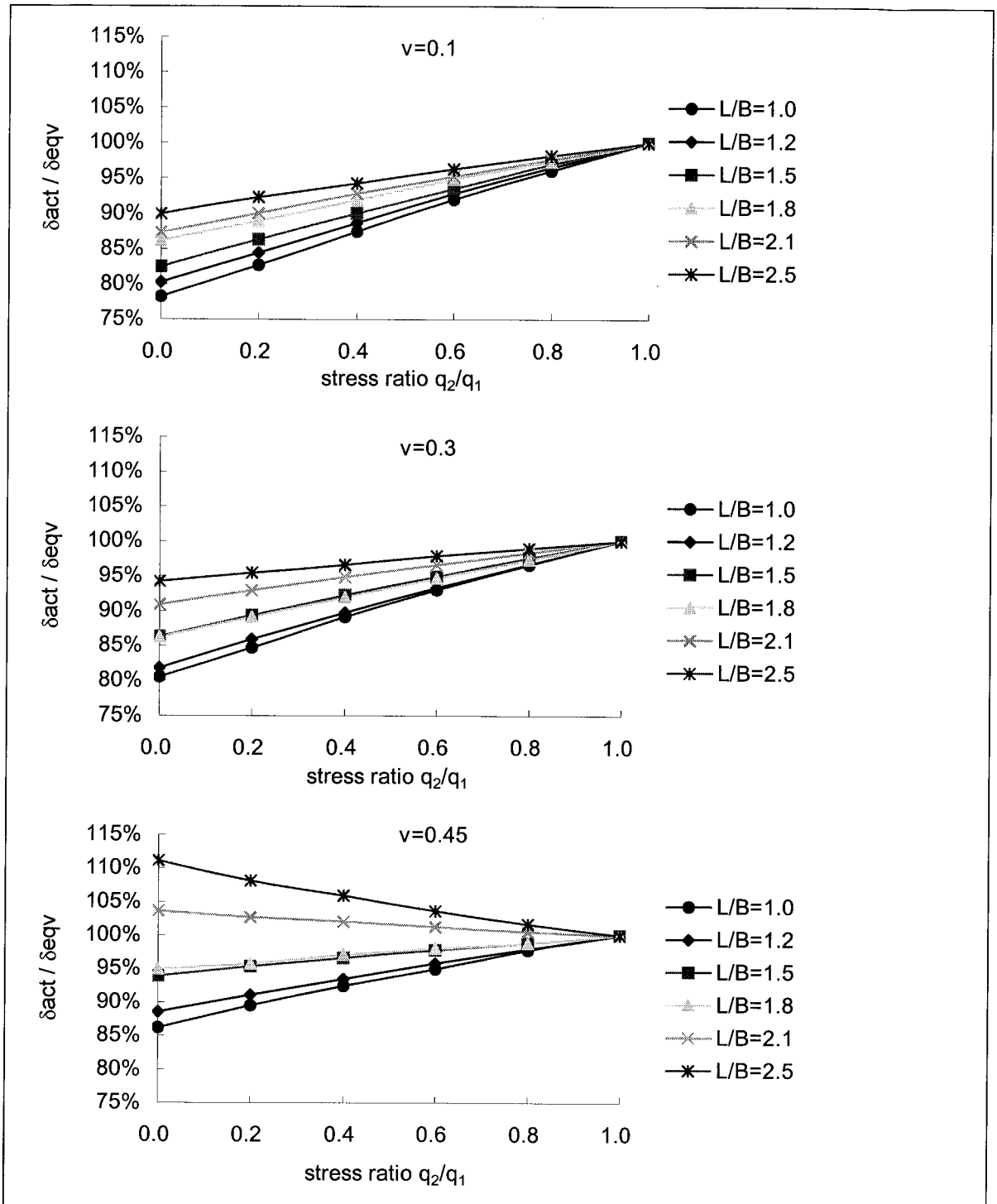

Figure 4-11 Comparison of settlement caused by actual and equivalent track pressure

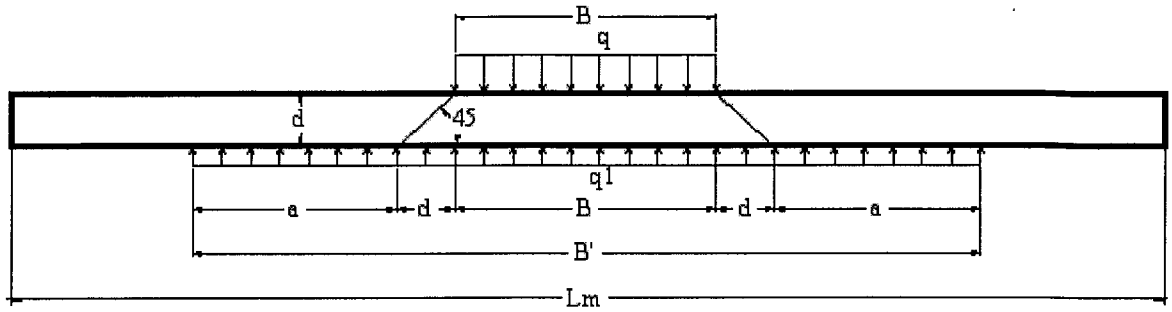

Figure 4-12 Diagram for determining the lateral spread width

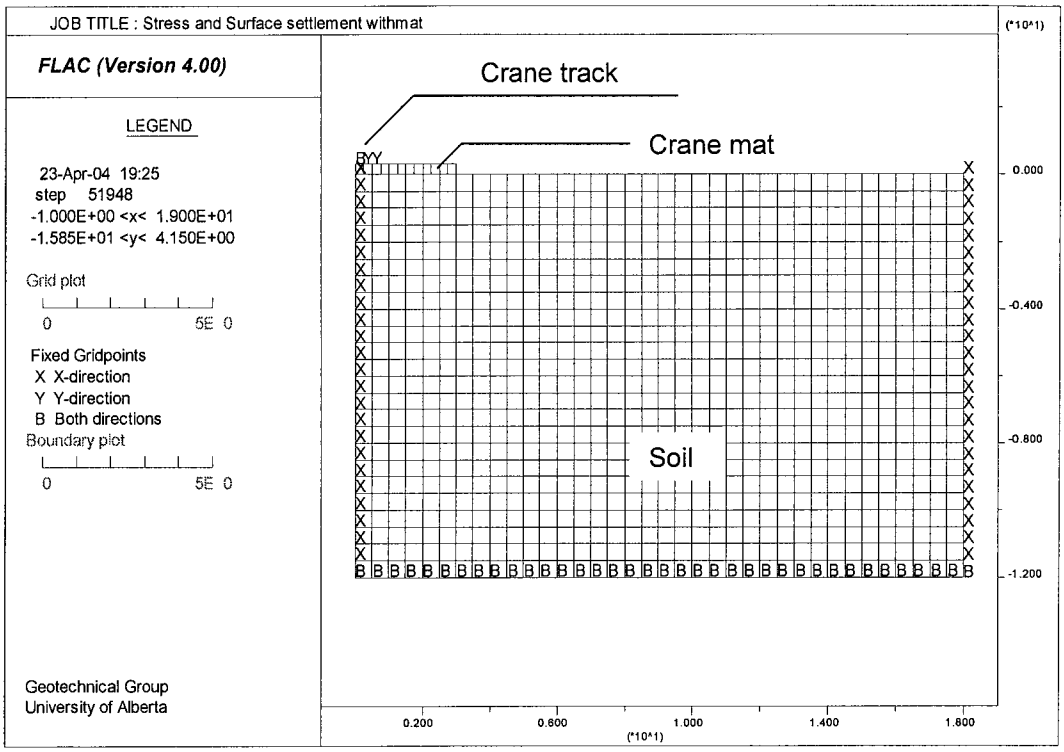

Figure 4-13 Model to determine track pressure for certain settlement

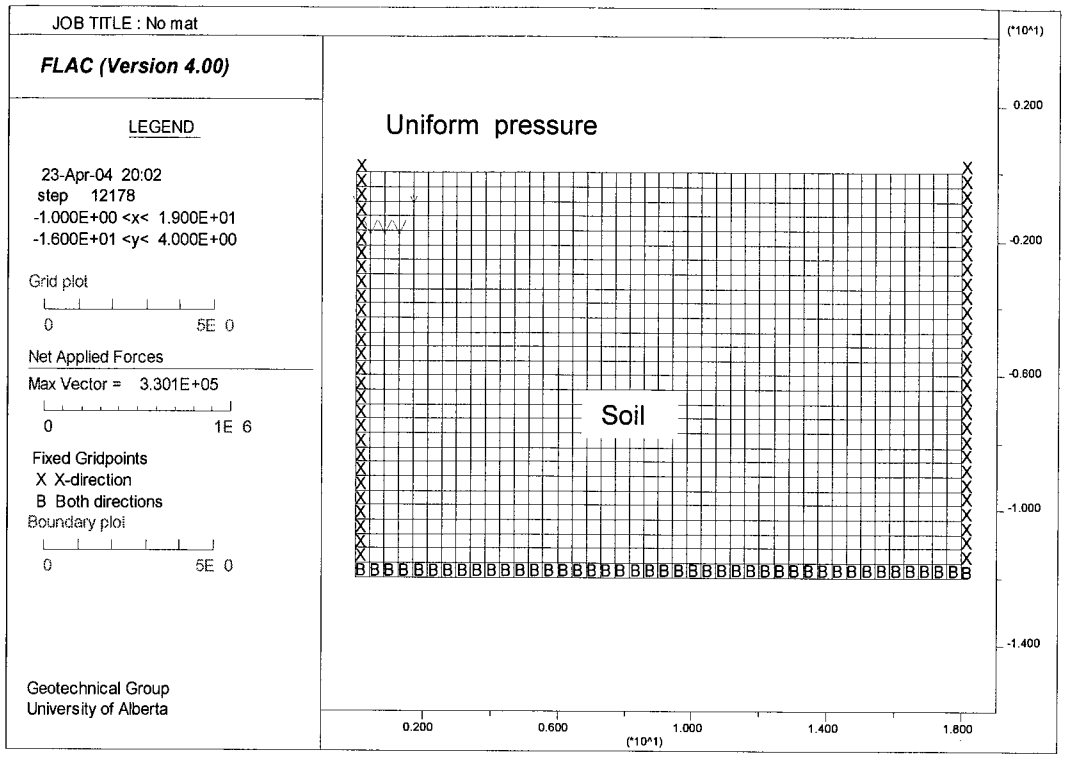

Figure 4-14 Model to simulate situations of crane with mats

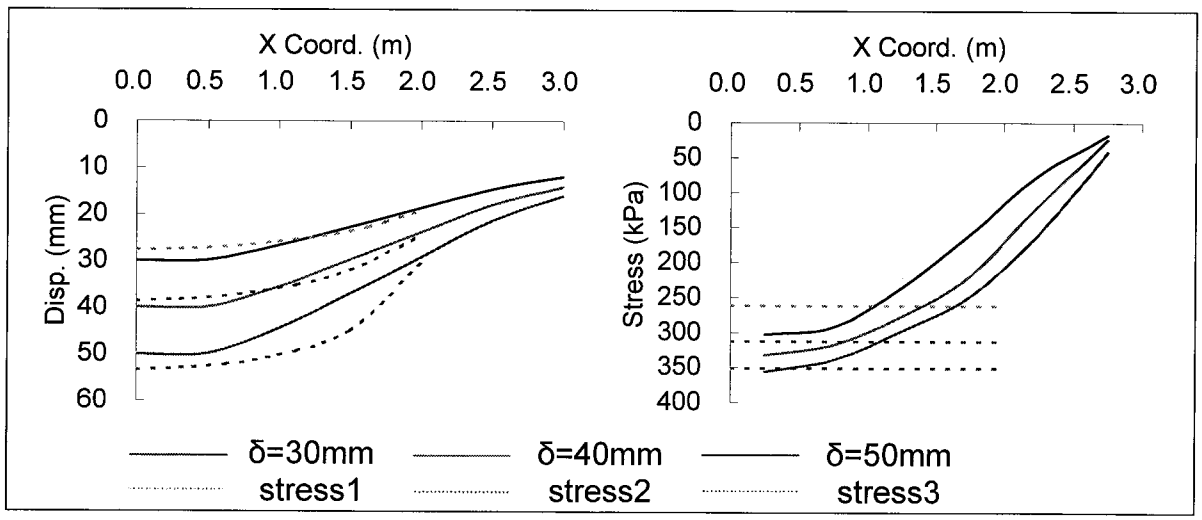

Figure 4-15 Typical settlement and stress profile using lateral spread width

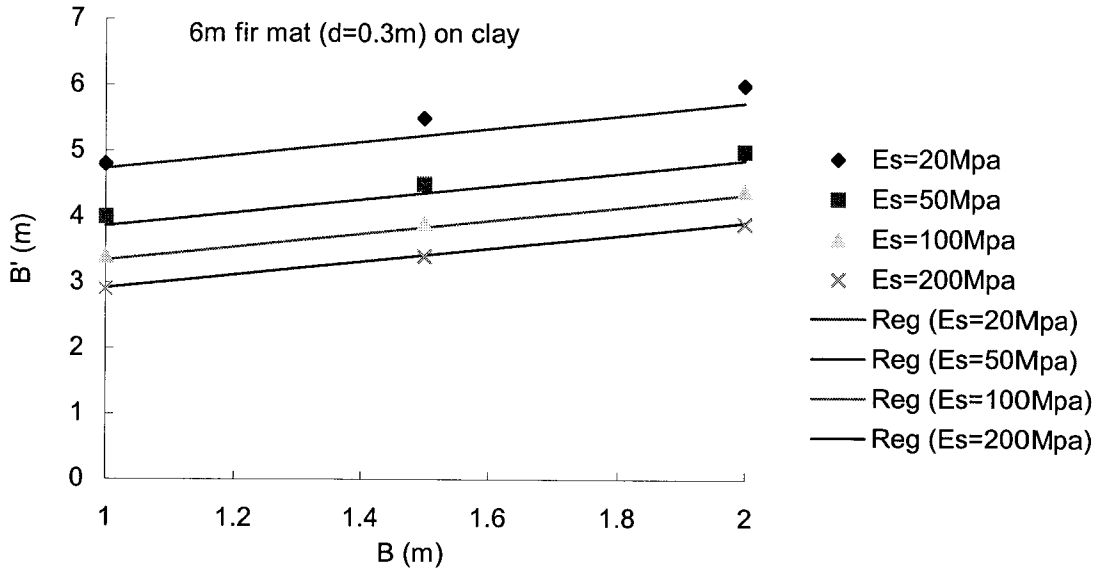

Figure 4-16 Correlations of lateral spread width with crane track width

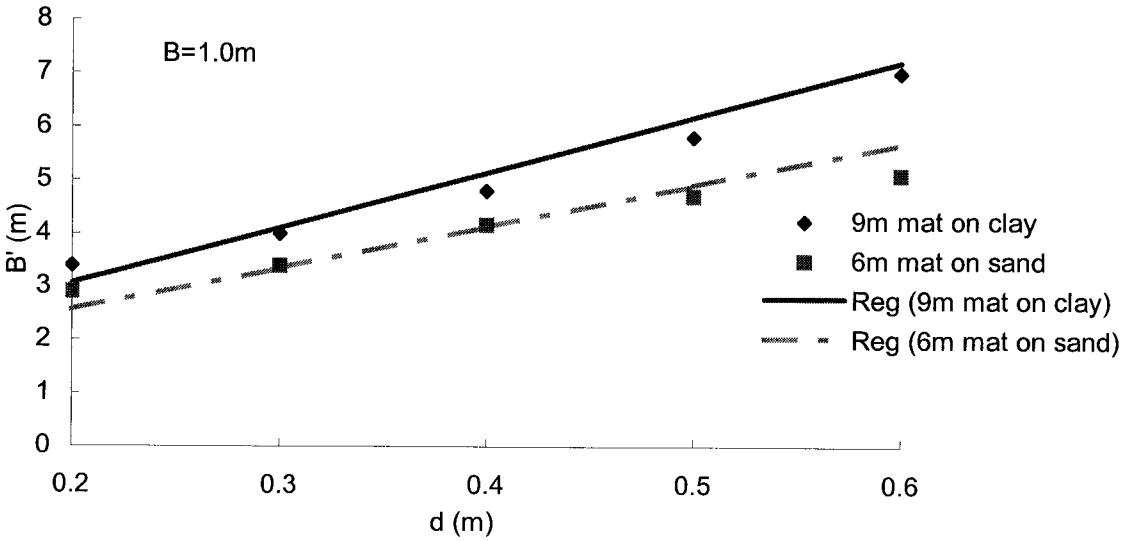

Figure 4-17 Correlations of lateral spread width with mat thickness

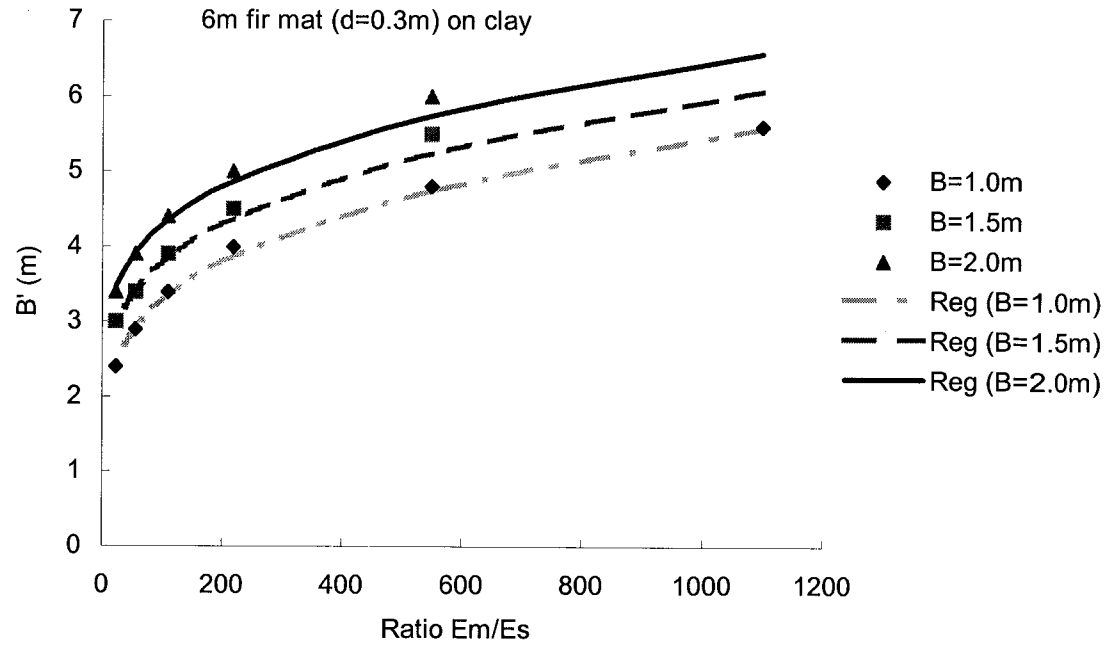

Figure 4-18 Correlations of lateral spread width with E_m/E_s for clays

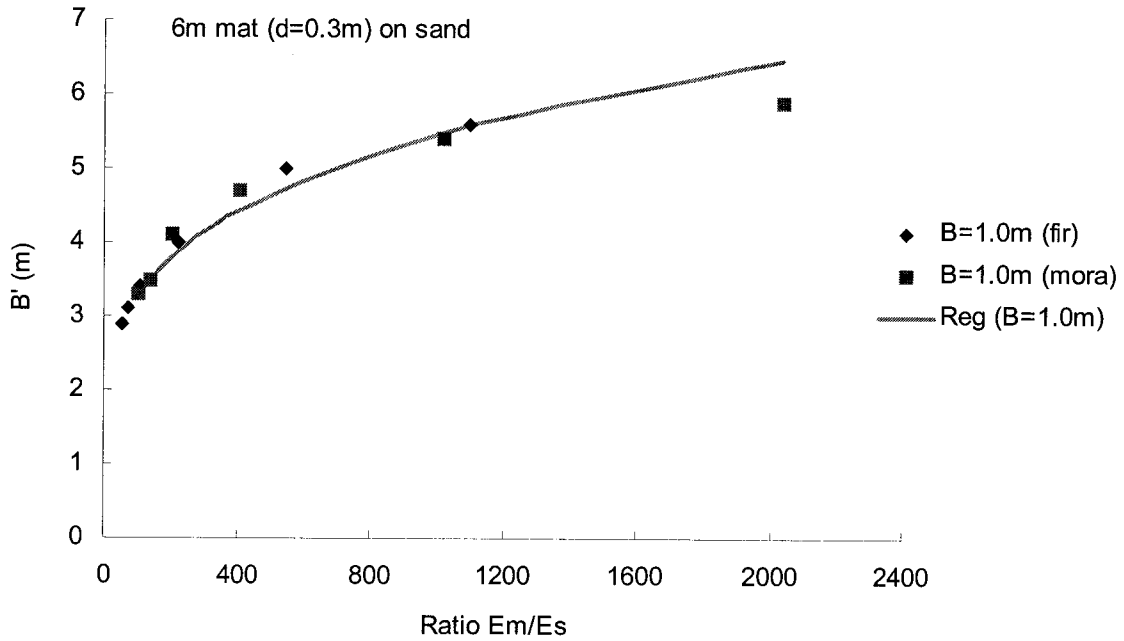

Figure 4-19 Correlations of lateral spread width with E_m/E_s for sands

5 BEARING CAPACITY FOR DIFFERENT TYPE OF SOILS

By using a series of simplifications including converting the out of levelness criterion to the maximum allowable settlement criterion, the use of equivalent pressure instead of the triangular or trapezoidal pressure and the lateral spread width of track pressure, the study of soil bearing capacity for crawler cranes becomes a traditional soil bearing capacity study for building foundations. The difference between these two is that the settlement for cranes is mainly initial settlement and the allowable settlement is a function of the crane dimension.

The most suitable and efficient way to determine the soil bearing capacity for crawler cranes is to perform a FEM/FDM analysis based on the above-mentioned simplifications. However, this kind of analysis is usually a time consuming procedure and may require special person to carry out. In comparison to the operation duration of the cranes, this analysis is too complicate to be applied in practice.

In order to provide some simple formulae to estimate the allowable bearing capacity for crawler cranes, three types of soil are used in the study:

- Sand and gravel, which represents most cohesionless soils
- Soft to medium clay, which represents most normally consolidated or slightly over consolidated cohesive soils
- Stiff clay, which represents heavily over consolidated soils like glacial till

For each kind of soil, both the situations for crane sitting on mats and directly on the ground are studied. The influence of ground water table is also considered. The formulae for allowable bearing capacity of soil are modified from the prevailing bearing capacity formula for foundations so as to be easily understood by geotechnical engineers. All the formulae proposed are based on theoretical analyses and simulation results.

5.1 Sand and gravels

The allowable bearing capacity of sand is usually governed by the settlement of the foundations. Since it is difficult to obtain undisturbed sample of sand, the elastic parameters of sand are often derived empirically from the in-situ SPT or CPT tests. Although it is straightforward to estimate the allowable bearing capacity by performing a settlement calculation with known elastic parameters, the empirical correlation between the allowable bearing capacity and SPT blow count N provides a simple and direct way. The Canadian Foundation Engineering Manual (CFEM) recommends using Meyerhof's method (Equation 2-24) to evaluate the allowable bearing capacity from SPT N value for sand.

Both Meyerhof's and Bowles' equations (Equation 2-24 and 2-25) are based on 25mm settlement for homogeneous sand with ground water below the failure zone of footing, which is usually one to one and a half times of the footing width (1B~1.5B) from the bottom of footing. Assuming linear elastic behavior of sand prior to failure, the allowable bearing capacity for crawler cranes can be expressed in the same way as Meyerhof's equation:

$$q_a = 1.5 \cdot \frac{[\delta]}{F} \cdot N \qquad for\ B \le 1.2m$$
$$q_a = \left(\frac{B+0.3}{B}\right)^2 \cdot \frac{[\delta]}{F} \cdot N \qquad for\ B > 1.2m \qquad (5\text{-}1)$$

where q_a = allowable bearing capacity (kPa)

$[\delta]$ = allowable settlement (mm)

B = footing width (m)

N= SPT blow count

F = factor to be determined later

F=3.125 from Meyerhof's equation (Equation 2-24)

F=2.08 from Bowles' equation (Equation 2-25)

The only difference between Equation 5-1 and Equation 2-24, 2-25 is that Equation 5-1 explicitly applies the allowable settlement. By using an allowable settlement of 25mm, it turns into one of them with an appropriate F value.

To find adequate value of factor F, two sets of computer models are constructed: one for cranes sitting on mats and the other for cranes sitting directly on the ground. Considering symmetry, only half of the track is considered. The model size for cranes with mats is Width X Depth = 3B X 2B and for cranes without mats is Width X Depth = 3B X 4B, where B is the footing width, for cranes with mats, B is the length of timber mat and for cranes without mats, B is the crane track width. Soil in the model is assumed to be a Mohr-Coulomb material with linear elastic behavior prior to failure. It was found that the track width B has little influence on the determination of factor F, and only a typical track width B=1.5m is used in the simulation. The typical mat length is chosen to be 6.0m. Figure 5-1 and 5-2 shows the typical configuration of these two sets of models.

5.1.1 Model calibration

Total 41 cases are picked from Burland and Burbridge's (1985) paper for the purpose of calibration of the models. The soil type, SPT blow count N, modulus of elasticity E of each case are listed in Table (5-1). Detailed information about the cases cited are presented in Appendix B. Computer models are built for each case and the modulus of elasticity of sand of each model is adjusted to yield the same amount of settlement as observed. This modulus is then applied in the two sets of crane models to generate pressure versus settlement profile. From there, the factor F can be determined.

Table 5-1 Cases for bearing capacity study of sandy soils

Case No.	Soil type	N	E (Mpa)	Case No.	Soil type	N	E (Mpa)
08/P	silty sand	10	60	91	sand	27	80
12/A	silty sand	17	80	92	sand	50	240
13/C	silty fine sand	15	12	03/A,B	sand	8	12
13A	silty fine sand	15	30	06/P,R	sand	30	120
78	silty fine sand	5	20	07/A	sand	35	100
50/B	silty fine sand	20	80	45	fine to coarse sand	18	120
57	fine sand	6	10	76	fine/coarse sand	20	180
14	fine sand	7	24	27	gravelly sand	47	240
64/C	fine sand	23	40	47/C	sand with gravel	18	36
81/C	fine sand	5	22	47/A,B	sand with gravel	27	60
81/D	fine sand	6	22	83	sand/gravel	20	200
81/E	fine sand	7	30	84	sand/gravel	14	180
81/F	fine sand	8	30	85	sand/gravel	10	180
61/A	fine sand	34	60	87	sand/gravel	34	120
59/M	fine to medium sand	40	60	58/A	sandy gravel	13	24
60/B	fine to medium sand	30	120	52/D3,J	sand/gravel	20	45
60/C	fine to medium sand	25	36	65	sand/gravel	25	180
30	fine/medium sand	20	100	52/C	sand/gravel	50	80
39/P	medium sand	16	36	52/A3	sand/gravel	30	60
61/B	compact moist sand	45	120	51	gravel	37	200
61/C1,C2	compact moist sand	45	72				

5.1.2 Bearing capacity equations

Figure 5-3 illustrates the variation of factor F with different soil type and SPT blow count for crane track sitting on the ground without mat. It can be found that the factor F nearly does not change with SPT N value. Two lines representing the factor F used in Meyerhof's equation and Bowles' equation are also shown in the plot. F = 2.08 used in Bowles' equation seems to be more reasonable for cranes sitting directly on the ground. For cranes sitting on mats, Figure 5-4 also shows no influence of SPT N value on the factor F. A value of F = 4.3 might be appropriate to estimate the allowable bearing capacity for cranes with mats. But this factor is much larger than that for cranes without mats. This can be contributed to the flexibility of mats and high load intensity right beneath the crane track. Since the maximum settlement at the center of crane mats is concerned in dealing with the bearing capacity for crawler cranes, and it can be

as much as two times of the settlement at the edge of a flexible footing. The high pressure beneath the track might yield the soil locally and cause larger settlement.

Another aspect to be considered is the strength of the soil. This can be significant if the footing width is small and most applicable for cases where cranes sitting on the ground without mats. To prevent the crane from bearing capacity failure and limit the soil behaving within the linear elastic zone, a factor of safety of 2.0 may be appropriate for cranes. Using Meyerhof's ultimate bearing capacity equation (1956), the allowable bearing capacity of sand from the strength aspect is:

$$q_a \le \frac{q_u}{FS} = \frac{32.8 \cdot B \cdot N}{2} \approx 16 \cdot B \cdot N \qquad (5\text{-}2)$$

However, this equation is only applied to cases where cranes without mats. For cranes with mats, since the footing width is relatively large, Equation 5-1 with Equation 5-2 should be combined and applied appropriate factor F to it. The allowable bearing capacity of sand and gravel for crawler cranes can be written as:

- For cranes sitting on the ground without mats

$$\begin{aligned} q_a &= 1.5\frac{[\delta]}{2.08} \cdot N \le 16B \cdot N \qquad B \le 1.2m \\ q_a &= \left(\frac{B+0.3}{B}\right)^2 \cdot \frac{[\delta]}{2.08} \cdot N \le 16B \cdot N \qquad B > 1.2m \end{aligned} \qquad (5\text{-}3)$$

- For cranes with mats

$$q_a = \left(\frac{B'+0.3}{B'}\right)^2 \cdot \frac{[\delta]}{4.3} \cdot N \qquad (5\text{-}4)$$

where B = crane track width

B' = lateral spread width of track pressure

Since the allowable settlement is related to the crane track length L as shown in Chapter 4, Equation 5-3 and 5-4 can be rewritten as the function of crane track length:

- For cranes sitting on the ground without mats

$$\begin{aligned} q_a &= 3L \cdot N \le 16B \cdot N && B \le 1.2m \\ q_a &= 2\left(\frac{B+0.3}{B}\right)^2 \cdot L \cdot N \le 16B \cdot N && B > 1.2m \end{aligned} \tag{5-5}$$

- For cranes with mats

$$q_a = 1.2\left(\frac{B'+0.3}{B'}\right)^2 \cdot L \cdot N \tag{5-6}$$

5.1.3 Influence of ground water

Since the submergence of cohesionless soils will decrease the unit weight by half, the ultimate bearing capacity should be reduced by up to one-half for ground water table higher than the base of footing. If the water table is at a depth greater than 1~1.5B below the bottom of the footing, there is no effect on it. Therefore, the allowable bearing capacity for cranes without mats should be modified as Equation 5-7 for ground water higher than the base of footing.

$$\begin{aligned} q_a &= 3L \cdot N \le 8B \cdot N && B \le 1.2m \\ q_a &= 2\left(\frac{B+0.3}{B}\right)^2 \cdot L \cdot N \le 8B \cdot N && B > 1.2m \end{aligned} \tag{5-7}$$

If ground water table is at intermediate position, the allowable bearing capacity for cranes without mats can be interpolated linearly from Equation 5-5 and 5-7.

For cranes with mats, since the ultimate bearing capacity is usually much greater than the allowable bearing capacity from settlement criterion. No effect of ground water table should be considered.

Equation 5-7 is also applicable to silty sand in the determination of allowable bearing capacity for cranes without mats since its ultimate bearing capacity is usually only one-half of that for clean sand with same SPT blow count.

The allowable bearing capacity of granular soils can also be estimated from CPT test results since an empirical correlation between the CPT cone penetration resistance q_c and SPT blow count N exists. It is convenient to convert the CPT cone resistance to the equivalent SPT blow count N and then perform the allowable bearing capacity evaluation using the equations mentioned above.

5.2 Soft and medium clay

Soft clay is usually classified as clay with an undrained shear strength C_u less than 25kPa. The undrained shear strength of medium clay is generally between 25kPa to 50kPa. There exists a nearly proportional correlation between the undrained shear strength C_u and pre consolidation stress $C_u = 0.25\sim0.30p_c'$, as a result, the pre consolidation stress p_c' for soft and medium clay is usually not so high and the clay can be deemed as normally consolidated or lightly over consolidated.

5.2.1 Theoretical approach

From Equation 2-9 and 2-10, the allowable bearing capacity of saturated clay for cranes on a flat ground surface from strength aspect can be expressed as:

$$q_a = \frac{q_u}{FS} = \frac{cN_c s_c}{FS} = \frac{5.14 + B/L}{FS} C_u \qquad (5\text{-}8)$$

Since only immediate settlement is concerned in evaluating the bearing capacity for crawler cranes, the allowable bearing capacity from settlement aspect based on Equation 2-20 is:

$$q_a = \frac{E_u}{\left(1-\nu^2\right) B I_w} [\delta] \qquad (5\text{-}9)$$

where [δ] = allowable settlement of crane

E_u = undrained modulus of saturated clay

The undrained modulus of saturated clay is usually related to its undrained shear strength as $\lambda = E_u/C_u$ in practice. However, this relationship is only approximate and the ratio λ varies from 100 to1500 (Duncan and Bunchignani, 1976). Simons (1974) reported a wider range of values from 40 to 3000, he also pointed out that this ratio is highly depended on the shear stress level and the plasticity of the clay. The most likely range of λ ranges from 200 to 500 for normally or lightly over consolidated clay. The recommended value used for design is λ = 300. Theoretically, the Poisson's ratio for saturated clay is v = 0.5.

Since the strength of soft to medium clay is very low, only situations for cranes with mats are considered here. Recall Equation 4-11 and rewrite Equation 5-9 in term of λ and crane track length L as:

$$q_a = \frac{\lambda}{150 I_w} \frac{L}{B'} C_u \qquad (5\text{-}10)$$

It can be found that the allowable bearing capacity for saturated clay from both the strength aspect and settlement aspect is the function of its undrained shear strength and the L/B ratio of the footing. Figure 5-5 shows the variation of allowable bearing capacity with L/B ratio. The L/B ratio for cranes with mats is about 1.2 ~2.0. It can be seen from the figure that within this range the allowable bearing capacity from settlement criterion is generally greater than that from strength criteria with a factor of safety of 2.0 except for $\lambda < 300$ and $L/B<1.5$. As a result, Equation 5-8 with a factor of safety of 2.0 might be adequate to estimate the allowable bearing capacity of saturated clay for crawler cranes unless evidence shows a small E_u/C_u ratio for some problematic soils with high compressibility.

The ratio of immediate settlement to total settlement of normally consolidated clay is only about 0.2. In spread footing design, the total allowable settlement is about 65mm for clay. That means the allowable immediate settlement for foundations is about 13mm. It is far less than the allowable settlement for crawler cranes. This again shows that the allowable bearing capacity for cranes should be higher than that for buildings.

It has been shown by Davis and Poulos (1968) that for normally consolidated clay yielding and deviation from linear behavior will first occur when the factor of safety against a bearing capacity failure is between 4 and 8, for slightly over consolidated clays, the corresponding factor of safety at first yielding is 2 to 3. Therefore, it is not suggested to use a factor of safety less than 2.0 for soft and medium clay.

5.2.2 Verification from computer simulation

Computer models used in the bearing capacity study of soft clay have the same configuration as shown in Figure 5-1. The track width and length of timber mat are set to be 1.5m and 6.0m respectively. The soil within the model is assumed to be saturated with a Poisson's ratio v = 0.49. By varying the undrained shear strength C_u and E_u/C_u ratio, a series of pressure versus settlement profiles are obtained. Plots of pressure-settlement curves are shown in Figure 5-6 for each specific C_u. A straight line representing the allowable bearing capacity using a factor of safety of 2.0 is also included in each plot. It can be seen from the plots that the computer simulation results match the theoretical analyses very well. The typical allowable settlement for crawler cranes is about 35-50mm. Within this range, the allowable bearing capacity from settlement criterion is generally higher than that from the strength criterion using a factor of safety of 2.0, unless the E_u/C_u ratio is less than 300. That also confirms the use of Equation 5-8 with a factor of safety no less than 2.0 is valid to estimate the allowable bearing capacity of saturated soft to medium clay for cranes with mats.

5.2.3 The influence of ground water

Ground water has two effects on the bearing capacity of clay: It reduces the strength of soil therefore decreases the ultimate bearing capacity, on the other hand, the existing of water increases the incompressibility of soil mass and lower the settlement of ground under same amount of load. In another word, the existence of ground water decreases the allowable bearing capacity of clay from strength aspect but increases that from settlement aspect.

It is rather difficult to derive a separate set of equations dealing with allowable bearing capacity for unsaturated clays since many parameters need to be determined to describe its properties.

Since there is a theoretical relationship between the immediate settlement and the total settlement of clay as:

$$\frac{\delta}{\delta_u} = \frac{1-\nu'}{1-\nu_u} \tag{5-11}$$

where δ = total settlement

δ_u = immediate settlement

ν' = final Poisson's ratio

ν_u = Poisson's ratio of saturated soil

The total settlement can be treated as the settlement of clay above ground water table and the immediate settlement is the settlement of its saturated counterpart of the same soil. Poisson's ratio for saturated clay is 0.5 and for clay above ground water table, it normally ranges from 0.1 to 0.3.

Therefore, the settlement of clay above ground water table is about 1.4 to 1.8 times of that of saturated clay from Equation 5-11. Since a factor of safety of 2.0 is appropriate to represent the settlement of saturated clay, the use of a factor of

safety from 3.0 to 3.5 might be adequate to estimate the allowable bearing capacity of clay above ground water table for crawler cranes.

5.3 Stiff clay

Stiff clay is classified as clay with undrained shear strength over 50kPa. In this range, the clay usually has an over consolidated ratio greater than 4 and can be treated as heavily over consolidated soil. The typical range of ratio $\lambda = E_u/C_u$ is reported to be from 300 to 700.

5.3.1 Theoretical approach

Similar analysis for soft and medium clay is carried out here. Both cases for cranes with mats and without mats are studies. For crane without mats, Equation 5-10 is rewritten by using a different allowable settlement formula as:

$$q_a = \frac{\lambda}{180 I_w} \frac{L}{B} C_u \qquad (5\text{-}12)$$

Figure 5-7 and 5-8 show the allowable bearing capacity of stiff clay from both strength and settlement aspect for cranes with mats and without mats respectively. Similar to soft to medium clay, the allowable bearing capacity for cranes with mats is generally controlled by the strength of soil with a factor of safety of 2.0. The plot of allowable bearing capacity for cranes without mats shows that the allowable bearing capacity from settlement is much greater that that from strength aspect with a factor of safety of 2.0. As a result, a factor of safety of 2.0 is adequate to estimate the allowable bearing capacity of stiff clay for crawler cranes no matter the crane is sitting on the mats or not.

5.3.2 Verification from computer simulation

Two sets of computer models are constructed to testify the results from theoretical analysis: One for cranes with mats which is similar to that built for soft and medium clay unless the soil parameters used in the model is different. The other for cranes sitting on the ground without mats, which is similar to that used

in the study of bearing capacity of sand and gravel for cranes without mats. Figure 5-9 and 5-10 show a series plots of pressure-settlement curve for each specific undrained shear strength value used in the simulation. Again, these plots testify the results from theoretical analysis.

5.3.3 The influence of ground water

Similar to soft and medium clay, the influence of ground water will result in a larger factor of safety used in evaluating the allowable bearing capacity for cranes with mats. Since the allowable bearing capacity from the strength aspect with a factor of safety of 2.0 is adequate to represent the allowable bearing capacity from settlement aspect for saturated stiff clay, a factor of safety of 3.0 to 3.5 should be applied to estimate the allowable bearing capacity of stiff clay above ground water table for cranes with mats.

For cranes without mats, the allowable bearing capacity from settlement aspect is much higher than that from strength aspect with a factor of safety of 2.0 for saturated stiff clay. The use of FS=2.0 only represents 10mm settlement shown in Figure 5-10. Even for stiff clay above ground water table, this settlement is only about 14mm to 18mm, which is less than the allowable settlement for cranes. Therefore, a factor of safety of 2.0 is still valid in estimating the allowable bearing capacity of stiff clay above ground water table for cranes sitting directly on the ground without mats.

5.4 Bearing capacity for layered soil

It is nearly impossible to find a simple solution for allowable bearing capacity of layered soil for cranes because the failure surface and stress distribution differ from that of homogeneous soil. The precise method to find the allowable bearing capacity of layered soil for cranes is to perform a FEM/FDM analysis. However, it is a time-consuming process. In practice, two possible ways can be followed to determine the allowable bearing capacity for cranes:

- Use the minimum allowable bearing capacity using parameters from the weakest layer of soil. This allowable bearing capacity may be far less than the actual bearing capacity of soil.

- Use the weight average parameters of each layer based on their thickness. This method works very well if there is no large difference in the parameters between each layer. The allowable bearing capacity from this method can be either conservative or not.

Several computer simulations are also carried out for layered soil, but the result is quite diverse and no conclusion can be drawn from there. An idea about using another weight to account for the induced strain within each layer in the weighted average method may be testified in the continuing study.

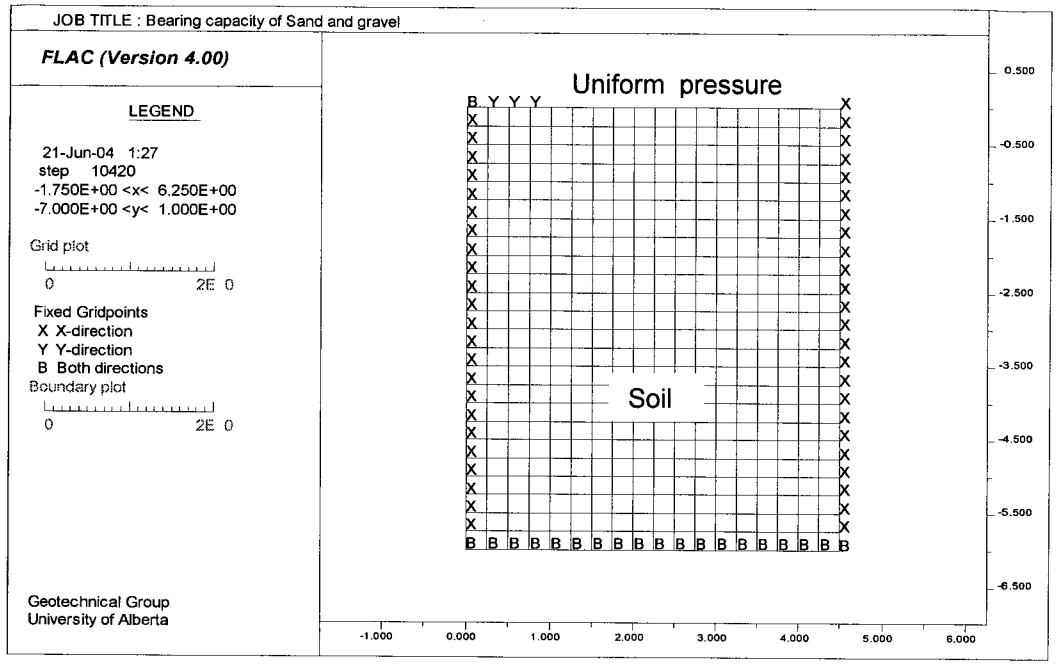

Figure 5-1 Model for bearing capacity study of sand for crane without mats

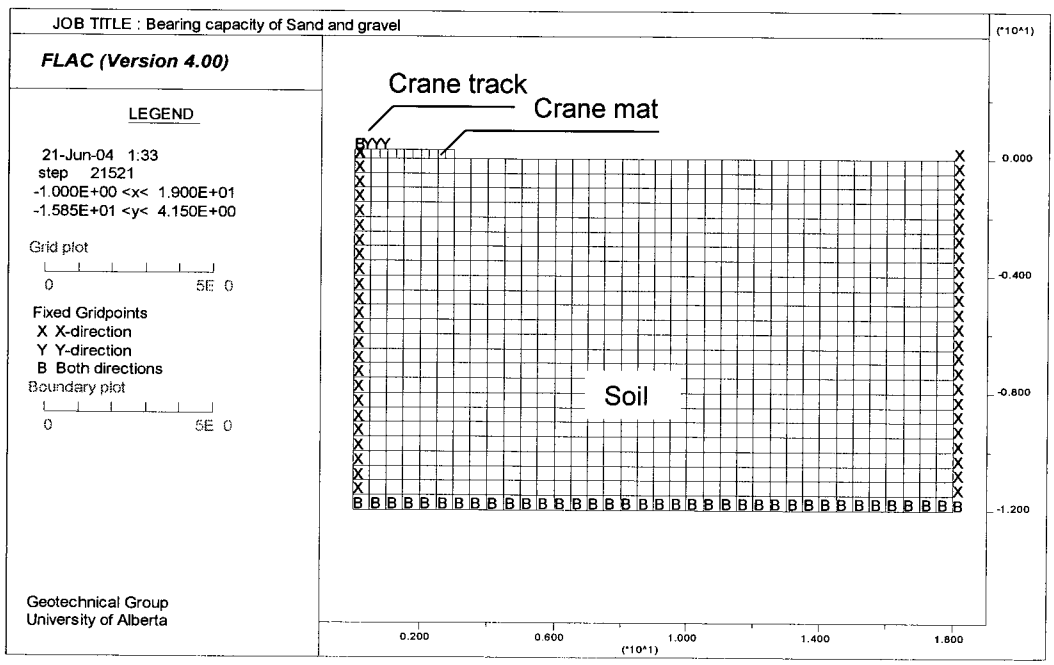

Figure 5-2 Model for bearing capacity study of sand for crane with mats

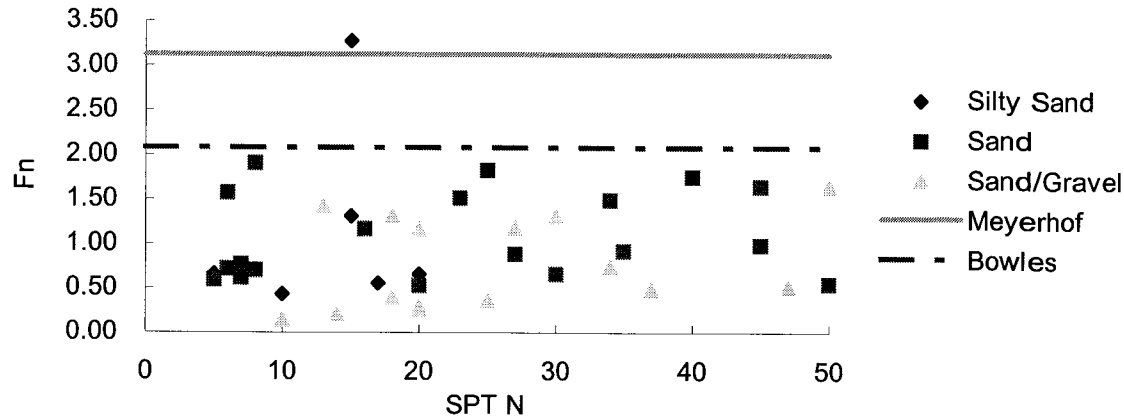

Figure 5-3 Factor F for crane without mats

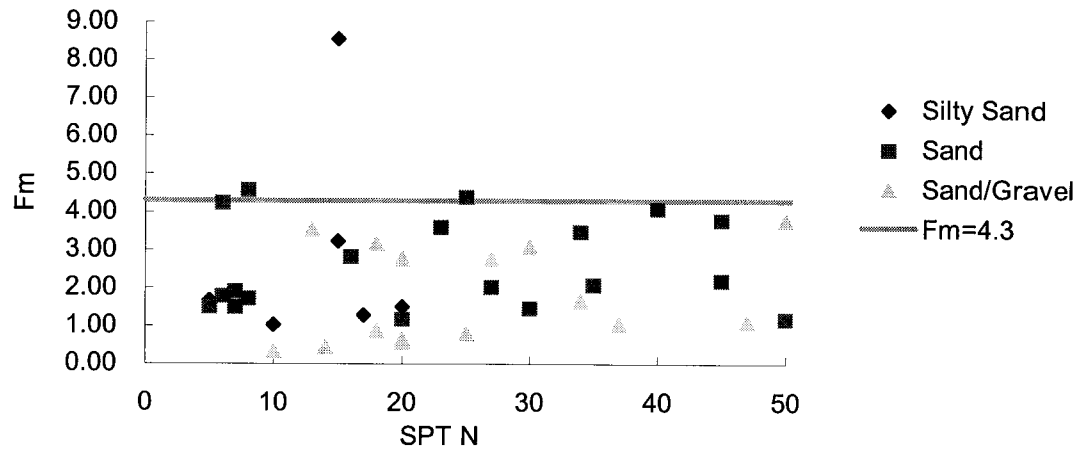

Figure 5-4 Factor F for crane with mats

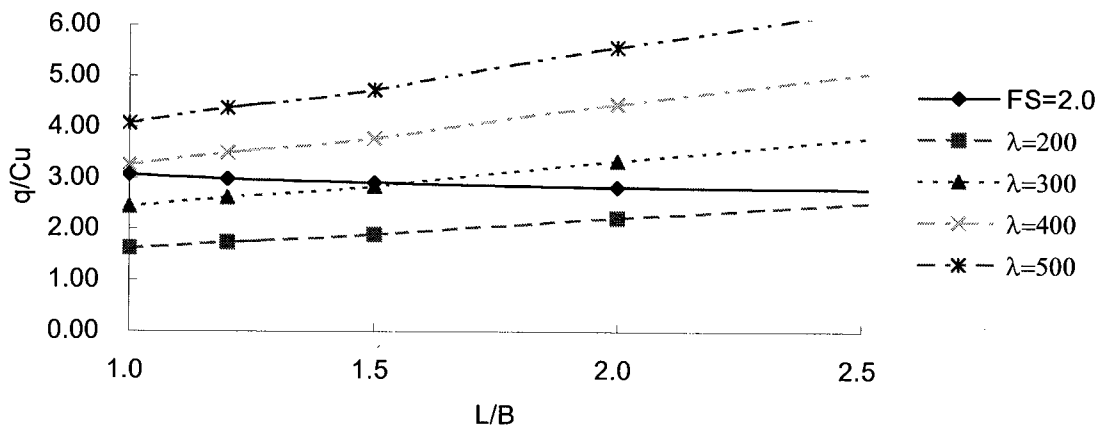

Figure 5-5 Bearing capacity of soft clay from theoretical analysis

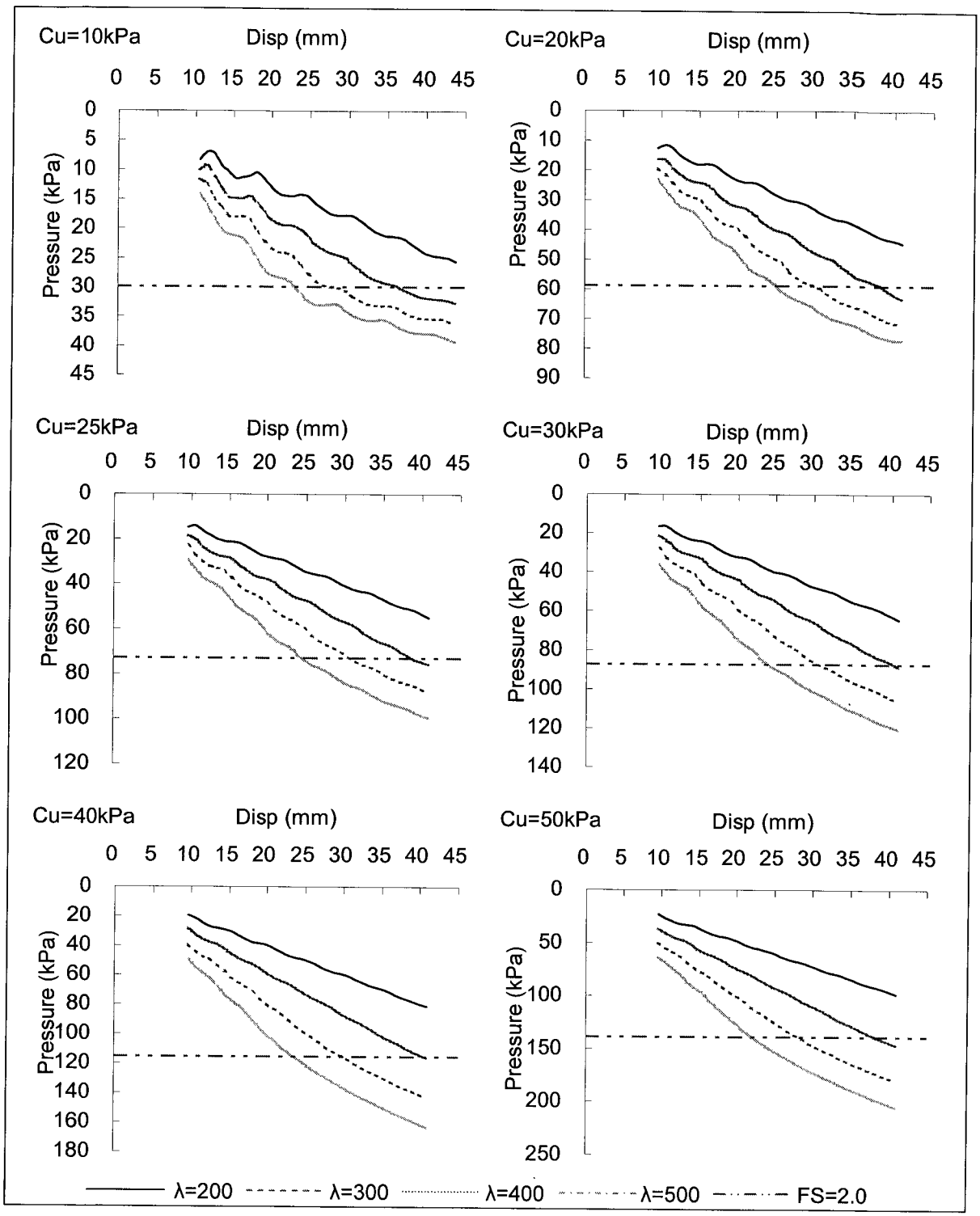

Figure 5-6 Load immediate settlement curve of soft clay for crane with mats

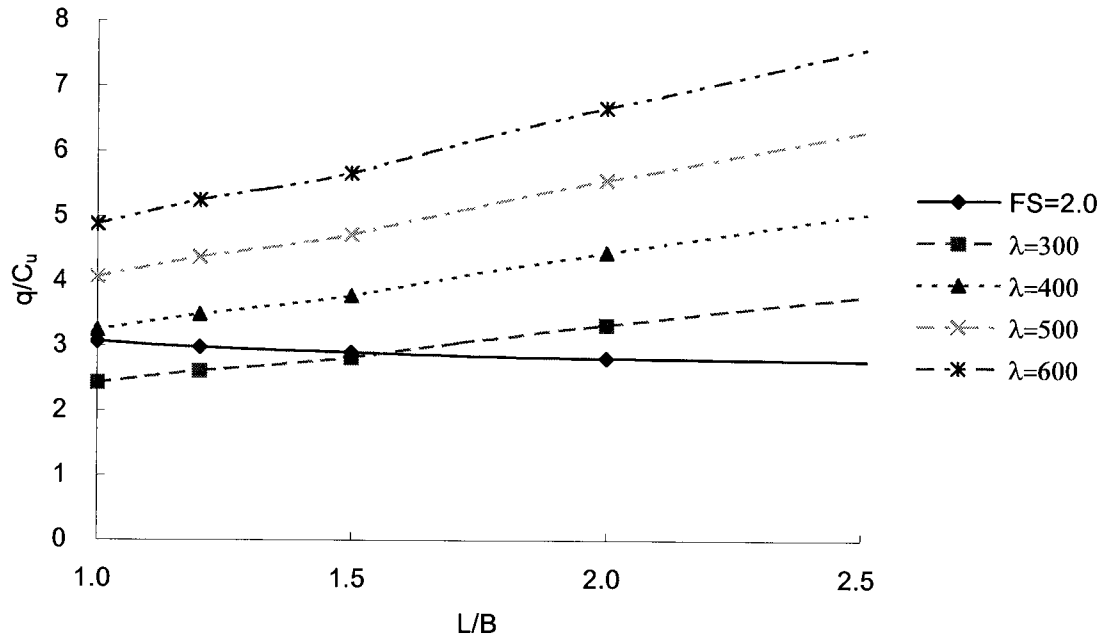

Figure 5-7 Bearing capacity of stiff clay for crane with mats

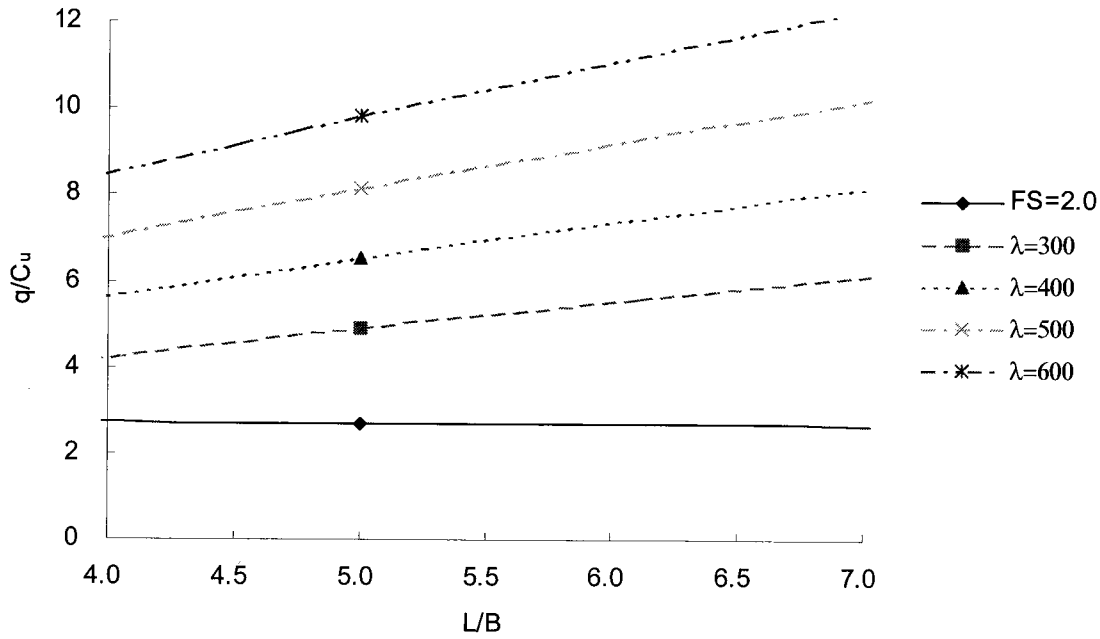

Figure 5-8 Bearing capacity of stiff clay for crane without mats

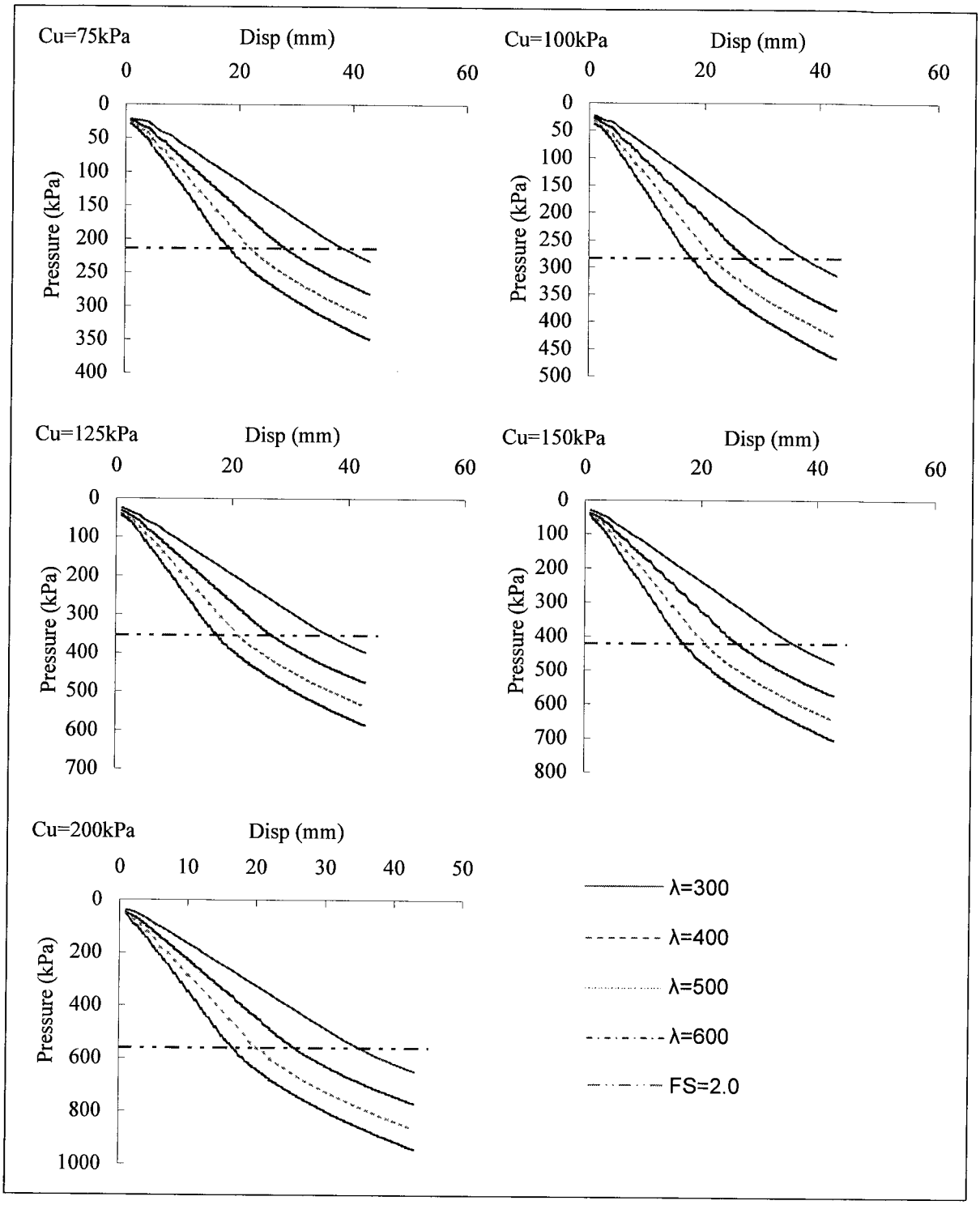

Figure 5-9 Load immediate settlement curve of stiff clay for crane with mats

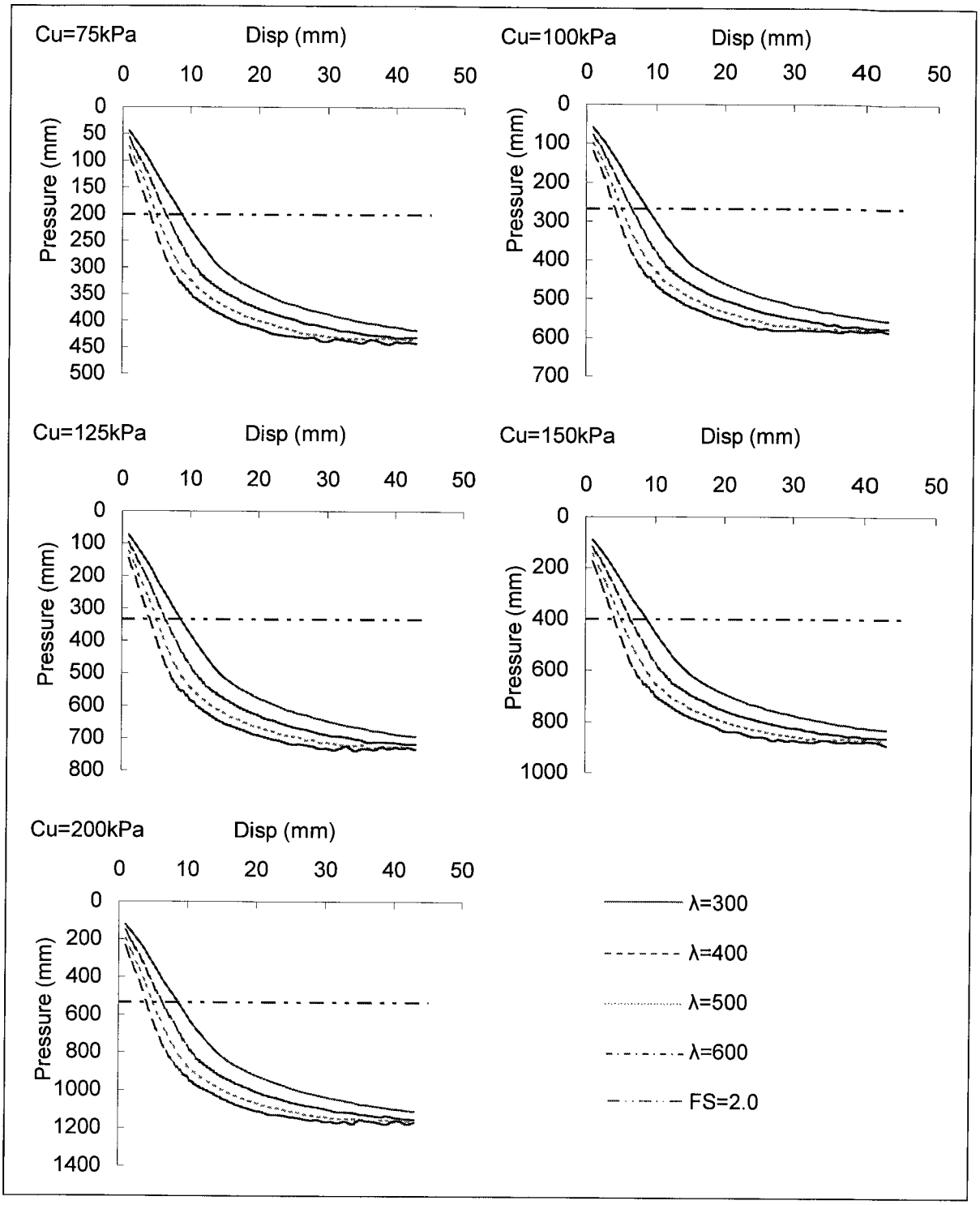

Figure 5-10 Load immediate settlement curve of stiff clay for crane without mat

6 CASE STUDIES OF LOAD-SETTLEMENT RESPONSES FOR CRANES

Besides theoretical analyses and computer simulations, six lifts on three different sites have been studied. They are:

1. Test lift using a 400mt DEMAG CC2000 at Brighton Beach
2. Life to replace and reinstall vessel "G" using a 600mt DEMAG CC2800 at Fort Nelson, B.C.
3. Lifts of Fractionator, Burner and Reactor using a 1250mt DEMAG CC8800 at Fort McMurray, Alberta

6.1 Field Observation

The objective of field observation is to obtain the ground settlement and the corresponding track pressure. Knowing these two sets of data, computer models can be built to back analyze the soil parameters and predict the soil bearing capacity for cranes.

To directly measure the displacement of ground right beneath the crane track using electronic devices like LVDT is rather difficult since the devices must be mounted on fixed reference objects. This kind of reference object can be either a structural component of a building or a slip free pile buried far and deep enough from the crane that the pile will not move due to the crane load. The latter is more realistic since these piles can be located according to the points that need to be measured. However, it is a time-consuming and expensive alternative. Moreover, the layout of these piles can be affected by the existing pipeline or other obstructions that can not be located as desired. Other problems associated with electronic devices include not easy to be calibrated and may not work properly at extremely low temperature.

Traditional survey technology using the level to shoot a scaled target was used in this study since it provides a simple and cost effective way to do the measurements.

One level transit on each side of the crane is usually set to measure the vertical displacement of each track. They were calibrated and can reach an accuracy of about 0.2mm based on the average of three shots on the same target with double scales at a distance about 12m with no wind. However, an accuracy of 0.5mm can be achieved in general condition with only one shot on the target, which is suitable for the measurement of the ground response.

The preferred locations for levels should be close to the targets and out of the settlement influence zone of the crane; 10m to 30m from the targets is the most desirable distance. A benchmark or reference point is also used to check the movement of the level and eliminate the influence of it.

The targets used in the settlement monitoring were originally made of 60cm long lath mounted with 2 measuring tapes. The measuring tapes are of 0.5mm difference in major scale to achieve a higher precision. One of the problems with the targets is that the lath shrinks with time and the measuring tapes have to be readjusted. Therefore the lath was abandoned later and only one measuring tape mounted on the crane track was used as shown in Figure 6-1 since the crane slews so quickly that it is impossible to take both shots on one target at a time. Although the settlement of the ground is the main concerned, the vertical displacement of the crane track is much easier to be measured and may well represent the ground settlement because the compressive displacement of the timber mat and crane track is relatively small. The maximum track pressure of a crane is rarely over 2Mpa. The compressive displacement of a 30cm thick fir mat caused by this amount of pressure is only about 1mm. The modulus of steel is more than 300 times higher than fir mat. Therefore, the displacement within crane track due to compression is imperceptible. Even though another layer mat may be needed in some cases, since the track pressure is spread through the first layer of mat, the pressure acting on the second layer is much smaller than the first layer and the compressive displacement within the second and following layers is negligible.

Since the settlement profile along the crane track is close to a straight line, only two end points on each track need to be monitored. These two end points are chosen to be the points right above the first and last rollers contacted to the ground. Figure 6-1 also illustrates the typical layout of levels and targets for the settlement observation. Although it is of interest to put some targets along a single timber mat to find the deformation profile of the mat, it is nearly impossible to track more than three target points simultaneously during the crane lift.

The most direct and precise way to measure the track pressure of a crane is to bury several pressure meter beneath the crane track. However, it is also the most expensive way. An alternative is to calculate the track pressure rather than measurement using the manufacture's software with knowing the detailed crane load information. All the track pressure information used in the case studies is from the later one.

The crane configuration, load and lift radius can be obtained from lift plan. However, more precise information from the computer mounted on the crane is usually available and used in the evaluation of track pressure.

During the crane lift, the displacement of targets mounted on crane tracks are monitored and recorded at an interval of about 5 minutes. The detailed crane load information including the load, radius, boom orientation angle are also recorded simultaneously. These recorded information are then used to calibrate the elastic properties of soil and estimate the ground bearing capacity for crawler cranes.

6.2 Soil properties determination

The soil properties of each site were first interpreted from the site investigation reports and then calibrated by computer simulation using the observed settlement and track pressure.

Except for the Brighton Beach case, the site investigation reports of the other two sites are fairly general and for the purpose of characterizing the ground condition

of the whole site. The local soil properties may differ from the general site and need to be calibrated before performing the bearing capacity prediction.

This calibration procedure involves using two sets of computer models with one perpendicular to the crane tracks (Section A) and the other along the crane tracks (Section B and Section C) as shown in Figure 4-2. Timber mats are included in the models to represent the real work situation and avoid error from simplification. To account for the rigid effect of crane tracks, steel blocks with the same dimension of the tracks are placed onto the timber mats in those models and the track pressure is applied on the steel block rather than directly on timber mats. The modulus of the steel block is reduced properly to yield equivalent rigidity of the crane track.

Unlike models built for the track pressure spread width study, models perpendicular to crane tracks include both tracks therefore the width of the model is chosen to be 6B+S, where B is the width of the footing or the timber length and S is the span of the crane tracks. The depth of the model is set to be 2B as discussed in Chapter 4.

Although model along tracks is not very precise in simulating the real case, it is the only choice to evaluate the differential settlement of each crane track. A series measures were applied to limit the errors caused by the model to an acceptable level. These measures include:

- Spread track pressure over a wider area

Since the crane track with mat can be treated as a spread footing with a dimension of B' x L, where L is the track length and B' is the lateral spread width of track pressure. In order to model such a spread footing, the track pressure used in the model should be spread over the width B' correspondingly.

- Using proper model size

As discussed in Chapter 4, the model width along the crane track direction should be about 6L, however, the appropriate model depth should be about 2B' rather than 2L. In practice, the lateral spread width B' is usually close to the length of timber mat B. For this reason, the model depth used in case studies is chosen to be 2B for section along crane track.

- Check the simulation results with those from Section A

The best way to avoid large errors caused by the model itself when modeling sections along crane tracks is to compare the results from the model with those from model perpendicular to crane track. Since the two sets of models use the same soil properties and track pressures, settlement from those two models should be equal or close. This is also useful to testify the validity of spreading track pressure over a width area and model size used in the simulation.

The inputs and outputs of these models are the track pressures and the corresponding settlements. Although settlement is recorded at an interval of about 5 minutes in field observation, only several critical situations such as initial, load pickup, boom at a special angle are used in the computer simulation.

The soil parameters used in the models are then adjusted by trail and error to yield similar amount of settlement to that observed for each critical situation. It should be pointed out that the observed settlements are always the settlement difference from its initial situation. While the settlements from computer models are the absolute settlement. To make these two comparable, it is necessary to deduct the initial settlement from the model result.

6.3 Evaluation of soil bearing capacity using different approaches

The soil bearing capacity can be estimated with known soil properties and the dimension of footing. It is useful to compare the values of soil bearing capacity from different approach to find out which one is most suitable to evaluate the soil bearing capacity for cranes.

The first approach is to evaluate the bearing capacity from strength aspect. Using Vesić's equation (Equation 2-9) to estimate the ultimate bearing capacity of soil and then apply a factor of safety 2.0 or 3.0 to it. A factor of safety of 3.0 is usually used in foundation design for buildings and a factor of safety of 2.0 is thought to be suitable for bearing capacity evaluation for cranes.

The second approach is to evaluate the bearing capacity from settlement. The bearing capacity is determined to yield equal to or less than a certain amount of the total settlement of the footing. This certain amount of settlement is taken to be 25mm for sandy soil and 65mm for clayey soil. This approach combined with the first approach is typically used in the bearing capacity determination for building foundations.

The third approach is to evaluate the bearing capacity using the method and equations proposed in Chapter 5. And the last approach is to predict the bearing capacity from computer simulation. The ground is further loaded to yield maximum allowable settlement for cranes as calculated from Equation 4-11. Since the soil properties have been calibrated from the field observation, this approach should yield the closest result to the real value.

Comparison of the bearing capacity from these four approaches is helpful to tell which one is suitable to estimate the bearing capacity for cranes and test the validity of equations proposed in Chapter 5 from real cases.

6.4 Detail study of each case

6.4.1 400mt DEMAG CC2000 at Brighton Beach, Ontario

- Crane configuration

The project at Brighton Beach, Ontario is to install support grids for Brighton Beach Power in February 2003. Two 400mt DEMAG cranes, one CC2000 crawler crane, and a 600mt AC1600 all terrain crane were utilized for the lifts. Only the crawler crane CC2000 is studied here. Two layers of 300mm thick fir

mats were laid beneath each crane track in order to spread the track pressure over a wider area.

Two test lifts were monitored by the field persons to avoid excessive settlement for this crane. The test lift #3 involving moving the grid out of the way for future test was studied. The detailed information used in this study including the crane configuration, the track pressure, the soil properties and the settlement from computer simulation is provided in Appendix E.

- Ground condition

A detailed site investigation for this site has been carried out. Two boreholes were drilled to depths between 9.75m and 10.36m below the ground surface in the crane mat area on January 22nd and 27th, 2003. Standard penetration test (SPT) and sampling was carried out at selected intervals. In situ vane test was also carried out in soft strata. Base on the borehole logs, the strata can be simplified into 4 major layer. From the ground surface, there is a 0.9m thick sand and gravel fill over 1.5m compact silty sand, below that is 1.8m firm silty clay followed with more than 6m thick soft silty clay. The ground water level is about 1.5m from the ground. Table 6-1 and Figure 6-2 show the stratification of the ground.

Table 6-1 Soil stratification of Brighton Beach case

Depth (m)	Soil Description
0.00 - 0.88	Sand and gravel fill
0.88 - 2.43	Silty sand, compact, fine to medium, trace gravel
2.43 - 4.27	Silty clay to clayey silt, laminated, stiff to firm, grey
4.27 - 10.05	Silty clay, firm to soft, grey, some sand, trace gravel

The bottom silty clay layer only has an undrained shear strength of about 25kPa from in-situ vane test and even less (about 9kPa) from the remolded vane test. The soil is normally consolidated and may have large amount of settlement. In general, the ground condition is very poor and low bearing capacity is expected.

- Field settlement observation

The original field observation record is enclosed in Appendix C. Only several settlement records with enough information to calculate the track pressure were used in the comparison with the simulation results. The maximum settlement during the lift deviates from the initial condition of the crane about 30mm.

- Track pressure determination

Since this crane is an old model and no software is available to calculate the track pressure directly. The track pressures used in computer models were calculated by the manufacture using a program STUMAX. The crane is first assumed to be outrigger supported and with the same configuration. The outrigger load can be calculated by STUMAX with knowing the detailed crane configuration, load, radius and boom orientation. Then the outrigger loads on each side of the crane can be equivalent to the track pressure. The detailed procedure to convert the outrigger loads to track pressure is presented in Appendix D.

- Computer modeling

As stated previously, three sections shown in Figure 4-2 are modeled. The typical dimension and configuration of these models are illustrated in Figure 6-3. The properties of the timber mats used in the models are listed in Appendix A.

Assume the crawler frame is about 300mm thick for this crane, to simulate the crane track by using a steel block, the modulus of this steel block must be reduced to have the same rigidity as the crane track. The equivalent Young's modulus of this steel block should be $E' = 206GPa \cdot 0.3m / 1.5m = 41.2GPa$ for Section A and $E' = 206GPa \cdot 0.3m / 6.0m = 10.3GPa$ fro Section B and C.

The strength and elastic properties of the soils used in the models are first interpreted from the SPT test and field vane test results of the site investigation report and then calibrated using the computer models. The Poisson's ratios of

these soils are obtained from Table 4-3. No test was carried out on the sand and gravel fill. All the material parameters are obtained from other tests conducted on the same material obtained from the Syncrude Mildred lake site in Fort McMurray.

The track pressures used in models for Section B and C were spread to a wider range B'=5.7m from Equation 4-24 as discussed before.

- Result form compute modeling

After a series of adjustment to the soil properties used in the computer models, the settlement from the computer simulation should match those from field observation. However, noticeable differences exist between the two. Table 6-2 shows the comparison of these two sets of data.

Table 6-2 Comparison of settlement from field observation and computer simulation for Brighton Beach case

Crane activity	Observed settlement (mm)				Computer simulation (mm)			
	A	B	C	D	A	B	C	D
Sitting	0	0	0	0	0	0	0	0
Load on	-3	30	-13	7	2	27	-17	12
Boom over front	-2	26	-7	7	-6	24	-16	20
Boom over front right	-3	24	-5	6	-7	16	-7	22
Boom over right side	-2	21	-4	6	-2	8	3	17

The major reasons for the difference between the result of computer modeling and field observation can be attribute to:

1. The error in track pressure determination. The track pressure used in the analysis is not the real pressure but the value from theoretical calculation.
2. The error caused by the model. It has been discussed before that models along crane tracks are not very accurate in simulating the real condition and may cause some errors.
3. The ignorance of crane soil interaction. This interaction will cause track pressure redistribution and lead to more error.

4. The errors of field observation. This may involve a series of errors from the instrumentation, targets setup and the observation etc.

5. The defect in site preparation. This may cause gaps between the crane and timber mats and between the timber mats and the ground.

6. The assumptions on soils. Any simplification did on the ground and soil will cause errors in the simulation results. However, it is impossible to perform a simulation without simplification.

In general, the settlements from computer simulation are comparable to those from field observation. Another important result is that the settlement from the models for Sections B and C matches that from models for Section A very well. This shows that the use of the lateral spread width B' and the model size is appropriate.

- Bearing capacity evaluation and comparison

Detailed bearing capacity evaluation using different approaches is enclosed in Appendix F. The complete load settlement curve from computer simulation is presented in Figure 6-4. The ultimate bearing capacity from load settlement curve q_u=263kPa is less than the calculated value q_u=443kPa from bearing capacity equation using weighted average method. It is because of the large difference in soil properties between each layer that may lead to large amount of error in the bearing capacity calculation using weighted average method. Table 6-3 shows the comparison of bearing capacity using different approaches. It can be found from the table that the bearing capacity from the proposed method in Chapter 5 is close to that from computer simulation. The allowable bearing capacity from settlement criterion of buildings is too conservative since the soft silty clay is normally consolidated and subjects to large total settlement. The allowable bearing capacities from conventional method (settlement of foundations), the proposed method and computer simulation result are also illustrated in Figure 6-4 to demonstrate the comparison.

Table 6-3 Comparison of bearing capacity using different approach for Brighton Beach case

Method	FS=2.0	FS=3.0	Settlement of foundations	Proposed method	Computer simulation
Allowable bearing capacity (kPa)	221	148	30	148	119

6.4.2 600mt DEMAG CC2800 at Fort Nelson, B. C.

- Crane Configuration

The project at Fort Nelson, B. C. is to replace four vessels of Duke Energy Gas Plant in June 2003. Only the replacement of vessel "G" that caused the maximum settlement of the ground is monitored. This includes two lift activities: removing the old vessel and reinstalling a new vessel.

Two DEMAG cranes are used to perform the lifts: one 600mt CC2800 crawler crane and one 150mt AC335 all terrain crane. The main lift was carried out by the CC2800 and the all terrain crane was used as a tail crane to help handling the load. Again, the information used in this study is enclosed in Appendix E as well.

- Ground condition

No site investigation was carried out specifically for the crane lifts. Only a site investigation report written in 1968 for the whole plant is available to study the ground condition. Based on the 1968 report, boreholes #23 and #26 reveal some stratification information around crane the working area. A test hole from 1963's investigation was taken to a depth of 23m in the till deposit. Bedrock should be therefore at some greater depth below ground surface in this area. Since the general ground elevation at this location is 431.75m while the existing processing plant is at an elevation of about 431m, it is believed that the top 0.75m soil was removed during the construction of the G&H train. The major subsurface stratification of this area is shown in Table 6-4. It consists of only two layers of clay till below 600mm sand and gravel fill which was used for site preparation. The till in this area is principally medium plastic clay containing numerous

pebbles and shale pieces. It has high shear strength and low compressibility due to the process of glaciations in its geological history. No ground water was observed at a depth of 5.5m from the 1968's site investigation.

Table 6-4 Soil stratification of Fort Nelson case

Depth (m)	Soil description
0.0 - 0.6	Sand and gravel fill
0.6 - 2.3	Clay till, weathered, medium consistency
2.3 - 5.4	Clay till, unweathered, stiff

A 50-100mm thick pavement for the access to the G&H train is believed to be under the right track of the crane and covered by this fill. One layer of 300mm thick fir mats is placed on the sand and gravel fill beneath each crane track.

Besides the site investigation report, load tests prior to the lifts have been done by Duke Energy at various locations around the crane working area to check the compressibility of the ground. The tests were carried out by first placing 3 pieces of 6mx1.2mx0.3m timber mats side by side on the ground and measure the level of the mats. Then 13 pieces of 10mt crane superlift counterweights were added one by one onto the mats and levels were taken at a certain intervals. The results from load tests were used in soil properties calibration as well.

- Field settlement observation

One level was set at each side of the crane to monitor the settlement. Four targets were mounted on both ends of each track. Another four targets were mounted at the outside end of the timber mats to measure ground deformation away from the crane track. A benchmark was used to check the movement of the levels during observation. The layout of levels and targets and the original records of settlement observation are shown in Appendix C.

It was found that less than 1mm settlement was observed on the targets away from the crane track and most of the settlement occur right beneath the crane

track. The maximum settlement recorded during the lift is 14.4mm from the initial sitting condition of the crane.

- Track pressure determination

Track pressures used in this case study were also obtained from manufacture's calculation given the detail crane load information. However, the pressures were provided in imperial unit and the precision is 1ksf (kips/ft^2). This may cause as much as 24kPa error in the calculated track pressure.

- Computer modeling

Computer models were constructed in the same way as that for the case of the Brighton Beach. Since the crane dimension is different from that used in Brighton Beach, the equivalent modulus for the steel block used in models here are E'=41.2Gpa for Section A and E'=13.7Gpa for Section B and C by assuming the thickness of crawler frame is 400mm. The other major difference between the two sets of models for this case and for the case of Brighton Beach is the lateral spread width B' used in Section B and C. Based on the soil and mat properties, the lateral spread width used in this case should be B'=4.7m. No ground water is considered in this case since there is no evidence of low ground water table.

The load tests did by Duke Energy was modeled as well. It is useful to test the results from models for crane lifts. The model size and configuration for this case are presented in Figure 6-5.

- Result from computer modeling

The results from computer simulation show great consistency with that observed for load tests as illustrated in Figure 6-6, whereas, the settlement for the crane lifts only generally match the observation as shown in Table 6-5. Besides the reasons explained in the Brighton Beach case, other factors may cause the difference are:

1. The mats are not continuous. The actual mat layout is different from that as designed and gap between mats exists as shown in Figure 6-7.

2. The existence of pavement under the right track of the crane (Settlement point C and D).

3. The non-precision of calculated track pressure.

4. The movement of the crane. The crane traveled during the lift and the targets moved as well. This may be the reason of the large difference shown in the bottom 2 rows of the removal of old vessel "G" and the bottom row of the reinstall of new vessel "G" in Table 6-5.

Table 6-5 Comparison of settlement from field observation and computer simulation for Fort Nelson case

Removal of old vessel "G"								
Crane activity	Observed settlement (mm)				Computer simulation (mm)			
	A	B	C	D	A	B	C	D
Sitting	0	0	0	0	0	0	0	0
Load on	-9	14	-4	9	-2	13	-4	12
Boom up	-	14	-4	11	1	7	1	7
Boom over front right	-	-	-4	14	1	7	1	7
Boom over right side	-	12	4	15	2	9	1	7
Reinstall of new vessel "G"								
Crane activity	Observed settlement (mm)				Computer simulation (mm)			
	A	B	C	D	A	B	C	D
Sitting	0	0	0	0	0	0	0	0
Load on	-2	0	1	3	1	2	5	5
boom over front right	-	-	0	4	2	1	5	5
Boom over front	3	3	1	1	2	1	7	6
Boom down	2	7	1	4	-3	6	3	11

Again, the settlements from the computer simulation are in general comparable to those from field observation. And the use of the lateral spread width B' and the model size is shown to be appropriate for this case.

- Bearing capacity evaluation and comparison

Same as the Brighton Beach case, detailed bearing capacity evaluation using different approaches was also carried out and enclosed in Appendix F. The comparison of the results is shown in Table 6-6. A complete load settlement curve from computer simulation along with the allowable bearing capacities using different approaches are presented in Figure 6-8. It can be found from the table that the bearing capacity from proposed method in Chapter 5 is again much closer to that from computer simulation. Comparing to the ultimate bearing capacity from computer simulation, an overall factor of safety of 3.4 is appropriate for this case. The bearing capacity from settlement criterion of buildings is too conservative and a factor of safety of 2.0 seems to overestimate the soil bearing capacity without any consideration to the settlement of the crane.

Table 6-6 Comparison of bearing capacity using different approach for Fort Nelson case

Method	FS=2.0	FS=3.0	Settlement of foundation	Proposed method	Computer simulation
Allowable bearing capacity (kPa)	734	489	200	315-368	327

6.4.3 1250mt DEMAG CC8800 at Fort McMurray, Alberta

- Crane Configuration

A 1250mt DEMAG CC8800 crane was utilized to perform several heavy lifts for the installation of large vessels at the Coker Plant for the Syncrude UE-1 project at Fort McMurray, Alberta.

Total three lifts were monitored and studied including the lift of a 550mt fractionator on November 26th, 2003, the lift of the upper part of burner vessel 340mt BX-2 on December 08th, 2003 and the lift of upper part of reactor vessel 390mt RX-3B on January 11th, 2004. The detailed information used in this study is also enclosed in Appendix E.

- Ground Condition

The geotechnical investigation report prepared by Thurber Engineering Ltd. on March 30th, 2001 for the whole UE-1 project was used to determine the ground condition of the crane working area. Boreholes Tel007, Tel008 Tel009 and Tel034 represent the soil profile around that area. Figure 6-9 illustrates the layout of the crane and the soil stratification. Since the final ground is about 1.8m higher than that from the borehole logs, the ground is believed to have been raised by sand and gravel fill as suggested in the site investigation report. Therefore, total five layers of soils are involved in this area as listed in Table 6-7.

Table 6-7 Soil stratification of Fort McMurray case

Depth (m)	Soil Description
0.00 - 1.80	Sand and gravel fill
1.80 - 2.40	Sand fill, compact, fine to medium, brown
2.40 - 4.60	Native sand, compact to very dense, fine to coarse, brown to grey
4.60 - 5.80	Clay till, very stiff, dark grey, sandy, silty, occasional sand lens
5.80 -	Oilsand, very dense, dark brown-black, with siltstone interbedded

The observed ground water table is about 0.6m below the original ground surface and therefore should be at a depth of 2.4m from the raised ground.

- Crane mats layout

Three layers of crane mats under each crane track were used in the lift of fractionator. They are 6m long mora mats, 6m long fir mats and 9m long fir mats from top to bottom.

For the other two lifts, only a layer of 6m long mora mats on a layer of 6m long fir mats were placed over the crane working area. However, four pieces of 300mm thick 6m x 3m steel mats instead of mora mats were used at both ends of each track to reduce the tilting of the crane.

Another special feature of the crane mats layout for the lift of BX-2 and RX-3B is that the mats are not perpendicular to the crane tracks but at an angle about 45° to the crane tracks. But this can not be modeled in a 2-D program and the mats are assumed to be perpendicular to the tracks in the models.

- Field settlement observation

Since the crane track is about 2.7m high, it is convenient to tape the measuring targets directly on the crane track. This is believe to be simple and will cause less error. Due to the limitation of the working space, only one level was used in the monitoring of the lift of fractionator and the lift of BX-2. The original survey records and layout of targets for these three lifts are also enclosed in Appendix C.

- Track pressure Determination

Similar to the Fort Nelson case, the track pressures for these three lifts were calculated by the manufacture providing the detailed load information and crane configuration.

- Computer modeling

Since the ground condition and mat layout for the lift of BX-2 and RX-3B are all the same. Only two sets of models need to be built for the three lifts. Similar to the previous two cases, three sections were modeled for each set of models as well. Following the principle that was used in modeling the crane tracks, the equivalent modulus was also applied to model the steel mats. The configuration and dimension of the models are shown in Figure 6-10 and Figure 6-11.

A lateral pressure spread width of B'=6.0m calculated from Equation 4-24 based on the soil and mat properties is used for Section B of both sets of models.

- Result from computer modeling

The comparison of settlement from computer simulation and field observation is presented in Table 6-8. From the table it can be found that the computer simulation generally matches the field observation for all the three lifts. Most difference between these two can be attributed to the reasons as discussed in the Brighton Beach case and the Fort Nelson case.

Table 6-8 Comparison of settlement from field observation and computer simulation for Fort McMurray case

Lift of fractionator								
Crane activity	Observed settlement (mm)				Computer simulation (mm)			
	A	B	C	D	A	B	C	D
Sitting	0	0	-	0	0.0	0.0	0.0	0.0
Partial load on	-2.9	3	-	17.2	-0.3	3.7	1.6	4.7
Full load on	-6.2	13	-	31.8	-6.2	15.1	-0.4	18.6
Boom over front right	-6.1	13.5	-	35.6	-4.7	12.1	2.6	17.0
Lowering load	-6.3	13.4	-	35.4	-4.0	10.1	4.6	16.4
Lift of burner BX-2								
Crane activity	Observed settlement (mm)				Computer simulation (mm)			
	A	B	C	D	A	B	C	D
Sitting	0	0	-	0	0.0	0.0	0.0	0.0
Full load on	-1.8	7.8	-	6.1	-0.2	9.7	-3.3	7.5
Boom over front	-	7.5	-	6.7	-0.2	9.7	-3.3	7.5
Lowering load	-2.3	7.1	-	8.2	-1.1	9.5	-3.3	7.5
Lift of reactor RX-3B								
	Observed settlement (mm)				Computer simulation (mm)			
	A	B	C	D	A	B	C	D
Sitting	0	0	0	0	0.0	0.0	0.0	0.0
Full load on	0.8	4	-0.5	2.2	2.4	6.1	-0.6	4.7
Boom over front	0.2	3.8	-0.6	3.3	2.4	6.1	-0.8	3.9
Lowering load	0.1	3.7	-0.5	3.7	3.3	6.3	-0.8	3.9

A maximum settlement of more than 35mm was observed at the front right corner of the crane during the lift of fractionator and only about 18mm was calculated using the computer model. This settlement occurred while the main boom of the crane slew over its front to right corner. At this boom orientation, the settlement of the front right corner should be equal or a little bit higher than that of the front left corner of the crane. But the observed settlement of the front left corner of the crane is only 13.5mm, which is again far less than the observed settlement of the front right corner. The existence of open gap within layers of crane mats may be the possible reason in explaining this large excessive settlement observed. The timber mats may suffer distortion due to weathering and gap may exist between each layer of mats. Most of the gaps may be closed with the preload of the crane.

However, the use of three layer timber mats increases the chance of open gap and may cause excess movement due to gap closure. The deflection of the top layer mats shown in Figure 6-12 may support this point.

- **Bearing capacity evaluation and comparison**

Detailed bearing capacity evaluation using different approaches was also carried out and enclosed in Appendix F. The comparison of the results is shown in Table 6-9. A complete load settlement curve from computer simulation along with the allowable bearing capacities using different approaches are presented in Figure 6-13. It can be found from table 6-9 that Equation 5-6 proposed in Chapter 5 is closer to that from computer simulation. An overall factor of safety for this case is about 3.6 comparing to the ultimate bearing capacity from computer simulation. Using settlement criteria for foundations and Meyerhof's method will underestimate the bearing capacity for cranes. Since the ground is mainly comprised of sand and gravel, a factor of safety of 3.0 could also overestimate the soil bearing capacity.

Table 6-9 Comparison of bearing capacity using different approach for Fort McMurray case

Method	FS=2.0	FS=3.0	Settlement of foundation	Meyerhof's method	Proposed method	Computer simulation
Allowable bearing capacity (kPa)	1054	703	400	370	583	597

6.4.4 Summary of case studies

All these three cases illustrate that the use of 2-D program in modeling the 3-D bearing capacity problem can yield reasonable results by using proper model size. To determine the bearing capacity for crawler cranes by using a settlement criterion typically for building foundations is usually too conservative and not suggested to use. And to evaluate the soil bearing capacity for cranes by simply using a factor of safety of 2 or 3 can either overestimate or underestimate it. A FEM or FDM analysis will provide an appropriate estimation of soil bearing

capacity for crawler cranes. A suitable alternative is to using the method proposed in Chapter 5, which is proved by these cases to yield close result to that from a FEM or FDM analysis.

Using more than two layers of timber mats is not recommended since it may cause more open gaps within the mats. And computer simulation of the fractionator lift shows that the use of 9m long mats at the bottom layer does not contribute too much in the bearing capacity increase.

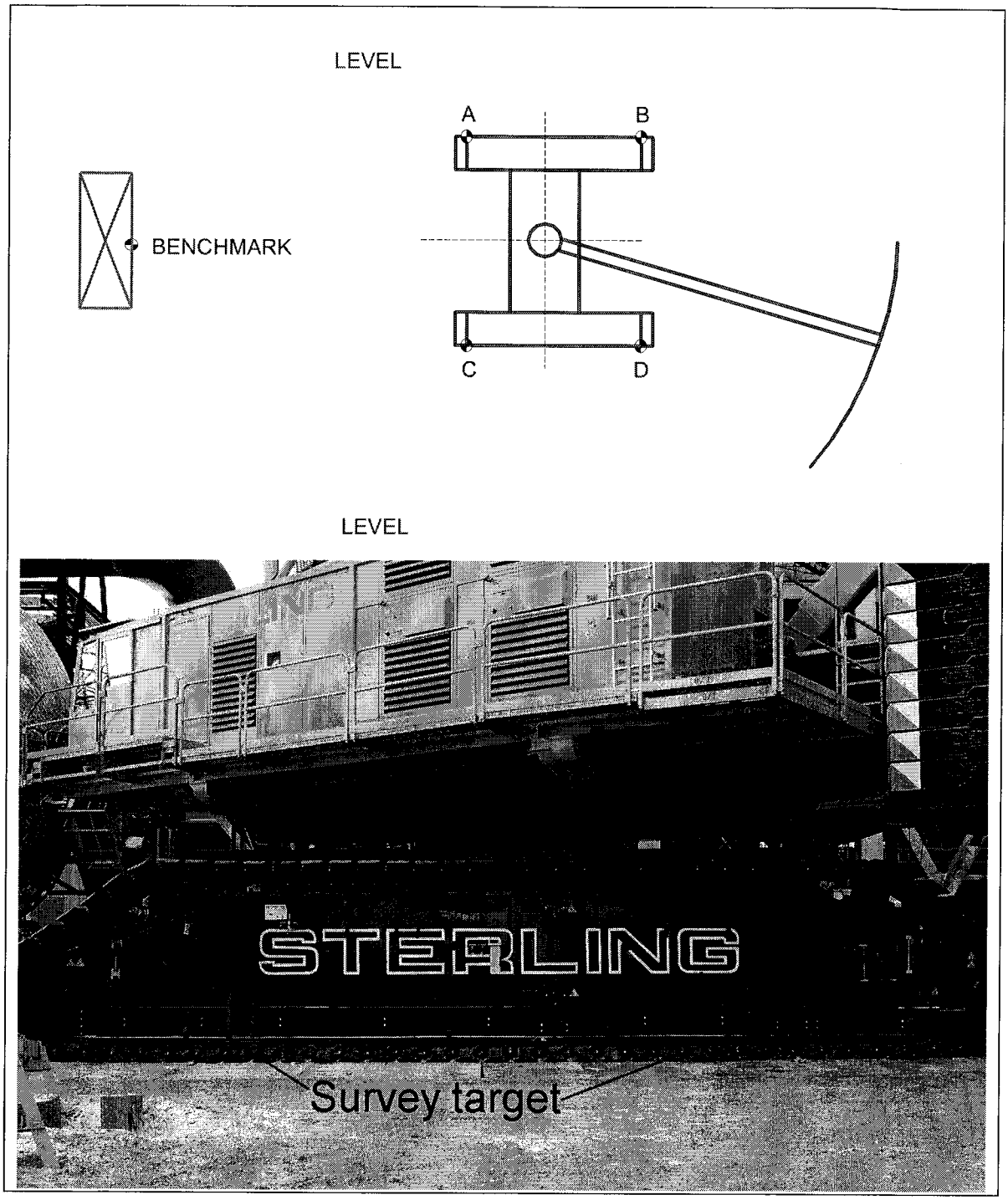

Figure 6-1 Typical level and targets layout for settlement observation

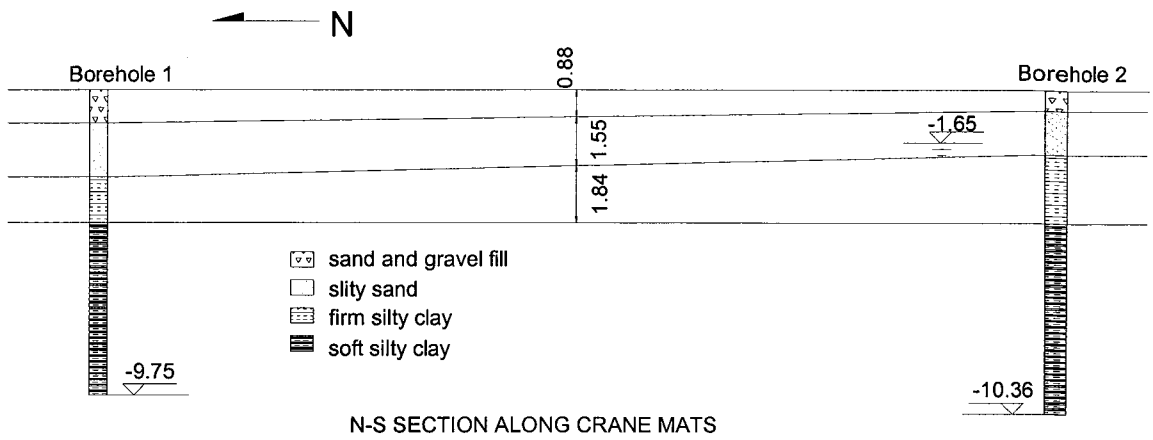

Figure 6-2 Soil stratification of Brighton Beach case

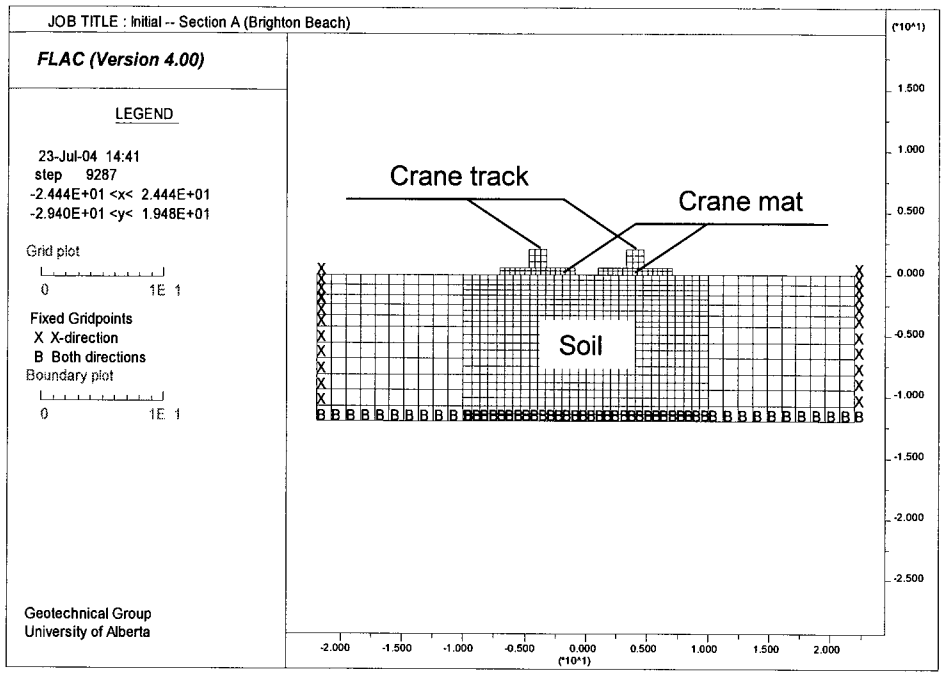

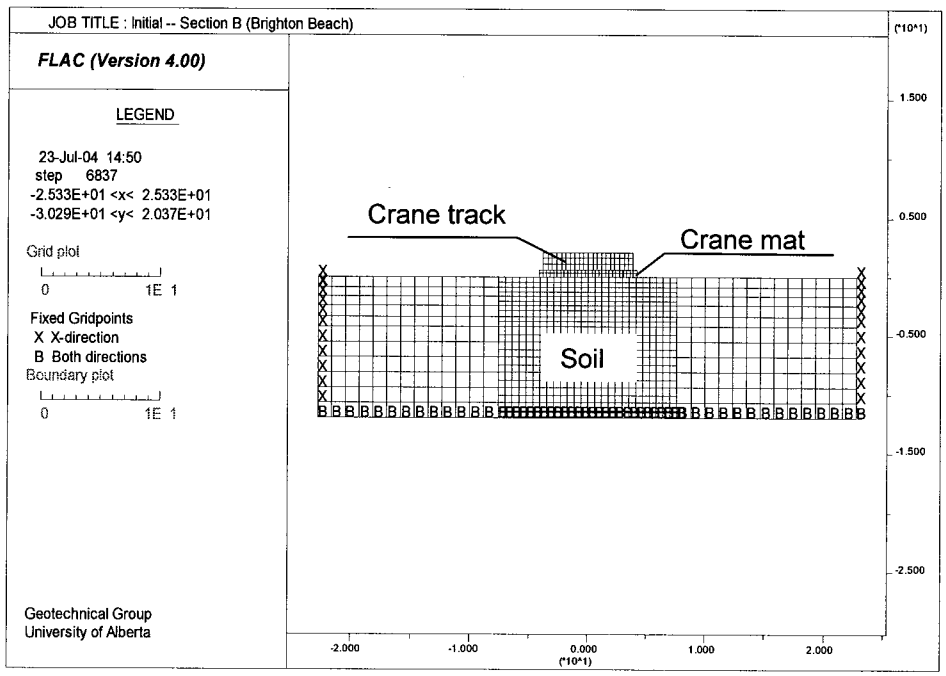

Figure 6-3 Model configuration for Brighton Beach case

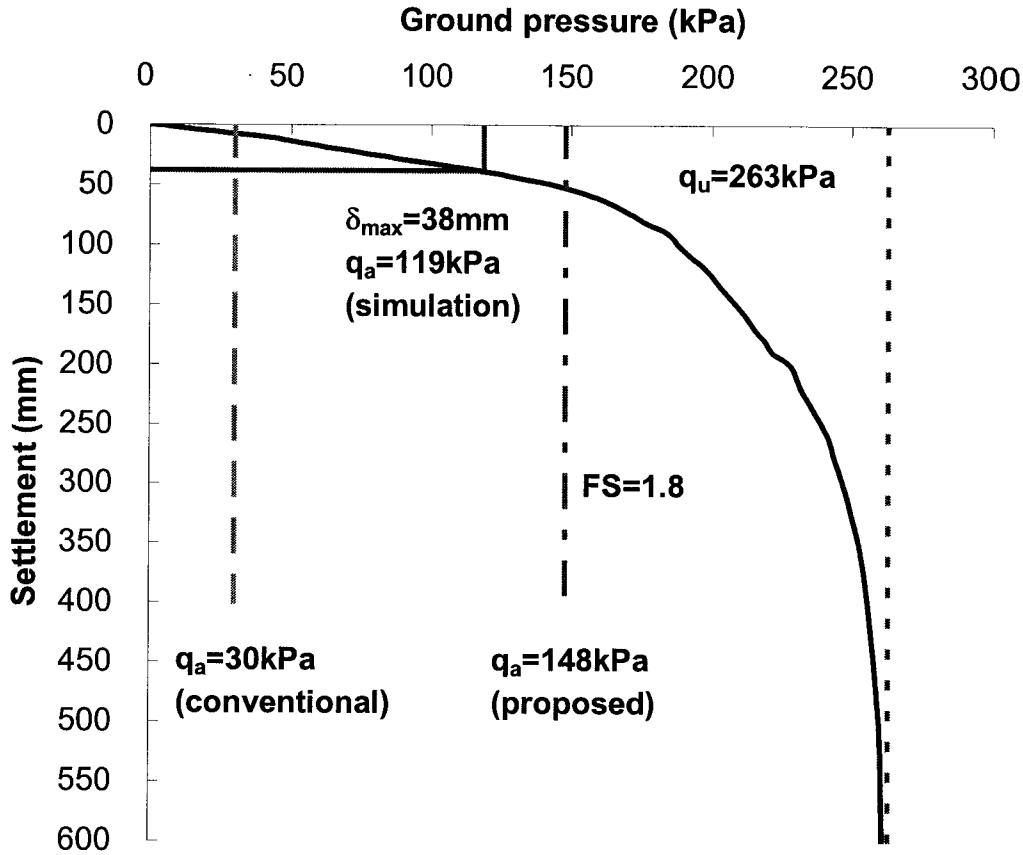

Figure 6-4 Load settlement curve for Brighton Beach case

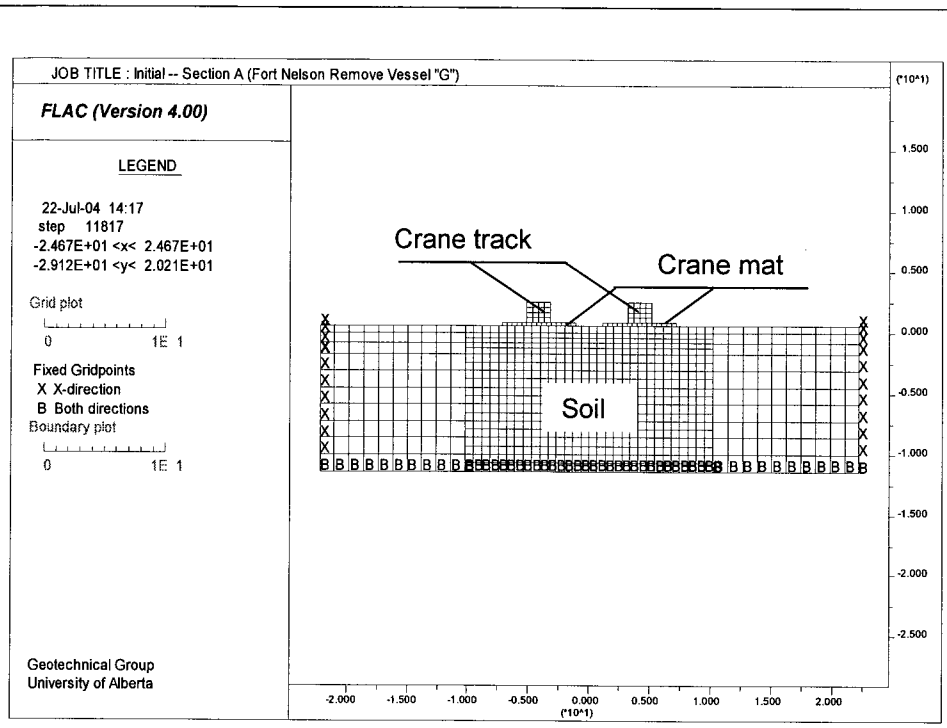

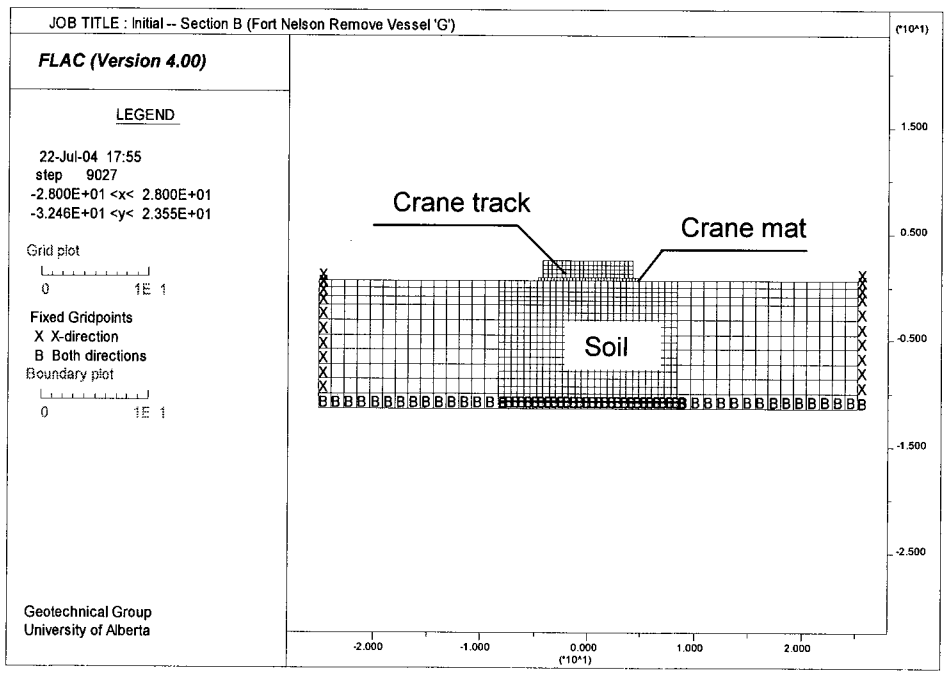

Figure 6-5 Model configuration for Fort Nelson case

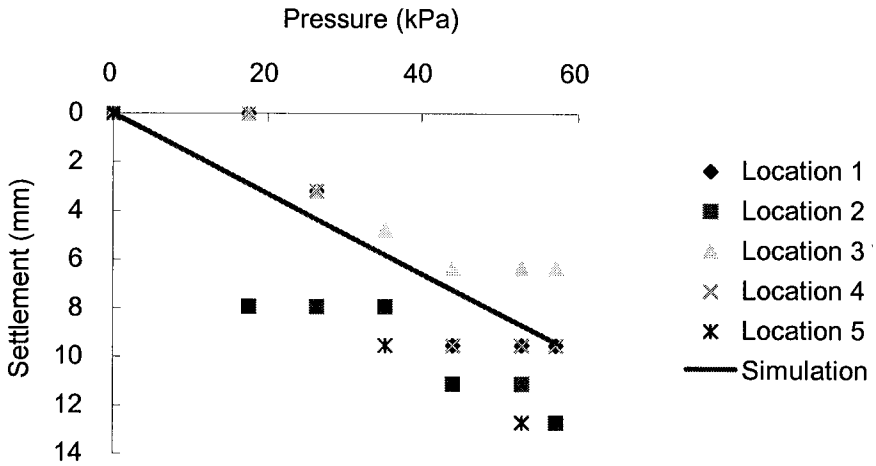

Figure 6-6 Comparison of settlement from field observation and computer simulation for the load test at Fort Nelson

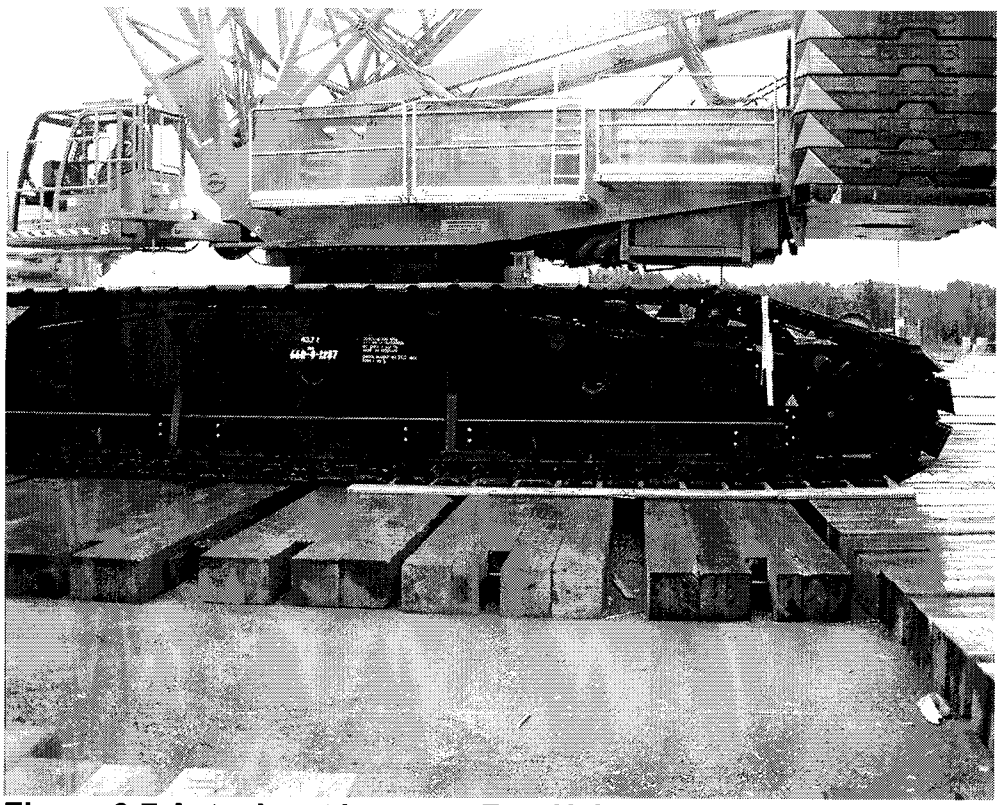

Figure 6-7 Actual mat layout at Fort Nelson

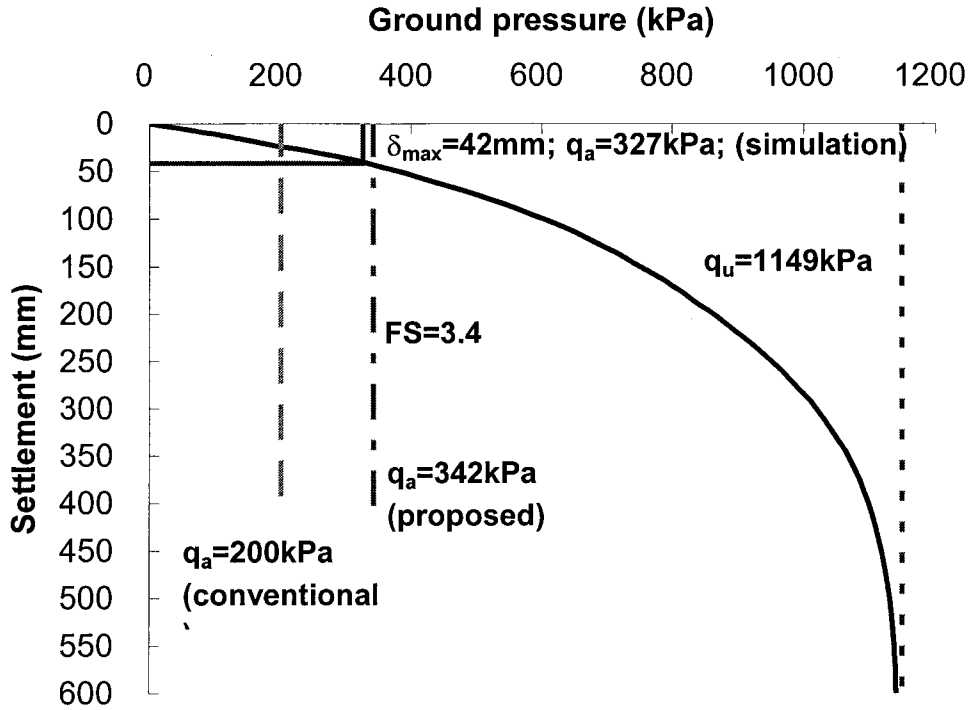

Figure 6-8 Load settlement curve for Fort Nelson case

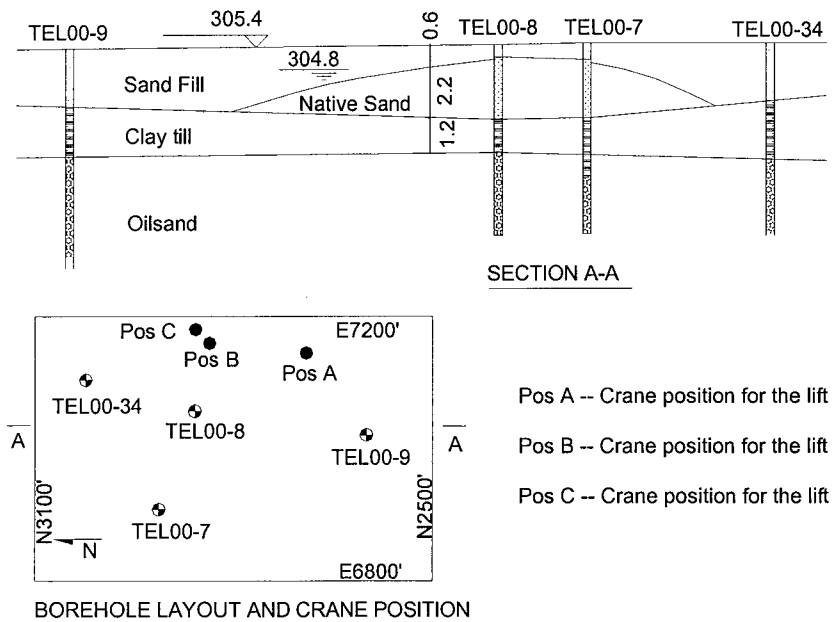

Figure 6-9 Crane layout and soil stratification of Fort McMurray case

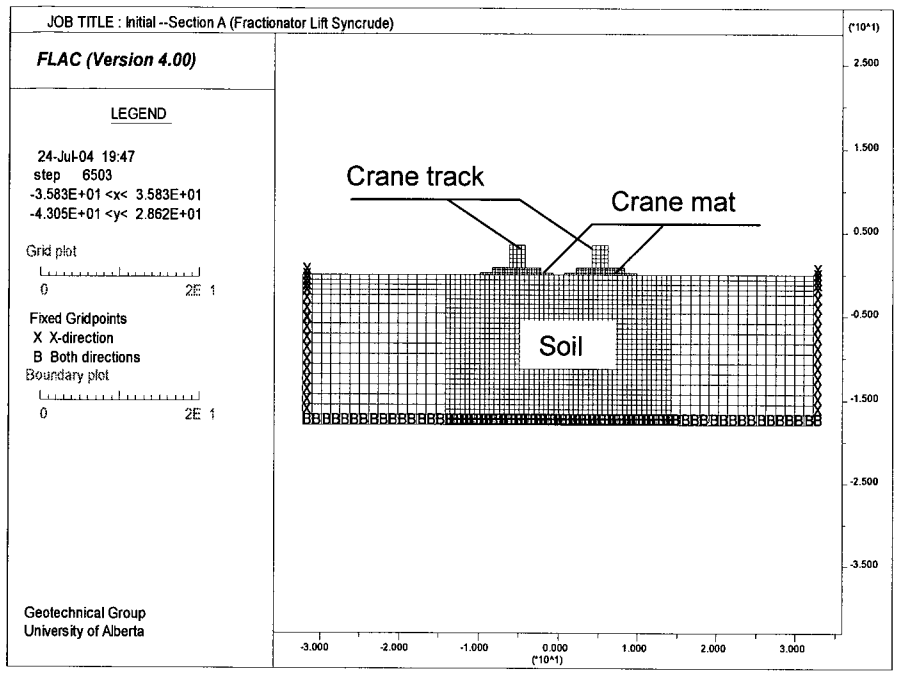

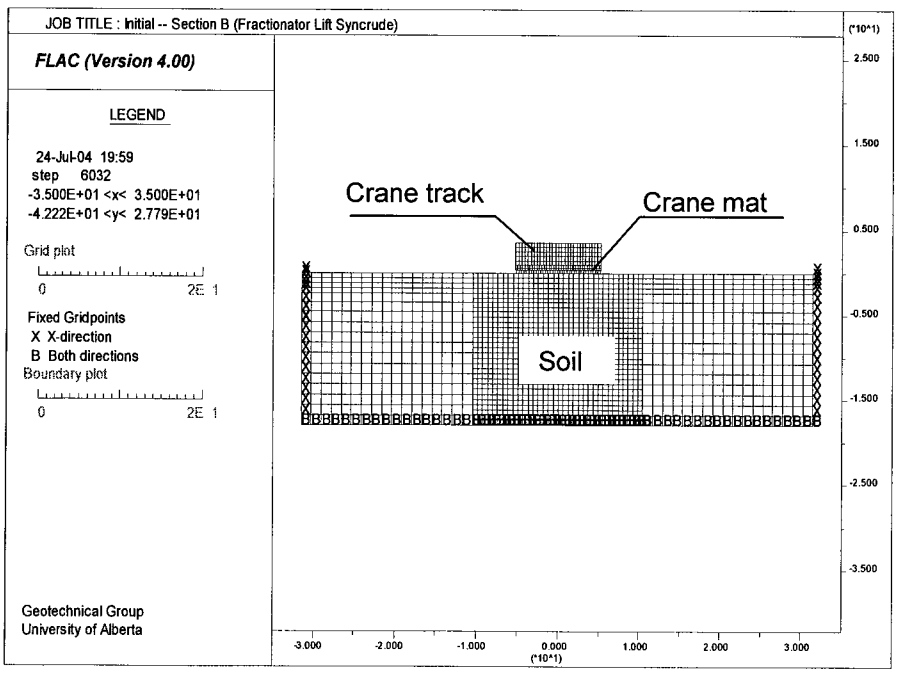

Figure 6-10 Model configuration for the Fractionator lift at Fort McMurray

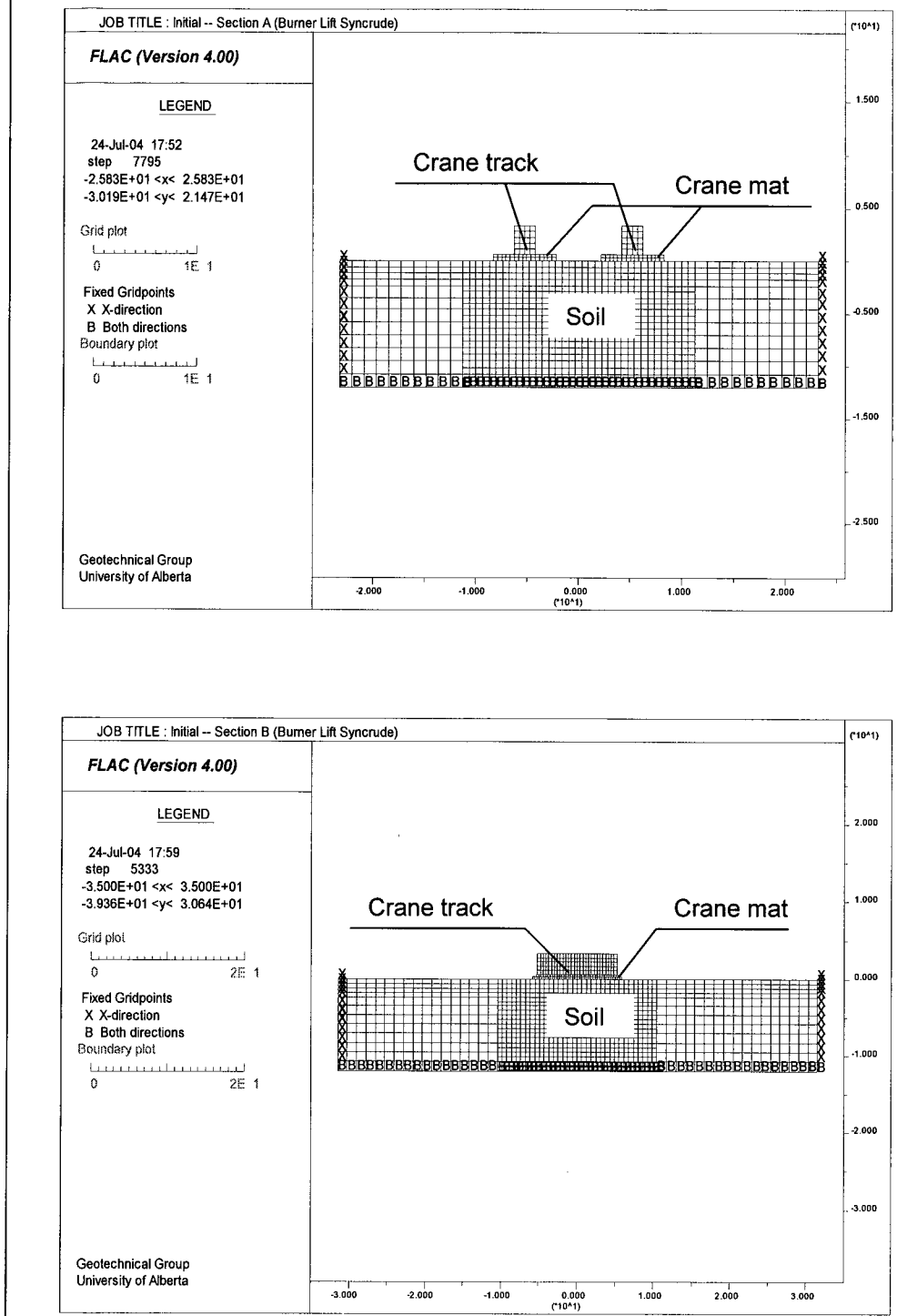

Figure 6-11 Model configuration for the lift of burner and reactor at Fort McMurray

Figure 6-12 Deflection of timber mats during the lift of fractionator at Fort McMurray

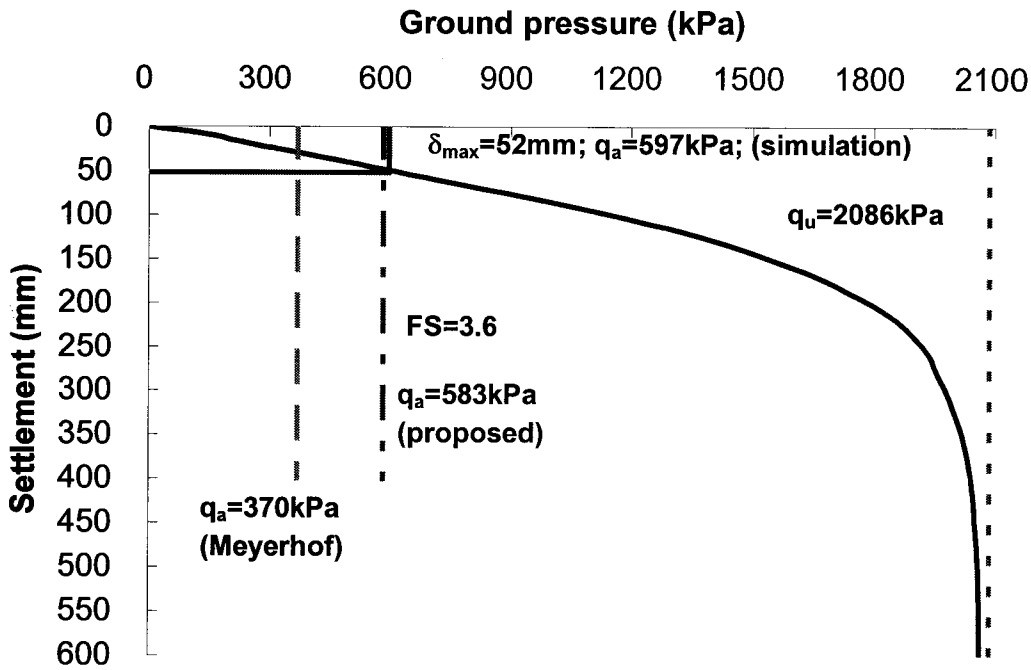

Figure 6-13 Load settlement curve for Fort McMurray case

7 CONCLUSION AND RECOMMENDATIONS FOR FURTHER RESEARCH

One of the major contributions of this study is the conversion of a crane problem to a shallow foundation problem. The relationship of these two problems was being explored. Both analytical and field studies have been carried out in the determination of soil bearing capacity for crawler cranes. Only two typical scenarios were studied: cranes sitting on the ground surface without mats and cranes supported by timber mats under each track.

The crane tracks or tracks with mats can be treated as two separate spread footings. The major difference between these two cases is the footing width used in bearing capacity determination. The length to width ratio L/B of a footing plays a very important role in affecting the performance of the footing.

The out of levelness of a crawler crane during its operation should be within 1%. A 0.5% may be due to the uneven ground surface during site preparation and another 0.5% is assumed to be the maximum allowable tilting caused by the differential settlement of the ground. This maximum allowable tilting can be converted to the maximum allowable settlement of the ground by using Equation 4-11 and Equation 4-12.

The crane track pressure is usually not equally distributed over the track length. A uniformly distributed equivalent pressure is proposed in Equation 4-18 to simplify it and suggested to use in the bearing capacity determination.

The lateral spread width of crane track pressure through timber mats is of great importance in this study. Equation 4-24 provides a general form to estimate this width. This width is treated as the width of the spread footing to simulate the track with mats scenario as well.

Directly applying the traditional bearing capacity calculation used for building foundations to crawler cranes is proven to be not appropriate and may lead to large amount of error. The bearing capacity calculated from allowable settlement for buildings is usually too conservative. And simply using a factor of safety of 2.0

or 3.0 without any consideration of settlement may either overestimate or underestimate the bearing capacity for crawler cranes.

Back analyses of the three cases provide good support to the use of equivalent pressure, lateral spread width and model size for computer simulation. It is also important to testify the validation of method proposed in the estimation of bearing capacity for crawler cranes.

The ground is classified into 3 categories: soft clay, stiff clay and sand and gravel for the convenience of bearing capacity evaluation.

For saturated soft clay and stiff clay, Equation 5-8 with a factor of safety of 2.0 is appropriate to estimate the bearing capacity for cranes with mats. The footing width B used in Equation 5-8 is the lateral spread width B' defined in Equation 4-24. If the ground water is more than 2B' below the ground surface, this factor of safety should be replaced by 3.0 to 3.5. If the crane is sitting directly on the ground surface without mats, a factor of safety of 2.0 could be always used despite the ground water conditions for stiff clay. It is not suggested to use crane without mats on soft clay.

For sand and gravel, Equation 5-7 and Equation 5-5 is applicable for cranes without mats with and without the influence of ground water. A linear interpolation may be carried out to evaluate the bearing capacity while the ground water is at an intermediate depth. Equation 5-6 is suitable for crane with mats despite the ground water condition.

For layered soils, it is suggested to perform a FEM or FDM analysis to determine the bearing capacity for cranes. If the variation of soil properties is not too much between each layer, a weighted average of the soil parameters by depth might be applicable and provides reasonable estimation.

A typical design procedure used for the estimation of ground bearing capacity for crawler cranes is suggested in Figure 7-1.

Future study on bearing capacity for crawler cranes and other large mobile equipments might focus on the advantageous weathering effect of top layer soil since those equipments are sitting directly on the ground and the top layer of soil has great impact on the ground bearing capacity. Another research direction is to perform more sophisticated three dimensional computer modeling to eliminate errors arose from track pressure simulation, 2-D simulation and other simplifications. Since the crane track pressures used in this study are only from calculation and may contain certain amount of error, it is recommended to measure the actual track pressure distribution by burying pressure cells beneath the crane track in the future lift studies.

DISCLAIMER

The study on soil bearing capacity for crawler cranes only focuses on the general situation where a crane is sitting directly on flat ground or with mats beneath its tracks to spread the track pressure over a wider area. The conclusion made in this study is only valid with crane staying far enough from any slope surface or underground facility that the crane track pressure will have no influence on stability of the slope or the performance of underground facility. The study so far is only based on normal soils and the conclusions may not be applicable for problematic soils such as sensitive clay, loose sand, loess, and organic soils. These soils may require special attention for them to support crawler cranes.

The equations proposed in this study should only be applied by experienced geotechnical engineer who understands the limitations of these equations and the ground condition within the crane influence area.

Figure 7-1 Procedures to determine the bearing capacity for crawler crane

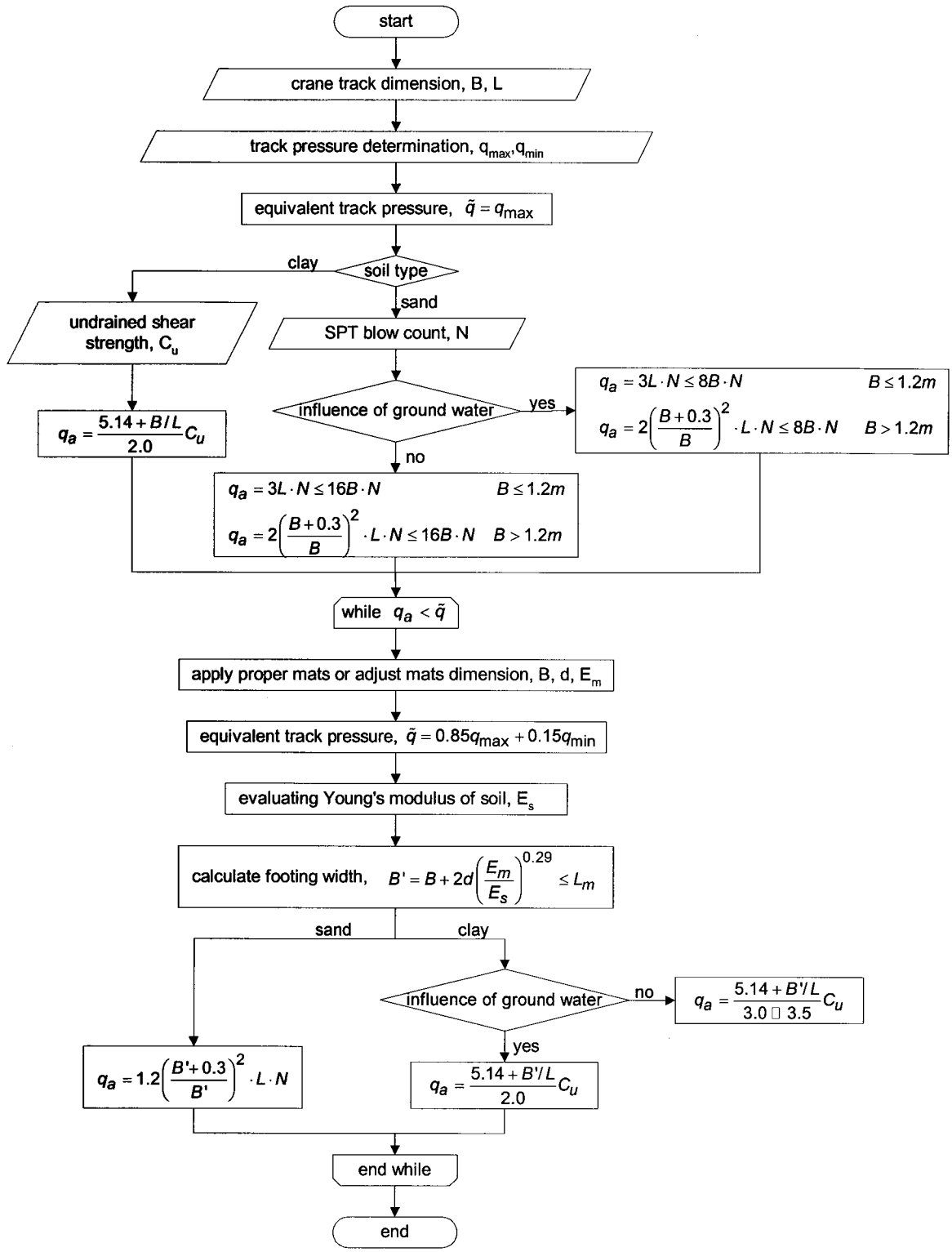

8 REFERENCES

ASME B30.5-2000, Mobile and locomotive cranes, American Society of Mechanical Engineers, New York, 2000, pp.1-28

Becker, R., The great book of mobile cranes volume 1 - Handbook of mobile and crawler crane technology, KM Verlags GmbH, Griesheim, Germany, 2001

Bowles, J. E., Foundation analysis and design, 3rd ed., McGraw-Hill, New York, 1982, pp.130-207

Bulter, F. G., Heavily over-consolidated clay, Proceedings of the conference on settlement of structures, Review paper: Session III, Cambridge, John Wiley & Sons, New York, 1974, pp.531-578

Burland, J. B., Broms, B. B. and De Mello V. F. B., Behaviour of foundations and structures, State-of-the-art report, Proc. 9th Int. Conf. Soil Mech. and Foundation Eng., Balkema: Rotterdam, Vol.3, pp. 495-546

Burland, J. B. and Burbridge, M. C., Settlement of foundations on sand and gravel, Proc. Institution of Civil Engineerings, London, 78-Part 1, pp.1325-1381

Burland, J. B. and Wroth, C. P., Settlement of buildings and associated damage, Proceeding of the conference on settlement of structures, Cambridge, John Wiley & Sons, New York, 1974, pp. 611-654

Cernica, J. N., Geotechnical engineering: foundation design, John Wiley & Sons, New York, 1995, pp.113-148

Coduto, D. P., Foundation design: principles and practices, 2nd ed., Prentice Hall, New Jersey, 2001, pp.170-300

Davis, E.H. and Poulos, H. G., The use of elastic theory for settlement prediction under three-dimensional conditions, Geotechnique, Vol.18, 1968, pp.67-91

Eslaamizaad, S., and Robertson, P. K., Cone penetration test to evaluate bearing capacity of foundations in sands, Geotechnical center, University of Alberta, Edmonton Canada, 1996

ISO 4305:1991(E), Mobile cranes - determination of stability, International Organization for Standardization, Geneva, 1991, pp.44-47

John Laing Construction Ltd. and Sir William Halcrow & Partners Ltd., Crane stability on site - an introduction guide, Construction Industry Research and Information Association, London, 1996, pp.48-50

Jumikis, A. R., Soil mechanics, R. E. Krieger, Malabar, 1984, pp. 612-653

Keenan, F. J., Shear strength of wood beams, Forest products journal, 1974, Vol. 24(9), pp.63-70

Ko, H. Y. and Scott, R. F., Bearing capacities by plasticity theory, Journal of the soil mechanics and foundations division, ASCE, Vol.99, No. SM1, Proc. paper9497, 1973, pp.25-43

Meyerhof, G. G., Penetration tests and bearing capacity of cohesionless soils, Journal of soil mechanics and foundation division, ASCE, Vol. 82, No. SM1, 1956

Meyerhof, G. G., Some recent research on the bearing capacity of foundations, Canadian geotechnical journal, Vol.1, no.1, 1963, pp.16-26

Meyerhof, G. G., The ultimate bearing capacity of foundations, Geotechnique, Vol.2, 1951, pp.301-330

Newlin, J. A., Heck, G. E. and March, H. W., A new method for calculating horizontal shear in wood beams, Eng. News-record, 1933, Vol. 110, pp.594-596

Poulos, H. G. and Davis, E. H., Elastic solutions for soil and rock mechanics. John Wiley & Sons, New York, 1974

Shapiro, H. I., Shapiro, J. P., and Shapiro, L. K., Cranes and derricks, 3rd ed., McGraw-Hill, New York, 1999

Simons, N. E., Normally consolidated and lightly over-consolidated cohesive materials, Proceedings of the conference on settlement of structures, Review paper: Session II, Cambridge, John Willey & Sons, New York, 1974, pp. 500-530

Stalnaker, J. J. and Harris, E. C., Structural design in wood - 2nd ed., Chapman& Hall, New Jersey, 1997

Stuart, J. G., Interference between foundations, with special reference to surface footings in sand, Geotechnique, 1962, Vol. 12, No.1, pp.15-22

Teng, W. C., Foundation design, Prentice-Hall, New Jersey, 1962, pp.113-191

Terzaghi, K. and Peck, R. B., Soil mechanics in engineering practice, John Wiley & Sons, New York, 1948, pp.201-217, 407-443

Terzaghi, K., Theoretical soil mechanics, John Wiley & Sons, New York, 1943, pp.118-143

Tomlinson, M. J., Foundation design and construction, 5th ed., Longman, London, 1986, pp.72-182

Vesić, A. S., Analysis of ultimate loads of shallow foundations, Journal of the soil mechanics and foundations division, ASCE, Vol.99, No. SM1, Proc. paper 9480, 1973, pp.45-73

Wood engineering handbook - 2nd ed., Forest products laboratory, Prentice Hall, New Jersey, 1990

APPENDIX A

Engineering Properties of Douglas-fir & Mora Used in Case Studies

1. Elasticity properties

Wood is an orthotropic material; that is, it has unique and independent mechanical properties in the direction of three mutually perpendicular axes-longitudinal (L), radial (R) and tangential (T).

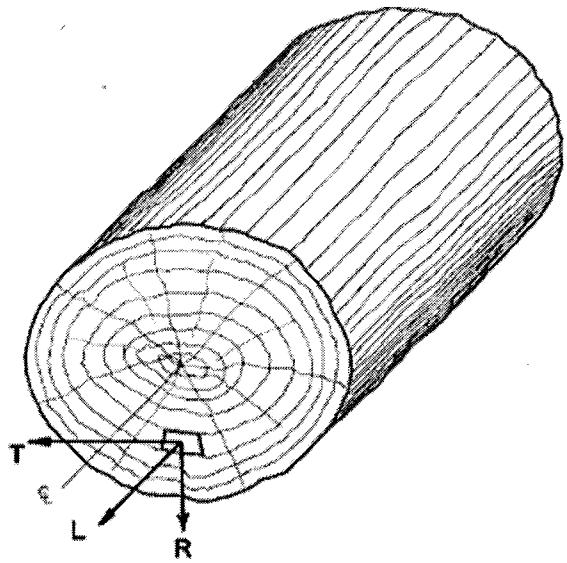

Twelve constants are needed to describe the elastic behavior, three moduli of elasticity E, three moduli of rigidity G, and six Poisson's ratio μ.

Only nine of them are independent, since $\frac{\mu_{ij}}{E_i} = \frac{\mu_{ji}}{E_j}, \quad i \neq j; i, j = L, R, T$

The longitudinal modulus of elasticity (E_L) is most commonly used, while other moduli are usually expressed as a ratio of it.

2. Strength properties

The most commonly measured strength properties are: the modulus of rupture in bending (F_b), compression parallel to grain (F_c), compression perpendicular to grain ($F_{c\perp}$), shear strength parallel to grain (F_v) and tensile strength parallel to grain (F_t).

3. Influence factors & allowable strength

There are many factors other than the material variability affecting the strength properties of wood. A series of reduction factors are used to account for the effects of moisture content, defects, load duration, and other effects related to the shape of wood element. Thus the allowable strength is considerably low in comparing to the measured strength of clear wood. The general process of adjustments needed to obtain allowable stresses for commercial timber products

can be expressed as follows where bending is used as an example (Stalnaker and Harris, 1997):

$$F_b = \left(\bar{X} - 1.645s\right) x F_{TIME} x F_{MOISTURE} x F_{DEPTH} x F_{GRADE} X \frac{1}{F_{SAFETY}} \qquad \text{(A-1)}$$

where F_b = allowable bending stress

$\bar{X}$ = average strength of small clear specimens tested wet

s = standard deviation

F_{TIME} = adjustment factor for duration of load

$F_{MOISTURE}$ = adjustment factor for moisture content

F_{DEPTH} = adjustment factor for depth

F_{GRADE} = strength ratio for the grade

F_{SAFETY} = factor of safety

Other allowable stresses have the similar form as the allowable bending stress. Although a factor of safety of only 1.3 is used in the above equation, the overall strength reduction is more than 10.0 for shear parallel to grain.

4. Typical values from literatures

Table A-1 presents typical value of engineering properties of Douglas-fir and Mora based on air-dry (12% moisture content) condition. These values are not factorized and represent the average properties of small clear specimens. No elastic ratios and Poisson's ratios are available for Mora.

5. Properties from Lab Test Result

Two 12"x12"x6.5' Douglas-fir timbers and two Mora timbers were tested on May 10, 2002 at University of Alberta Structural Lab. Another piece of 12"x4'x20' Mora mat was also tested on July 30, 2002 at Lehigh University. The major strength

properties calculated from the test results are listed in Table A-2. There is no moisture contents data from UA while the Mora mat tested at Lehigh has very high moisture content about 47%.

Table A-1 Typical engineering properties of Douglas-fir and Mora (modified from Wood engineering handbook/Forest product laboratory—2nd ed.,)

Properties	Douglas-fir	Mora
Specific gravity	0.48	0.95-1.04
Modulus of elasticity E_L (GPa)	12.2	20.4
Bending strength F_b (Mpa)	86.2	152.4
Compression parallel to grain F_c (Mpa)	47.9	81.7
Compression perpendicular to grain $F_{c_\perp}$ (Mpa)	4.3	15.9
Shear parallel to grain F_v (Mpa)	9.2	13.1
E_T/E_L	0.050	-
E_R/E_L	0.068	-
G_{LR}/E_L	0.064	-
G_{LT}/E_L	0.078	-
G_{RT}/E_L	0.007	-
μ_{LR}	0.29	-
μ_{LT}	0.45	-
μ_{RT}	0.39	-
μ_{TR}	0.37	-
μ_{RL}	0.04	-
μ_{TL}	0.03	-

TableA-2 Lab test result of Douglas-fir and Mora

	E_L (GPa)		F_b (Mpa)		F_v (Mpa)	
	UA	Lehigh	UA	Lehigh	UA	Lehigh
Mora	13.1	20.2	51.7	89.5	4.6	2.2
Douglas-fir	8.6	--	32.6	--	3.3	--

The test configuration at UA is not suitable to measure any of the three properties listed above since the timber tested is too short and the mat undergoes a combination shear and bending failure. Although Lehigh's test is appropriate to measure E_L and F_b, the high moisture content of the test sample may lead to large error of the test result, especially for the bending strength.

6. Allowable shear strength for crane mat

Timber mats are relatively week in shear parallel to grain. Shear failure causes a long horizontal split at beam mid-depth. The traditional design to prevent shear failure is to compare the actual shear stress with the adjusted allowable shear stress, which is:

$$f_v \leq F_v' \qquad \text{(A-2)}$$

where $f_v = VQ/Ib$ (for rectangular members $f_v = 1.5V/A$)

$$F_v' = C_H \cdot f_d \cdot F_v$$

F_v = allowable shear stress for typical structural timber

C_H = shear stress factor

f_d = load duration factor

The allowable shear stress is based on the assumption that a full length split is present, so if end splits are known to be minor and will not grow in length, the allowable shear stress should multiply by the shear stress factor C_H. The value of shear stress factor ranges from 1.0 to 2.0 based on the split and shakes condition of the timber ends.

Another factor accounting for the duration of load should also be applied to the allowable shear stress since the duration of maximum crane load will not last longer than 1day. The allowable shear stress should be multiplied by another factor of 1.33 for this effect.

Newlin, et. al. (1933) argued the effect of "two-beam action" would lower the horizontal shear stress. Keenan (1974) found the shear strength is a function of sheared area. All the works done by the researchers showed that the allowable shear strength is underestimated.

Deterioration of wood has less impact on the shear strength than the other properties of wood. Studies show that in early stage of decay (5 to 10% weight loss), the probable remaining shear strength is about 80% of its original strength while tension parallel to grain is only about 40% left.

In general, the allowable shear strength of timber used as crane mat might be obtained by multiplying the traditional allowable shear strength of it by a factor of 1.33 to 2.0 depending on the condition of the mat.

7. Parameters used in the study of soil bearing capacity for cranes

Although wood is a typical orthogonal isotropic material, its elastic properties in the radial direction and in the tangential direction are very close and can be treated as transverse isotropic material, especially in 2-D analysis where only properties in two directions are involved.

- Mat Geometry

The mat is typically formed by bolting four pieces of 290mm x 290mm x 6.1m timbers at an interval of 1.8m together. The influence of holes and bolts is usually ignored. Another type of mats involved in this study is formed by bolting five pieces of 290mm x 290mm x 9.1m timbers together. This type of long mat is used for the lift of fractionator at Fort McMurray to distribute the track pressure to a wider area.

- Density

The density of mat is determined from the specific gravity at air-dry condition. That is:

$$d_{fir} = 0.48x(1+12\%)x1000 = 540(kg/m^3)$$
$$d_{mora} = 0.98x(1+12\%)x1000 = 1100(kg/m^3)$$

- Elastic parameters

90% of the modulus of elasticity of fir from Table A-1 is used in the analysis since the moisture content of the fir mat used on site (17.7%) is a little bit higher than air-dry condition. However, no reduction on the modulus of elasticity of mora mat was applied.

Other elastic parameters used in the analysis are derived from the modulus of elastic using the ratio provided in Table A-1. The ratios for mora are taken to be the same as those for fir since no further information available.

- Strength parameters

Since the allowable bending stress is about an order of magnitude higher than the allowable shear stress of the same timber and the moment acting on the crane mats is relatively low, only the allowable shear stress is concerned for crane mats. The allowable shear stress used in this study is determined from the traditional allowable shear stress by multiplying a factor of 1.5.

$$F_V' = 9.2 \times (1 - 1.645 \times 14\%) \times 0.50 / 4.1 \times 1.5 = 1.3 Mpa\ (fir)$$
$$F_V' = 13.1 \times (1 - 1.645 \times 14\%) \times 0.50 / 4.1 \times 1.5 = 1.8 Mpa\ (mora)$$

The parameters of timber mat used in the study are summarized in Table A-3.

Table A-3 Summary of timber parameters used in the study

Parameters of mat	Douglas fir	Mora
Dimension L x W X H (m x m x m)	6.1x1.17x0.29 9.1x1.46x0.29	6.1x1.17x0.29
Density (kg/m^3)	540	1100
E_L (Gpa)	11.0	20.4
$E_T = E_R = 0.059E_L$ (Mpa)	647	1205
$G_{LR} = G_{LT} = 0.071E_L$ (Mpa)	779	1450
$G_{RT} = 0.007\ E_L$ (Mpa)	76.8	143
$\mu_{TL} = \mu_{RL}$	0.04	0.04
$\mu_{TR} = \mu_{RT}$	0.38	0.38
F_v (Mpa)	1.3	1.8

APPENDIX B

Detailed Cases Cited from Burland and Burbridge for The Study of Bearing Capacity of Sand and Gravel

Case No.	Principal soil type	N	Grade	Method	Dimensions (m)			Hw (m)	Hs (m)	foundation pressure (kPa)			ρi (mm)	Δρ (mm)	ti (days)	Remarks
					B	L	D			q_{gross}	q'_{net}	Δq'				
3/A	sand	8	VI	C	3.3	14	1.8	1.6	>25		52		20		1000	
3/B	sand	8	VI	C	3.3	14	1.8	1.6	>25		52		35		1000	
6/P	sand	30	III	C	6	16	2.8	-1.5	>15		162		10.5		600	
6/R	sand	30	III	C	6	16	3.6	-2.3	>15		162		11		600	
7/A	sand	35	III	C	5.5	16	2.9	-1.6	>15.4		93		6.5		1800	
8/P	silty sand	10	V	C	2.6	22	2	0	>18		147		12		500	
12/A	silty sand	17	IV	C	5.3	53	2.6	-0.5	>14.8		121		6-12		300	
13/A	silty fine sand	15	V	C	19	19	0	1			80		52		400	
13/C	silty fine sand	15	V	C	0.8ϕ	-	0	1			78		7		1	
14	fine sand	7	VI	C	29.4ϕ	-	0	0	25		164		143		120	measured edge settlement 130mm
27	gravelly sand	47	II	C	60ϕ	-	5.2	-3.7	60	417		417	45	45	880	
30/1-7	fine/medium sand	20	IV	SPT	3	4.8	1.5	4	8		231			52	6	hard clay below 26m
30/8					3.4	5.4	1.7	4	8		247		8.1		1460	range of ρi=6.6-11.2mm
30/9-15					3.7	5.9	1.8	4	8		139-290		12.2		1460	
30/16-18					4	6.4	2	4	8		97-225		10.4		1460	range of ρi=6.4-16.5mm
30/19-30					4.3	6.9	2.1	4	8		102-161		7.5		1460	range of ρi=6.1-9.1mm
30/31-32					4.6	7.4	2.3	4	8		113-166		7.1		1460	range of ρi=3.6-11.2mm
30/33-43					4.9	7.8	2.5	4	8		97-199		5.1-8.1		1460	
30/44					5.5	8.8	2.6	4	8		139		8.7		1460	
30/45					6.1	9.8	3	4	8		161		9.4		1460	
30/46					6.4	10	3.2	4	8		150		10.2		1460	

Case No.	Principal soil type	N	Grade	Method	Dimensions (m)			Hw (m)	Hs (m)	foundation pressure (kPa)			ρi (mm)	Δρ (mm)	ti (days)	Remarks
					B	L	D			q_{gross}	q'_{net}	Δq'				
30/47-48	fine/medium sand	21	IV	SPT	6.7	11	3.4	4	8		113		14.5		1460	
30/49-50	fine/medium sand	22	IV	SPT	7	11	3.5	4	8		177		4.1-5.8		1460	
39/P	Medium sand	16	IV	SPT	2.5ϕ	-	0	10	>50	254			11		1	12 plate tests: ρ=6.3-20.5mm
39/P	Medium sand	16	IV	SPT	1.0ϕ	-	0	10	>50	245			9.9		1	4 plate tests: ρ=7.0-14.0mm
45/A	Fine to coarse sand	18	IV	C/SPT	13	32	2.1	0	19.2	193			21		488	
45/B		18	IV	C/SPT	13	27	2.1	0	19.2	193			18		580	
45/C		18	IV	C/SPT	13	23	2.1	0	19.2	193			14		488	
47/A	sand with gravel	29	III	SPT	1.2	1.2	2.6	>2.5	>20		215		2.5		1	
47/B		26	III	SPT	1.2	1.2	2.6	>2.5	>20		215		1.5		1	
47/C		18	V	SPT	1.2	1.2	2.6	>2.5	>20		215		8.6		1	
50/B	silty fine sand	20	IV	SPT	15.2ϕ	-	0.3	1.8	>8.9		33		2.8		207	
51/A-H	gravel	37	III	SPT	4	7	5	5.6	7		518		7.6-11.9		880	
52/C	sand /gravel	50	II	SPT	1.2	1.2	0.5	dry	4.1		300		4.5		1	
52/A3		30	III	SPT	0.9	0.9	1.2	3.7	6.1		300		4		1	
52/D3		20	IV	SPT	0.9	0.9	3.1	0.9	6.1		300		6.7		1	
52/J		20	IV	SPT	0.9	0.9	1.2	1.8	3.4		300		2.7		1	
57	fine sand	6	VI	C	3.5	3.5	-	>5	>14		123		90		1000	ρi=60-130mm
58/A	sandy gravel	13	V	SPT	1.1	1.1	1.2	1.5	-		78		2		125	
59/M	sandy gravel	40	III	C	1	1	0	3	>25		294		5		1	
60/B	sandy gravel	30	IV	C	21.7	22	3	0-3	>25	148			19.8		366	
60/C		25	IV	C	1	1	3	0-3	>25		196		6		1	model tests
61/A	fine sand	34	III	C	1	1	0	>2	-		220		3.6		1	model tests
61/B	compact moist sand	45	II	C	1	1	0.5	>2	-		564		4.4		1	model tests
61/C1		45	V	C	1	1	0.5	0	-		339		6		1	model tests
61/C2		45	V	C	1	1	0.5	0	-		284		4.7		1	model tests

Case No.	Principal soil type	N	Grade	Method	Dimensions (m)			Hw (m)	Hs (m)	foundation pressure (kPa)			ρi (mm)	Δρ (mm)	ti (days)	Remarks
					B	L	D			q_{gross}	q'_{net}	Δq'				
64/C	fine sand	23	IV	SPT	11	22	17	-14	18	340		160		40	520	
65	sand/gravel	25	III	SPT	1.2	1.2	0	-	-		320		2.8		1	
76	fine/coarse sand	20	IV	SPT	22.5	65	10	-2.5	>30	245-295			15-28		700	
78A	silty fine sand	5	VI	C	20	20	3	-1	32	85			116		854	
78B	silty fine sand	5	VI	C	20	20	3	-1	45	85			81		752	
81/C	fine sand	5	VI	C	0.9	0.9	0.3	deep	-		133		7.6		1	
81/D	fine sand	6	VI	C	0.9	0.9	0.9	deep	-		113		6.4		1	
81/E	fine sand	7	VI	C	1.2	1.2	0.2	deep	-		199		13		1	
81/F	fine sand	8	VI	C	1.2	1.2	0.9	deep	-		268		12.7		1	
83	sand/gravel	20	IV	SPT	17.6	84	11	-2.2	>37	240			21.2		822	
84	sand/gravel	14	V	SPT	16	43	7.3	-1.8	>23	228			17.9		488	
85	gravel/sand	10	V	SPT	20.5ϕ	-	3.5	2.5	>26	173			8		195	
87	sand/gravel	34	III	SPT	33.0ϕ	-	5.3	-2.5	8.2	216			43.8		532	
91	sand	27	III	SPT	24.4ϕ	-	0	-	-		120		14.3		7	
92/A	sand	50	II	SPT	2.1	2.4	2.4	-	-		584		4.4		1	
92/B			II	SPT	2.1	2.1	1.5	-	-		697		2.3		1	
92/C			II	SPT	1.8	2.8	1.5	-	-		575		2.7		1	
92/D			II	SPT	2.1	2.4	3	-	-		584		4.6		1	
92/E			II	SPT	2.1	4.1	3	-	-		347		1.8		1	

APPENDIX C

Original Field Observation Record for the Three Cases

Test lift #3 at Brighton Beach

Brighton Beach Power
Load Test #3: Feb.18,2003
Moving Grid out of the way for Feb. 19 test
CC-2000 in 'Initial Position' ('-' settle downward)

Time	Settlement (mm)				Remarks
	front left Point #1	rear left Point #2	front right Point #3	rear right Point #4	
13:36	0	0	0	0	Initial
14:11	-18	2	-5	6	Load on, over left front
14:13	-25	3	-6	11	
14:16	-27	3	-7	12	
14:19	-28	3	-3	13	
14:22	-29	4	-7	13	
14:25	-29	4	-7	14	raised load
14:30	-30	4	-7	14	
14:35	-30	3	-7	13	
14:40	-27	3	-7	8	start swing to right
14:42	-26	2	-7	7	load over front
14:44	-24	2	-5	5	
14:47	-24	3	-6	5	load over right corner
14:49	-24	3	-6	5	
14:52	-24	3	-5	5	
14:54	-21	2	-6	4	load over right side
15:00	-24	2	-27	18	start track back
15:08	-27	3	-29	19	
15:12	-27	2	-30	15	holding
15:17	-27	3	-29	14	
15:36	-23	4	0	10	track forward, boom over side
15:40	-24	3	0	9	
15:48	-24	4	-2	9	
16:00	-23	4	-2	8	
16:16	-23	3	-2	9	
16:38	-23	4	-1	9	
17:00	-24	4	0	9	
17:03	-27	2	-32	17	track back
17:25	-29	4	-33	16	
17:38	-28	3	-32	17	weight off

Layout of targets and levels at Fort Nelson

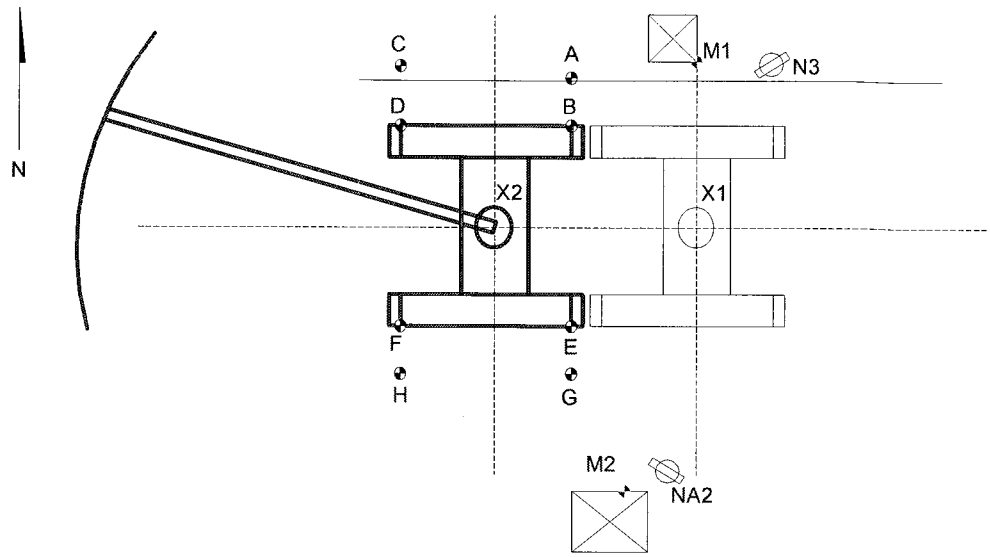

Layout of targets and levels for the lift of Fractionator at Fort McMurray

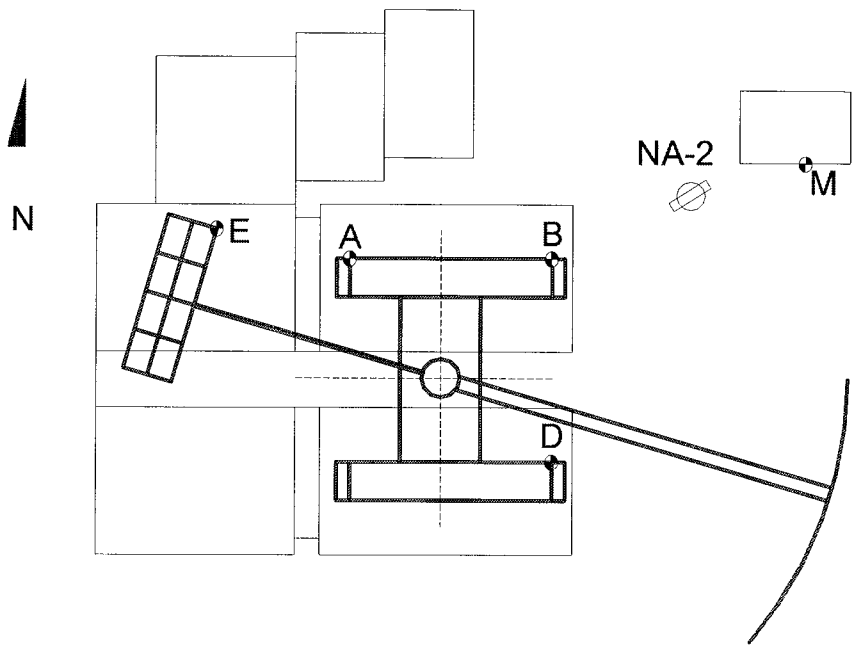

Layout of targets and levels for the lift of burner BX-2 at Fort McMurray

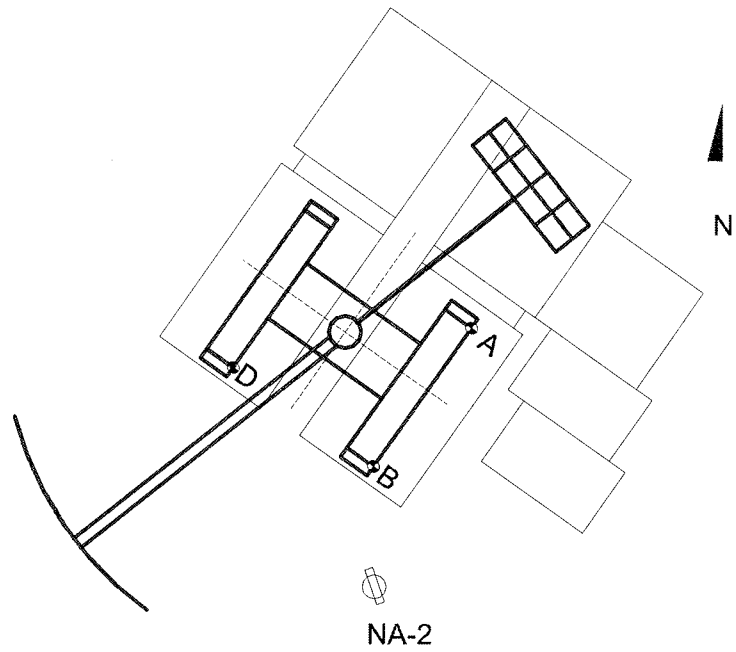

Layout of targets and levels for the lift of reactor RX-3B at Fort McMurray

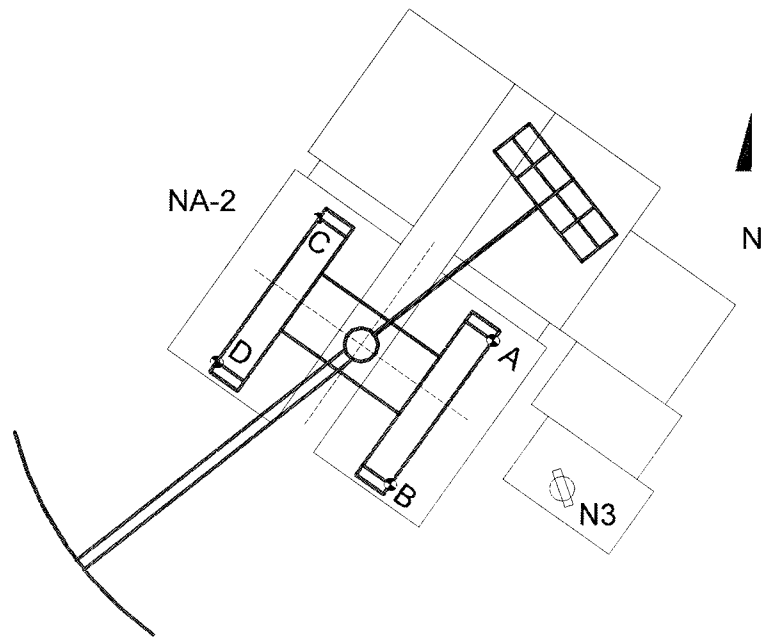

Survey record for the removal of old vessel "G" at Fort Nelson -1

Project	**Fort Nelson**
Crane	**DEMAG CC2800**
Level #	N3
Lift #	**Remove old vessel "G"**
Observer	**Xiteng Liu**
Date	**30-Jun-03**

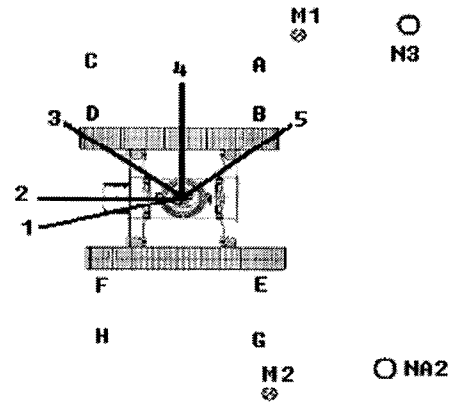

* BL -- Boom Location; unit in cm

TIME	BL	A		B		C		D		M1	Remarks
		L	R	L	R	L	R	L	R		
7:15	1	19.94	69.99	76.92	76.94	19.86	20.09	25.80	75.88	26.53	sitting at X2 position
7:55	1	19.88	69.96	76.54	76.56	19.96	20.07	26.74	76.82	26.54	load attached
8:01	1	19.89	69.94	76.51	76.54	19.96	20.07	26.74	76.82		load on
8:07	1							26.78	76.85	26.55	boom up
8:10	1							26.82	76.86		
8:26	1			76.54	76.59			26.86	76.95		start tracking back at 8:31
8:39	1			75.11	75.14			27.70	77.76	26.52	initial at X1 position
8:43	1	19.95	70.02	75.13	75.16			27.79	77.85		start slewing north
8:46	3			75.11	75.15			28.07	78.13		boom over front right
8:48								28.15	78.25		
8:50				75.79	75.82			28.06	78.14		
8:55	4			75.87	75.91			28.11	78.20		boom over right side
8:56	4			75.90	75.92			28.10	78.16		
9:02	4			75.96	76.01			28.45	78.51		slew back, increase radius
9:05								28.43	78.50	26.53	
9:41	3-4			75.87	75.90			28.23	78.29		finish

Survey record for the removal of old vessel "G" at Fort Nelson -2

Project **Fort Nelson**

Crane **DEMAG CC2800**

Level # **NA2**

Lift # **Remove old vessel "G"**

Observer **Brian Gerbrandt**

Date **30-Jun-03**

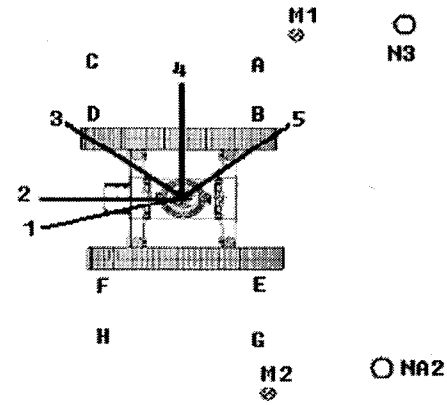

* BL -- Boom Location; unit in cm

TIME	BL	E		F		G		H		M2	Remarks
		L	R	L	R	L	R	L	R		
7:15	1	20.38	20.32	73.18	73.18	30.00	30.00	24.53	74.45	26.72	sitting at X2 position
7:55	1	19.51		74.30		30.00		24.51			load attached
8:01	1	19.52		74.61							load on
8:26	1			74.59						26.71	start tracking back at 8:31
8:39	1			79.23							initial at X1 position
8:43	1	19.40		79.36						26.72	start slewing north
8:50		19.04		79.01						26.72	
8:55	4	19.04		78.97							boom over right side
9:17	3-4	18.54		78.75						26.73	
9:41	3-4	18.75		78.59						26.75	finish

Survey record for the reinstallation of new vessel "G" at Fort Nelson

Crane	**DEMAG CC2800**
Level #	**NA2 / N3**
Lift #	**Reinstall new vessel "G"**
Observer	**Brian Gerbrandt / Xiteng Liu**
Date	**30-Jun-03**

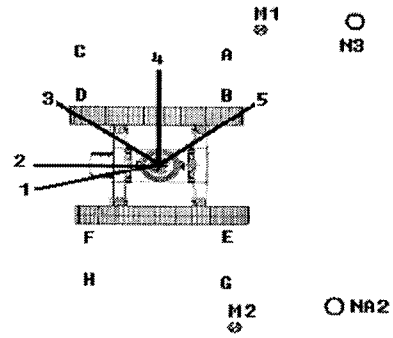

* BL -- Boom Location; unit in cm

TIME	BL	A		B		C		D		M1	Remarks
		L	R	L	R	L	R	L	R		
11:00	3-4	19.91	69.97	75.92	75.95	19.78	19.91	27.94	78.02	26.51	initial reading, no load
11:26	4			76.06	76.09			28.25	78.31		start swing back
11:31	3			75.91	75.94			28.33	78.38		boom over front right
11:35	2	19.93	69.98	76.04	76.07	19.80	19.93	28.07	78.11		boom over front
11:53	1	19.95	70.00	76.80	76.81	19.90	20.04	26.80	76.86	26.54	track to X2 position
12:05	1			76.83	76.84			27.04	77.11		boom down
12:20	1	20.00	70.04	76.79	76.82	19.87	20.08	27.09	77.17	26.56	lowering load
12:50	1	20.05	70.10	77.11	77.16	19.84	20.03	26.74	76.75	26.54	finish

TIME	BL	E		F		G		H		M2	Remarks
		L	R	L	R	L	R	L	R		
11:00	3-4	19.44		78.86		29.89		24.47	74.41	26.74	initial reading, no load
11:26	4	19.26		78.84						26.74	start swing back
11:35	2	19.73		79.11		29.87					boom over front
11:53	1	20.12		74.53						26.74	track to X2 position
12:05	1	20.01		74.88		29.85		24.52			boom down
12:10	1			74.92							
12:20	1	19.98		74.95		29.86		24.54		26.75	lowering load
12:50	1	20.71		74.25		29.86		24.5		26.75	finish

Survey record for the lift of fractionator at Fort McMurray

Project **Syncrude UE-1** Crane **DEMAG CC8800-SSL**

Lift **Fractionator** Level # **NA-2**

Date **26-Nov-03** Observer **Xiteng Liu**

* Pos -- Boom position, clockwise from front; unit in cm

* Point A is 1ft south to its original location

TIME	D	B	A	E	M	Pos (°)	Rad. (m)	Remarks
9:10	57.4	19.9	29.65	69.16	66.45	38.1	15.5	initial with riggings on
9:50	58.98	20.22	29.38	67.37		38.1	15.5	start picking up load with tail crane
10:05	59.07	20.2	29.36	67.45		38.1	15.5	
10:15	59.08	20.24	29.36			38.1	15.5	
10:16	59.12	20.2		66.63			15.5	start swing back to front
10:21	59.09	20.2	29.33			-1.8	15.5	end swing, start swing tail crane
10:35	59.16	20.25	29.34	66.52		-1.8		start booming down
10:45	59.18	20.24				-1.8		
10:50	59.4	20.35	29.3	61.42		-1.8		
10:53						-1.8	25.4	end booming, start walking tail crane
11:00	59.58	20.55	29.2	59.01		-1.8	25.4	
11:15	59.78	20.62	29.2	60.26		-1.8	25.4	
11:21	60.58	21.2	29.03	52.07		-1.8	25.4	straight vessel, tail crane off
11:25	60.63	21.28				-1.8	25.4	start lowering vessel
11:30	60.78	21.38	29.06	51.85	66.45	-1.8	25.4	holding, remove tail beam
14:40	60.84	21.53	29.06	52.81	66.43	-1.8	25.4	holding
14:46	60.8	21.53	29.12			-1.8	25.4	staring raising the vessel
14:55	60.87	21.57					25.4	start swing to right
15:00	60.95	21.4					25.4	
15:01	60.96	21.25	29.04				25.4	boom over front right corner
15:08	60.81	21.25	29.05			73.7	25.4	vessel over final position
15:15	60.94	21.24	29.02			73.7	25.4	start lowering the vessel
15:26	60.95	21.25	29.03		66.43	73.7	25.4	
15:36	60.92	21.25	29.03		66.44	73.7	25.4	

Survey record for the lift of Burner BX-2 at Fort McMurray

Project **Syncrude UE-1**

Lift **Burner BX-2**

Date **8-Dec-03**

Crane **DEMAG CC8800-SFVL**

Level # **NA-2**

Observer **Xiteng Liu**

* Pos -- Boom position, clockwise from front; unit in cm

* Points A and D are 1ft south to their original locations

TIME	D	B	A	Pos (°)	Rad. (m)	Remarks
8:07	80.76	34.43	42.74	-23	32.6	Initial with riggings
8:14	81.37	35.21	42.56	-23	32.6	load pick up
8:17	81.38	35.22		-23	32.6	
8:22	81.42			-23	32.6	
8:29	81.42	35.18		-23	32.6	start swing clockwise
8:31	81.43	35.18		0	32.6	boom over front
8:32	81.51	35.18				
8:36	81.55	35.18				
8:40	81.54	35.17	42.4	21	32.6	final position
8:45	81.52	35.14	42.5	21	32.6	
8:48	81.56	35.14	42.5	21	32.6	
8:52	81.56	35.15	42.52	21	32.6	
8:58	81.58	35.14	42.51	21	32.6	

Survey record for the lift of Reactor RX-3B at Fort McMurray

Project	**Syncrude UE-1**	Crane	**DEMAG CC8800-SFVL**
Lift#	**Reactor RX-3B**	Level #	**NA2 / N3**
Date	**11-Jan-04**	Observer:	**Brian Gerbrandt / Xiteng Liu**

* Pos -- Boom position, clockwise from front; unit in cm

* Points A and D are 1ft shorter to their original locations.

TIME	A	B	C	D	Pos (°)	Rad. (m)	Remarks
9:48	25.02	13.81	81.03	76.06	-41	29.9	sitting
10:16	25.06	14.16	80.96	76.26	-41	30.8	partial load picked up
13:28	25.1	14.21	80.98	76.28	-41	30.8	total load picked up
13:32	25.12	14.21			-41	30.8	hoist up
13:39	25.11	14.24			-41	30.8	holding for adjustment
13:41			80.98	76.28			
13:44	25.11	14.22	80.97	76.29			hoist up again
13:50	25.1	14.21					start to swing at 13:49
13:51				76.33			final position
13:52				76.39			boom over front left corner
13:55	25.07	14.22			-20	30.5	swing half way to front
13:58	25.04	14.19		76.39	0	30.5	boom over front
14:00	25.03	14.21	80.97	76.43	17.5	30.4	boom over final position
14:02	25.04	14.19			17.5	30.4	start lowering the load
14:08	25.03	14.18	80.98	76.43	17.5	30.4	holding load for 14 days

APPENDIX D

Convert Outrigger Force to Equivalent Track Pressure

Principle: Static force and moment equilibrium

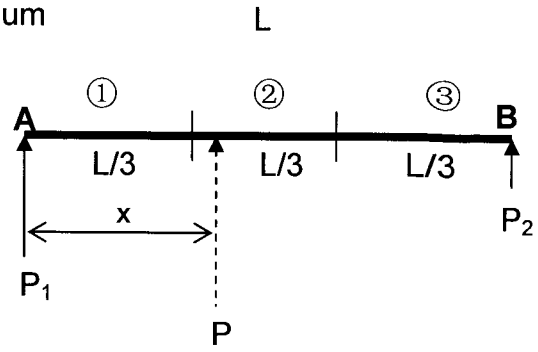

Assume the track has a length of L and width of B. Assume the force acting on outrigger 'A' is P_1 and on outrigger 'B' is P_2.

The equivalent total force and its acting point is:

$$P = P_1 + P_2$$

$$P \cdot x = P_2 \cdot L$$

$$or \quad P \cdot (L - x) = P_1 \cdot L$$

$$\therefore \quad x = \frac{P_2 L}{P} = \frac{P_2 L}{P_1 + P_2}$$

If $x \le L/3$ *or* $x \ge 2L/3$, the total force is in region ① or ③, the pressure distribution is triangular. If $L/3 < x < 2L/3$, the total force is in region ②, the pressure distribution is trapezoidal. (*Reason: triangular distributed pressure over length 'L' will have the equivalent force acting at 1/3 of the length.*)

Case 1: $0 < x \le L/3$ or $P_2 \le 1/2P_1$ (Triangular distribution)

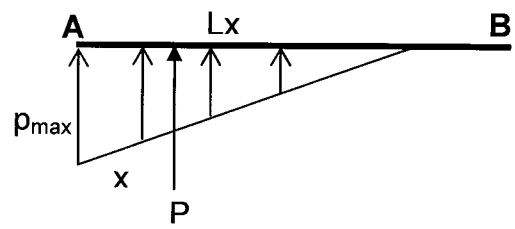

$$P = \frac{1}{2}(p_{max} \cdot L_x \cdot B)$$

$$P \cdot x = \frac{1}{2}(p_{max} \cdot L_x \cdot B) \cdot \frac{L_x}{3}$$

So, the bearing length and maximum pressure are:

$$L_x = 3x = \frac{3P_2 L}{P_1 + P_2}$$

$$p_{max} = \frac{2P}{L_x \cdot B} = \frac{2(P_1 + P_2)^2}{3P_2 \cdot L \cdot B}$$

Case 2: L/3< x< 2L/3 or $1/2P_1 \le P_2 \le 2\ P_1$ (Trapezoidal distribution)

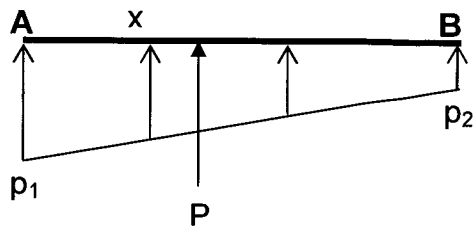

$$P = \frac{1}{2}(p_1 + p_2) \cdot L \cdot B$$

$$P \cdot x = \left[\left(\frac{p_1 + p_2}{2}\right) \cdot B \cdot L\right] \cdot \frac{L}{2} - \left[\frac{1}{2}\left(\frac{p_1 - p_2}{2}\right) \cdot B \cdot \frac{L}{2}\right] \cdot \frac{2L}{3}$$

So, the pressures at both ends are:

$$p_1 = \frac{4P_1 - 2P_2}{B \cdot L}$$

$$p_2 = \frac{4P_2 - 2P_1}{B \cdot L}$$

Case 3: $2L/3 \le x < L$ or $2P_1 \le P_2$ (Triangular distribution)

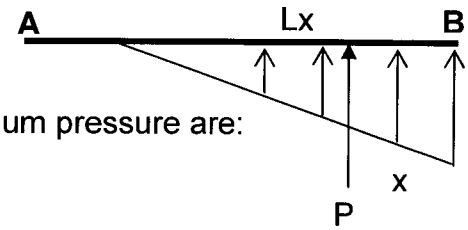

Similar to case 1, the bearing length and maximum pressure are:

$$L_x = 3(L - x) = \frac{3P_1 L}{P_1 + P_2}$$

$$p_{max} = \frac{2P}{L_x \cdot B} = \frac{2(P_1 + P_2)^2}{3P_1 \cdot L \cdot B}$$

APPENDIX E

Detailed Data Used in the Study of the Three Cases

➢ Crane configuration and load information

	Brighton Beach	Fort Nelson		Fort McMurray		
		removal "G"	reinstall "G"	Fractionator	Burner BX-2	Reactor RX-3B
Crane	DEMAG CC2000	DEMAG CC2800	DEMAG CC2800	DEMAG CC8800	DEMAG CC8800	DEMAG CC8800
Configuration	SSL	SSL/LSL	SSL/LSL	SSL	SFVL	SFVL
Boom length (m)	60	108	108	96	96	96
Mast length (m)	36	30	30	42	42	42
Jib length (m)	-	-	-	-	12	12
Jib offset angle (°)	-	-	-	-	13	13
Counterweight (t)	120	160	160	280	220	220
Central ballast (t)	-	-	-	100	-	-
SL-counterweight (t)	70 @ R13m	325 @ R15m	325 @R15m	640 @19m	640 @22m	640 @22m
Track length (m)	7.6	8.4	8.4	10.5	10.5	10.5
Track width (m)	1.5	2.0	2.0	2.0	2.0	2.0
Track span (m)	8.0	8.4	8.4	10.5	10.5	10.5
Equipment weight (t)	115	63.6	62.3	503.8	363.6	386.8
Rigging weight (t)	1.88	1.59	1.59	19.5	30.4	20.4
Load block (t)	5.55	3.59	3.59	39	39	17

➢ Crane track pressure

Crane activity	Load (t)	Radius (m)	Superstr. angle (°)	Bearing length (m)		Track pressure (kPa)			
				AB	CD	A	B	C	D
Test lift #3 at Brighton Beach									
Sitting	7.5	18	223	5.15	7.47	254	0	369.1	0
Load on	122.5	18	223	7.6	6.57	77.4	449.2	0	338.4
Boom over front	122.5	18	180	6.61	6.61	0	471	0	471
Boom over front right	122.5	18	136	6.57	7.6	0	338.4	77.4	449.2
Boom over side	122.5	18	90	7.6	7.6	125.6	115.3	294.3	284
Removal of old vessel "G" at Fort Nelson									
Sitting	5.17	66.4	182.9	8.4	8.4	287.4	0	287.4	0
Load on	68.7	66.4	182.9	8.4	8.4	95.8	383.2	47.9	383.2
Boom up	68.7	58.1	182.9	8.4	8.4	239.5	191.6	239.5	191.6
Boom over front right	68.7	58.1	134.5	8.4	8.4	239.5	191.6	239.5	191.6
Boom over right side	68.7	58.1	101.8	8.4	8.4	239.5	239.5	239.5	191.6
Reinstall new vessel "G" at Fort Nelson									
Sitting	5.17	70.1	123.4	8.4	8.4	239.5	191.6	143.7	95.8
Load on	67.5	58	102	8.4	8.4	239.5	239.5	239.5	191.6
Boom over front right	67.5	58	152	8.4	8.4	287.4	191.6	239.5	191.6
Boom over front	67.5	58	182.9	8.4	8.4	287.4	191.6	287.4	191.6
Boom down	67.5	66.4	182.9	8.4	8.4	95.8	383.2	95.8	383.2
Lift of fractionator at Fort McMurray									
Sitting	58.5	15.6	141.9	10.5	7.78	719	0	527	0
Partial load on	287	15.6	141.9	10.5	10.5	671	191.6	527	96
Full load on	584	26.1	181.8	10.5	10.5	288	767	288	767
Boom over front right	564	26.1	141.9	10.5	10.5	383	623	431	671
Lowering load	564	25.8	106.3	10.5	10.5	431	527	527	623
Lift of burner BX-2 at Fort McMurray									
Sitting	69.4	32.6	203	10.5	10.5	479	48	575	96
Load on	433	32.6	203	10.5	10.5	336	623	288	575
Boom over front	433	32.6	180	10.5	10.5	336	623	336	623
Lowering load	433	32.6	159	10.5	10.5	288	623	336	623
Lift of reactor RX-3B at Fort McMurray									
Sitting	37.5	29.9	221	10.4	10.5	431	0	575	96
Load on	332.8	30.8	221	10.5	10.5	479	336	479	383
Boom over front	332.8	30.5	180	10.5	10.5	479	336	479	336
Lowering load	332.8	30.4	162.5	10.5	10.5	527	336	479	336

➢ Soil properties from site investigation report

Brighton Beach

	Sand and gravel fill	Silty sand	Firm silty clay	Soft silty clay
Thickness (m)	0.88	1.55	1.84	>5.78
Unit weight γ (kN/m^3)	22.5	18.5	17.7	16.7
Relative density Dr (%)	-	85	-	-
Water content w (%)	7	11	24	43
Plastic limit PL (%)	--	--	--	23
Liquid limit LL (%)	--	--	--	50
SPT blow count N_{60}	--	24	6	1
Triaxial Cu (kPa)	--	--	--	31
In situ vane Cu (kPa)	--	--	65	25
Remold vane Cu (kPa)	--	--	32	9

Fort Nelson

	Weathered till	Unweathered till
Thickness (m)	1.7	>3.8
Unit weight γ (kN/m^3)	19.8	19.8
Moisture content w (%)	15-23	14-17
Plastic limit PL (%)	16-20	
Liquid limit LL (%)	31-57	
Initial void ratio e_0	1	
Compressive index C_c	0	
Re-compressive index C_r	0	
Unconfined compressive strength q_u (kPa)	240	420
SPT blow count N_{60}	16	28

Fort McMurray

	Sand fill	Native sand	Clay till	Oil sand
Thickness (m)	0.6	2.2	1.2	-
Unit weight γ (kN/m^3)	17.3	18	21	20.4
Relative density Dr (%)	60	82	-	-
Moisture content w (%)	13	22	11	13
Plastic limit PL (%)	-	-	13-16	-
Liquid limit LL (%)	-	-	20-36	-
SPT blow count N_{60}	20	40	46	>50
Cu (kPa)	-	-	240	-

➢ **Soil properties calibrated by computer simulation**

Site	Soil	Young's modulus E (Mpa)	Poisson's ratio ν	Friction angle ϕ (°)	Cohesion c (kPa)
Brighton Beach	Sand and gravel fill	150	0.15	48	0
	Silty sand	37.5	0.3	36	0
	Firm silty clay	19.5	0.49	0	65
	Soft silty clay	5	0.49	0	25
Fort Nelson	Weathered till	24	0.2	0	120
	Unweathered till	63	0.2	0	210
Fort McMurray	Sand and gravel fill	150	0.15	48	0
	Sand fill	33	0.3	36	0
	Native sand	55	0.3	36	0
	Clay till	120	0.49	0	240
	Oil sand	185	0.3	>50	-

➢ Settlement from computer simulation

Crane activity	Settlement from Section B, C (mm)				Settlement from section A (mm)	
	A	B	C	D	Track AB	Track CD
Test lift #3 at Brighton Beach						
Sitting	10.5	0.7	20.3	5.4	17.2	26.4
Load on	12.9	27.4	3.5	17.1	33.5	23.3
Boom over front	4.8	24.9	4.8	24.9	33.7	33.6
Boom over front right	3.5	17.1	12.9	27.4	23.3	33.5
Boom over right side	8.7	8.3	23.1	22.3	9.1	24.9
Removal of old vessel "G" at Fort Nelson						
Sitting	11.5	4.4	11.5	4.4	14.2	14.2
Load on	9.8	16.9	7.9	16.2	19.8	19.8
Boom up	12.5	11.4	12.5	11.4	13.5	13.5
Boom over front right	12.5	11.4	12.5	11.4	13.5	13.5
Boom over right side	13.3	13.1	12.5	11.4	13.8	13.5
Reinstall new vessel "G" at Fort Nelson						
Sitting	12.5	11.4	7.1	6.0	13.0	8.3
Load on	13.3	13.1	12.5	11.4	13.8	13.5
Boom over front right	14.4	12.1	12.5	11.4	15.7	13.6
Boom over front	14.4	12.1	14.4	12.1	15.9	15.8
Boom down	9.8	16.9	9.8	16.9	19.8	19.8
Lift of fractionator at Fort McMurray						
Sitting	15.9	3.6	10.1	0.1	18.1	31.2
Partial load on	15.6	7.4	11.7	4.8	17.7	13.7
Full load on	9.6	18.7	9.6	18.7	20.7	20.8
Boom over front right	11.2	15.7	12.6	17.1	17.4	18.9
Lowering load	11.9	13.7	14.7	16.5	15.1	18.1
Lift of burner BX-2 at Fort McMurray						
Sitting	8.5	2.7	10.5	3.9	10.9	13.5
Full load on	8.3	12.4	7.3	11.3	15.6	14.2
Boom over front	8.3	12.4	7.3	11.3	15.5	15.6
Lowering load	7.4	12.2	7.3	11.3	15.3	15.6
Lift of reactor RX-3B at Fort McMurray						
Sitting	7.3	1.6	10.5	3.9	9.5	13.6
Full load on	9.8	7.7	10.0	8.6	12.1	12.4
Boom over front	9.8	7.7	9.8	7.7	12.1	12.1
Lowering load	10.6	7.9	9.8	7.7	13.3	12.1

APPENDIX F

Evaluation of Bearing Capacity Using Different Approaches

- **Brighton Beach**

Based on the data presented in Appendix E, the equivalent footing length equals to the track length L=7.6m. The equivalent footing width is:

$B' = B+2d\ (E_s/E_m)^{0.29} = 1.5+2x0.6x(11000/150)^{0.29} = 5.7m$

The modulus of soil is chosen to be 150Mpa as the top layer soil since it has the greatest impact to the track pressure distribution and is considerable thick.

1) Allowable bearing capacity from strength aspect

Since the soil profile is layered, it is better to use weighted average parameters over depth rather than the parameters of the weak layer to estimate the ultimate bearing capacity. The values are presented in the following table taking the footing influence depth $D_f = B' = 5.7m$.

Unit weight (kN/m^3)	Friction angle (°)	Cohesion (kPa)
11.5	17	27

The ultimate bearing capacity from Equation 2-9 and 2-10 is:

$q_u = cN_cs_c+0.5\gamma N_\gamma s_\gamma = 27x12.3x1.29+0.5x11.5x3.56x0.7=443kPa$

Therefore, the allowable bearing capacities using a factor of safety of 2.0 and 3.0 respectively are:

$qa = qu/FS = 221kPa$ FS=2.0

$= 148kPa$ FS=3.0

2) Allowable bearing capacity from settlement criteria for foundations

The calculate depth of settlement for the footing is about two times of the footing width since the footing is close to square, or $D_f = 2B' = 11.4m$. The total allowable settlement for the footing is 65mm. Since major soils involved in the calculation are clays, large consolidation settlement is expected within these two clay layers.

The immediate settlement is evaluated using Schmertmann's method. Divide the soil profile into 6 layers from ground surface to a depth of D_f = 11.4m. Using the peak strain influence factor as $I_{\varepsilon p}$ = 0.6 since it is not sensitive. The equivalent modulus of elasticity used in Schmertmann's method of the clays are set to be two times of their Young's modulus since large confinement in depth. Try the allowable bearing pressure q=30kPa and calculation is illustrated in the following table.

Layer	Depth (m)	Es (mPa)	H (m)	z_f (m)	I_ε	$qI_\varepsilon H/Es$ (mm)
1	0.00-0.88	150	0.88	0.44	0.18	0.03
2	0.88-2.43	37.5	1.55	1.65	0.39	0.45
3	2.43-4.27	39	1.84	3.35	0.56	0.75
4	4.27-6.0	10	2.33	5.13	0.44	2.87
5	6.0-8.5	10	2.7	7.25	0.29	2.20
6	8.5-11.4	10	2.7	9.95	0.10	0.77
Total immediate settlement						7.1

No consolidation test has been carried out for the two clay layers, the empirical correlation C_c = 0.009 (w_L-10) between compressive index C_c and liquid limit w_L is used to estimate the consolidation settlement. The liquid limit of soft silty clay layer is about 50, so the compression index C_c =0.36. The initial void ratio of this layer is about e_0 = 1.44. The compressibility of the firm silty clay is assumed to be 1/3 of the soft silty clay. The vertical stress distribution is estimated using Boussinesq's elastic equation and a factor α is presented. However, since the upper soil is much stiffer than the lower, this method overestimates the stress in the clay layers. The settlement due to consolidation under uniform load q=30kPa is estimated in the following table:

Layer	Depth (m)	H (m)	z_f (m)	$C_c/(1+e_0)$	α	σ_i' (kPa)	σ_f' (kpa)	δ (mm)
1	2.43-4.27	1.84	3.35	0.05	0.70	50.8	71.8	13.8
2	4.27-6.0	1.73	5.13	0.14	0.44	64.5	77.7	19.6
3	6.0-8.5	2.5	7.25	0.14	0.26	81.9	89.7	13.8
4	8.5-11.4	2.9	9.95	0.14	0.16	100.9	105.6	8.0
Total consolidation settlement								55.2

The total settlement is 6.7+55.2=62mm < 65mm.

Therefore, the allowable bearing capacity using settlement criteria for foundation is q_a = 30kPa.

3) Allowable bearing capacity using proposed method

The soil is treated as two major layers, the sand and gravel on top and clay at bottom. Bearing capacities of these two layers are evaluated separately and a weighted average over depth is used as the approximate value for allowable bearing capacity.

The bearing capacity of the top layer using weighted average SPT blow count over depth of N=33 is:

$$q_{top} = 1.2L\left(\frac{B'+0.3}{B'}\right)^2 \cdot N = 1.2\times 7.6\times\left(\frac{5.7+0.3}{5.7}\right)^2 \times 33 = 333.5kPa$$

The bearing capacity of the bottom layer using weighted average undrained shear strength over depth of C_u =33 kPa is:

$$q_{bot} = \frac{5.14+B'/L}{FS}C_u = \frac{5.14+5.7/7.6}{2.0}\times 33 = 97.5kPa$$

Therefore, the overall bearing capacity using the proposed method is:

$$qa = \frac{q_{top}h_1 + q_{bot}h_2}{h_1+h_2} = \frac{333.5x2.43+97.5x8.97}{11.4} = 148kPa$$

4) Allowable bearing capacity from computer simulation

The model used to calibrate the soil properties for case study is further loaded to yield the maximum allowable settlement. This amount of load is deemed as the allowable track load. The bearing capacity is then derived by dividing this load over the footing width.

The load to cause a settlement of L/200 = 38mm is P= 676.4kN/m. Therefore, the allowable bearing capacity from computer simulation is:

$$q_a = P/B' = 676.4/5.7 = 119kPa$$

- **Fort Nelson**

Similar to Brighton Beach case, the equivalent footing dimension used in this case is L = 8.4m and $B' = B+2d\ (E_s/E_m)^{0.29} = 2.0+2x0.6x(11000/60)^{0.29} = 4.7m$.

1) Allowable bearing capacity from strength aspect

Again, the weighted average parameters for this case is listed in the following table:

Unit weight (kN/m^3)	Friction angle (°)	Cohesion (kPa)
20.1	10	150.6

The ultimate bearing capacity from Equation 2-9 and 2-10 is:

$$q_u = cN_cs_c+0.5\gamma N_\gamma s_\gamma = 150.6x8.35x1.16+0.5x20.1x1.22x0.77=1468kPa$$

Therefore, the allowable bearing capacities using a factor of safety of 2.0 and 3.0 respectively are:

$$qa = qu/FS = 734kPa \qquad FS=2.0$$

$$= 489kPa \qquad FS=3.0$$

2) Allowable bearing capacity from settlement criteria for foundations

Schmertmann's method is also used to estimate the immediate settlement. The soil is divided into 5 layers from ground surface to a depth of 2B' = 9.4m. The peak strain influence factor is again set to be $I_{\varepsilon p} = 0.6$. The equivalent modulus of elasticity for the clay tills is chosen to be 1.2 times of their Young's modulus since the confinement and the soil are not saturated.

Try the allowable bearing pressure q=200kPa and calculate the immediate settlement as illustrated the following table.

Layer	Depth (m)	Es (mPa)	H (m)	z_f (m)	Iε	q*IεH/Es (mm)
1	0-0.60	150	0.6	0.30	0.16	0.13
2	0.60-2.30	28.8	1.7	1.45	0.41	4.82
3	2.30-3.70	75.6	1.4	3.00	0.54	2.02
4	3.70-6.10	75.6	2.4	4.90	0.38	2.43
5	6.10-9.40	75.6	3.3	7.75	0.14	1.23
Total immediate settlement						10.6

The consolidation settlement mainly happens within the weathered clay till and unweathered clay till layers. The vertical stress is estimated using Boussinesq's elastic equation and a factor α is presented.

Assume the unweathered clay till is heavily over consolidated due to glaciations, the re-compressive index C_r=0.008 will be used in the consolidation settlement calculation. The settlement due to consolidation under uniform load q=200kPa is estimated as shown the following table:

Layer	Depth (m)	H (m)	z_f (m)	$C_c/(1+e_0)$	α	σ_i' (kPa)	σ_f' (kpa)	δ (mm)
1	0.60-2.30	1.7	1.45	0.03	0.92	29.5	213.5	43.8
2	2.30-3.70	1.4	3.00	0.005	0.76	60.1	212.1	3.8
3	3.70-6.10	2.4	4.90	0.005	0.52	97.7	201.7	3.8
4	6.10-9.40	3.3	7.75	0.005	0.3	151.2	211.2	2.4
Total consolidation settlement								53.8

The total settlement is 10.6+53.8=64.4mm < 65mm.

Therefore, the allowable bearing capacity using settlement criteria is 200kPa.

3) Allowable bearing capacity using proposed method

Since the thickness of sand and gravel fill is 0.6m, only the two clay till layers are used in the bearing capacity evaluation.

$$q_a = \frac{5.14 + B'/L}{FS} C_u = \frac{5.14 + 4.7/8.4}{3.0 \sim 3.5} \times 193.7 = 315 \sim 368 kPa$$

The undrained shear strength is taken the weighted average of the two layers. And a factor of safety of 3.0 to 3.5 is used since the soil is unsaturated.

4) Allowable bearing capacity from computer simulation

Similar to Brighton Beach case, the track load to yield maximum allowable settlement L/200 = 42mm is P = 1535kN/m from computer simulation.

Therefore, the allowable bearing capacity from computer model is:

$$q_a = P/B' = 1535/4.7 = 327kPa$$

- **Fort McMurray**

Similar to the above mentioned two cases, the equivalent footing size for this case is L=10.5m and B' = 6.0m since the calculated spread width is greater than the mat length 6.0m.

1) Allowable bearing capacity from strength aspect

The weighted average parameters for this case is listed in the following table using the information in Appendix E:

Unit weight (kN/m^3)	Friction angle (°)	Cohesion (kPa)
14	32	40

The ultimate bearing capacity from Equation 2-9 and 2-10 is:

$$q_u = cN_cs_c+0.5\gamma N_\gamma s_\gamma = 40x35.49x1.37+0.5x14x30.22x0.77=2108kPa$$

Therefore, the allowable bearing capacities using a factor of safety of 2.0 and 3.0 respectively are:

$$qa = qu/FS = 1054kPa \quad FS=2.0$$

$$= 703kPa \quad FS=3.0$$

2) Allowable bearing capacity from settlement criteria for foundations

Since cohesionless soils domain the subsurface profile, immediate settlement will be predominant and the total settlement can be predict by the three factors defined in Schmertmann's method as:

$$\delta = C_1 \cdot C_2 \cdot C_3 \cdot \delta_u$$

where $C_1 = 1 - 0.5(\frac{\sigma'_{zD}}{q_n}) = depth\ factor$

$$C_2 = 1 + 0.2\log(\frac{t}{0.1}) = time\ factor$$

$$C_3 = 1.03 - 0.03L/B \geq 0.73 = shape\ factor$$

δ = total settlement

δ_u = immediate settlement

q_n = net pressure applied by footing

σ'_{zD} = initial effective stress at bottom of footing

The soil is divided into 7 layers from ground surface to a depth of 2B' = 12m, the peak strain influence factor is chosen to be $I_{\varepsilon p}$ = 0.6. The equivalent modulus of elasticity for soils beneath ground water is chosen to be 1.2 times of their Young's modulus. The immediate settlement is calculated in the following table using a bearing pressure of q=400kPa.

Layer	Depth (m)	Es (mPa)	H (m)	zf (m)	Iε	q*IεH/Es (mm)
1	0.0 -1.80	150	1.8	0.90	0.25	1.20
2	1.80-2.40	33	0.6	2.10	0.45	3.27
3	2.40-3.60	66	1.2	3.00	0.60	4.36
4	3.60-4.60	66	1.0	4.10	0.53	3.19
5	4.60-5.80	144	1.2	5.20	0.45	1.51
6	5.80-8.0	222	2.2	6.90	0.34	1.35
7	8.0-12.0	222	4.0	10.00	0.13	0.96
Total immediate settlement						15.8

Total settlement in 50 years is:

$$\delta = C_1 \cdot C_2 \cdot C_3 \cdot \delta_u = 1 \times 1.54 \times 0.98x15.8 = 23.8mm < 25mm$$

Therefore, the allowable bearing capacity from settlement criteria for foundations is 400kPa.

3) Allowable bearing capacity using Meyerhof's method

$$q_a = 8 \cdot \left(\frac{B'+0.3}{B'} \right)^2 \cdot N = 8 \times \left(\frac{6.0+0.3}{6.0} \right)^2 \times 42 = 370kPa$$

The SPT blow count N is taken to be the weighted average over the failure zone of the footing in the above equation.

4) Allowable bearing capacity using proposed method

$$q_a = 1.2L \cdot \left(\frac{B'+0.3}{B'} \right)^2 \cdot N = 1.2 \times 10.5 \times \left(\frac{6.0+0.3}{6.0} \right)^2 \times 42 = 583kPa$$

5) Allowable bearing capacity from computer simulation

The load to yield L/200 = 52.5mm settlement is P = 3584kN/m from the computer simulation. Therefore, the allowable bearing capacity from the computer simulation is:

q_a = P/B' = 3584/6.0 = 597kPa